CENTER FOR COMPUTER AIDED DESIGN

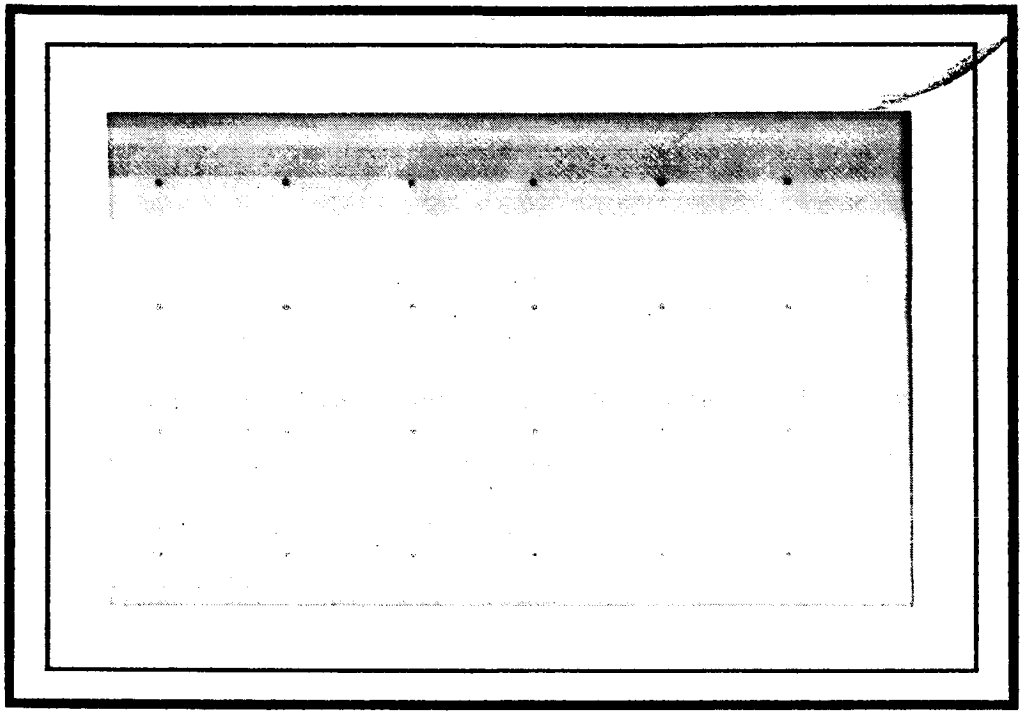

College of Engineering
The University of Iowa
Iowa City, Iowa 52242

Technical Report 84-12

DESIGN SENSITIVITY ANALYSIS AND OPTIMIZATION OF BUILT-UP STRUCTURES

Hee G. Lee
Kyung K. Choi and Edward J. Haug

Center for Computer Aided Design
College of Engineering
The University of Iowa

December 1984

Research was partially supported by
NASA Grant NAG-1-215

ABSTRACT

Design sensitivity analysis and optimization of built-up structures are formulated, analyzed, and solved numerically. A variational approach is used to incorporate both finite dimensional and distributed state and design variables in the same energy equation. Kinematic and natural boundary conditions at the interfaces between structural components of built-up structures are defined. Variation of the energy equation with the material derivative idea from continuum mechanics and introduction of an adjoint variational equation yield design sensitivity vectors and functions with respect to conventional and shape design variables. A unified method of shape design sensitivity analysis for static and eigenvalue problems, to complement the finite element method of structural analysis is developed. Standard shape design sensitivity forms are derived for structural components and may be applied to various kinds of built-up structures to obtain design sensitivity forms at the interfaces between structural components of built-up structures. This method provides potential for shape optimization of complex built-up structures. Numerical considerations for design sensitivity analysis and optimization are investigated. A basic study is carried out to check numerical accuracy of calculations by the finite element method. A characteristic function is introduced to treat stress constraints in finite dimensional shape optimization. Special attention is given to calculating shape design sensitivities for stress

constraints on elements that are adjacent to interfaces. Results of design sensitivity analysis and the related numerical considerations are used with a linearization method for iterative optimal design. A truss-beam-plate built-up structure is presented to illustrate use of the method.

TABLE OF CONTENTS

LIST OF FIGURES

LIST OF TABLES

LIST OF SYMBOLS

a	bilinear form
A	cross-sectional area of beam (truss)
$\bar{A}$	differential operator
$\bar{B}$	differential operator
b	design parameter
c	bilinear form
d	bilinear form; beam width
D	flexural rigidity of plate; elastic modulus tensor; differential operator
E	Young's modulus
f	distributed load
$\tilde{f}$	axial load
F	body force vector; function
g	function
G	shear modulus; function
h	plate thickness; beam height
$[H^i(\Omega)]^k$	various Sobolev spaces defined in Ω
I	moment of inertia
J	torsion constant
K	stiffness matrix
L	length
$\bar{L}$	virtual work
M	mass matrix; characteristic function

$M_x(M_y)$	bending moment
M_{xy}	twisting moment; corner force
n	outward unit normal vector
N	shape function
P	point load
q	displacement of truss
t	time parameter; thickness of plate
T	kinetic energy; applied torque; surface traction vector
u	design variable
U	strain energy
v	displacement of beam
V	velocity field
$V_x(V_y)$	shear force
w	displacement of plate
W	product space
W_i	weighting coefficient
$\hat{x}$	isolated point
$\tilde{x}$	position vector
y	eigenvector (eigenfunction)
$\tilde{y}$	position vector
z	state variable (displacement function)
Z	space of kinematically admissible displacement field
γ	boundary operator; interface
Γ	boundary of the system
δ	variation operator

ℓ	length; linear form
θ	angle of twist per unit length
ε	strain; small parameter
λ	adjoint variable
Λ	sensitivity coefficient
ν	Poisson's ratio
ζ	eigenvalue
ω	natural frequency; small angle
ρ	material density
τ	parameter
σ	stress
$\dot{\Phi}$	constraint function
ξ	normalized coordinate
η	normalized coordinate
Ψ	constraint functional
Ω	domain of the system
∇	gradient operator
∇^2	Laplacian operator
∇^4	biharmonic operator

CHAPTER 1

INTRODUCTION

1.1 Purpose, Motivation, and Scope

The research reported herein deals with variational methods of design sensitivity analysis and finite element numerical methods for iterative optimization of built-up structures, taking advantage of distributed parameter structural theory.

During the past decade matrix and finite element methods of structural mechanics have been used with nonlinear programming methods of optimization to create numerical methods for optimizing structures [1,2]. Recently, developments in distributed parameter structural optimization show rather clearly [3] that the unified variational theory of structural boundary-value problems can be used in design sensitivity analysis and optimization. Rigorous and practically computable results for structural components (beams, plates, plane elastic solids, and three dimensional elastic solids) have been demonstrated and used to solve component optimization problems [3].

The dichotomy between matrix and distributed parameter approaches to structure optimization is particularly evident when one considers complex built-up structures that consist of interconnected truss, beam, plate, shell, and other components. Virtually, all aircraft, vehicles, machines, and other mechanical structures are made up of combinations of a variety of such structural components. The matrix/finite element

approach is extendable to treat such classes of structures, which has been done to a limited degree in the literature. No attempt, however, has been made to develop a distributed parameter theory of structural optimization for built-up structures.

The principal objective of this research is to extend the theory of single component, distributed parameter design-shape optimization to treat built-up structures that are composed of interconnected components. Attention is restricted in this research to linear structural mechanics. The variational formulation, in the case of individual structural components, can be rigorously related to a virtual work or energy principle in mechanics. This result allows direct extension of energy ideas used in matrix methods to a distributed parameter formulation of built-up structures.

The approach taken in this research begins with an energy characterization of structural performance, namely Hamilton's Principle. Hamilton's Principle results in a variational formulation of the governing structural equations that is employed for design sensitivity analysis. Strong ellipticity properties of energy bilinear forms have been proved for individual structural components [4], yielding existence and uniqueness results for the associated variational equations and forming the foundation for a rigorous proof of differentiability of structural response with respect to design variables and shape. These mathematical properties are presumed to be satisfied, justifying use of direct variational analysis techniques that

were rigorously developed in individual structural components [5] for design sensitivity analysis of built-up structures.

The second principal objective of this research is to develop a unified shape design sensitivity analysis method to demonstrate substantial theoretical and computational advantages over previously used shape design sensitivity analysis methods for structural components. These new results are used in applications for optimal design of various kinds of built-up structures. The shape design sensitivity method developed follows directly from energy methods of solid mechanics and the material derivative idea of continuum mechanics. The result is a theory that can be stated almost completely in terms of concepts of mechanics, not requiring a detailed knowledge of functional analysis, even though such theory provides rigorous justification of these methods.

The final objective of this research is finite element implementation of the formulation developed. Finite element theory for built-up structures and variational equation theory [6] guarantee validity of the resulting finite element models.

The next section of this chapter presents a literature survey of topics and problems related to built-up structural optimization. Chapter 2 presents general distributed parameter theory for design sensitivity analysis of built-up structures.

With the variational equations and the material derivative idea from continuum mechanics for shape variations, static and eigenvalue design sensitivity analysis by the adjoint variable method on a variable

domain are carried out in Chapter 2. Chapter 3 presents a unified method for shape design sensitivity analysis for built-up structures, based on the formulation derived in Chapter 2 and taking advantage of direct application of design sensitivity forms to the various kinds of built-up structures. The interface conditions between structural components and the shape design sensitivity forms for basic built-up structural models involving beams, plates, and plane elastic solids are summarized.

Numerical considerations related to design sensitivity analysis and optimization are discussed in Chapter 4. In Chapter 5, a truss-beam-plate built-up structure is used to illustrate the numerical feasibility of design sensitivity analysis and optimization, through iterative optimization of a complex built-up structure. Finally, Chapter 6 presents a discussion and conclusions of the present study.

1.2 Literature Survey

One of the common means of achieving a high strength-to-weight ratio is to combine structural components as built-up structures. A substantial literature has developed on optimization of built-up structures.

One of the first treatments of built-up structure optimization was considered by Catchpole [7], who developed a method enabling rapid determination of the optimum cross-sectional dimensions of a compression surface having an unflanged integral stiffener. Symonds [8] presented the minimum weight design of a simply supported, transversely stiffened plate that is loaded in shear.

Problems of optimum design of stiffened cylinders or cylindrical shells, under either compression, lateral pressure, or combined axial compression and lateral pressure, with various types of stiffeners were considered by Nickel and Crawford [9], Crawford and Burns [10], Cohen [11], Burns and Almroth [12], Gerard and Papirno [13], Burns and Skogh [14], Burns [15-18], Gerard [19], Lakshmikantham and Becker [20], Block [21], and Shideler et al. [22].

In many of the earlier papers [9-22], optimization was achieved by parametric studies. This is a classical design method that is integral to the weight/strength and structural index concepts of minimum weight structural design [23]. Afterwards, optimal design has been achieved by the mathematical programming approach that was pioneered by Schmit [24]. For this approach, many algorithms are available that are guaranteed (theoretically) to produce at least a local optimum design.

Structural synthesis of stiffened cylinders or cylindrical shells was considered in several papers [25-33]. Kicher [25] treated the problem by using a constrained gradient method. Schmit et al.[26], and Morrow and Schmit [27] applied a Fiaco-McCormick type penalty function formulation to transform the basic inequality constrained minimization problem into a sequency of unconstrained minimization problems. Pappas and Amba-Rao [28] used a direct search algoritm with an interior-exterior penalty function formulation. Thornton [29] used the exterior penalty function method with least-square approximation. Jones and Hague [30] applied a different optimization search technique and

extended the work of Ref. 27. Pappas and Allentuch [31-33] utilized a direct search design algorithm and the golden search.

Many other papers considered minimum weight design of built-up structures, under a variety of loading conditions, constraints, configurations, and with a variety of optimization techniques [34-61].

Stroud and Sykes [34] showed the effect of slight meridional curvature. Lakshmikantham and Gerard [35] showed the effects of ring stiffeners of the isotropic skin. Kicher and Chao [36] treated the problem of stiffened fiber composite cylinders with the penalty function technique of Fiaco and McCormick. Weight optimization of reinforced spherical shells under external pressure was examined by Manevich and Kaganov [37]. An eccentrically stiffened wide panel under compression was investigated by Tvergaard [38].

An indirect, trial and error design procedure for axially compressed cylinders has been proposed by Rehfield [39]. Pappas and Allentuch [40] presented a procedure for circular, cylindrical, 'T' frame (ring) reinforced, submersible shells. Simitses and Aswani [41] found optimum stiffened cylinders that can safely carry a given hydrostatic pressure. Pappas and Allentuch [42] considered the pressure hull optimization using a general instability equation. Simitses and Ungbhakorn [43,44] have produced designs of axially compressed cylinders with various stiffeners. Kunoo and Yang [45,46] carried out design of cylindrical shells with different stiffeners, subjected to uniform axial compressive or bending load, by the method of steepest descent. This problem was also considered by Pappas and Moradi [47], by direct

optimization without use of approximation or limitations in the number of stiffener sizes.

Richards [48] considered optimum design of stiffened webs with supplementary skin stabilization. Søreide et al. [49] studied the design of stiffened plates in an ultimate limit state. Libai [50] presented design of a square plate with a single, eccentric, blade-type stiffener that is subjected to compressive edge loads.

Majumder and Thornton [51] presented a method to produce efficient piecewise uniform stiffened shells of revolution. Simitses and Giri [52] presented a design procedure of stiffened circular cylindrical shell geometries, subjected to pure torsion. Later they extended the design problem, combined with axial compression, with and without lateral pressure [53]. Design of stiffened cylindrical panels was considered by Toakley and Williams [54] for compression loading and by Simitses and Sheinman [55] for combined load.

Bronowicki et al.[56] presented the design of a shell with T-ring stiffeners subjected to a vibration constraint. Patnaik and Sankaran [57] treated stiffened cylindrical panels with constraints on natural frequencies, in the presence of initial stresses, using unconstrained minimization techniques and a finite difference scheme for design sensitivity analysis. Dobbs and Nelson [58] presented a method with fracture constraints that is capable of determining a fail-safe design, which is a logical extension of present structural optimization methods which include stress, displacement, buckling, frequency, and aeroelastic flutter constraints. Rao and Reddy [59] considered design optimization

of axially loaded, stiffened cylindrical shells for minimum mass with natural frequency, local and overall buckling strengths and direct stress constraints.

Simitses and Sheinman [60] solved the problem of optimizing stiffened, thin, circular cylindrical shells under uniform axial compression against general instability, in the presence of initial geometric imperfection. Patel and Patel [61] made an attempt to obtain a design of stiffened cylindrical shell under pure bending load, using a penalty function technique and complex method of Box.

However, all of these problems were solved by a matrix/finite element approach. The main emphasis of this research is on development of a distributed parameter structural theory for design sensitivity analysis and optimization, a unified method for shape design sensitivity analysis, and a method for finite element implementation of formulations achieved for numerical feasibility.

CHAPTER 2

DESIGN SENSITIVITY ANALYSIS OF BUILT-UP STRUCTURES, BASED ON DISTRIBUTED PARAMETER THEORY

2.1 Introduction

Distributed parameter structural theory [3,5] is applied here for design sensitivity analysis of built-up structures, for both static and eigenvalue problems with design variable and shape variations. Variational equations for structural components are obtained in Section 2.2 and a general variational formulation for built-up structures is presented in Section 2.3. For shape variation, the material derivative idea of continuum mechanics is introduced in Section 2.4. In Sections 2.5 and 2.6, static and eigenvalue design sensitivity analysis for both design and shape variations, respectively, are presented, using the variational/structural equations. The basic theory is originated from Ref. 5, where the reader may find more technical and mathematical developments.

2.2 Variational Equations of Structural Components

In order to be specific about properties of built-up structures, it is helpful to formulate variational equations for several structural components in a unified way, prior to delving into design sensitivity analysis. Three basic problems are defined in this section and are used in later sections. It is shown that the basic forms of all problems are identical.

2.2.1 Beam

Bending, torsion, axial deformation, and vibration of a beam are considered. For bending, the boundary-value problem, in operator form, is given as

$$\bar{A}z \equiv (EIz_{xx})_{xx} = f \quad , \qquad x \in (0, \ell) \tag{2.1}$$

$$\gamma z(0) = \gamma z(\ell) = 0 \tag{2.2}$$

where E is Young's Modulus, I is moment of inertia of the beam cross section, $f \in C^1[0,\ell]$ is distributed load, and γ is a boundary operator that gives the projection of structural displacements and perhaps their derivatives onto the exterior boundary.

For torsion, the differential equation for the angle of twist θ per unit length of the beam is [62]

$$\bar{A}\theta \equiv -GJ\theta_{xx} = T \quad , \qquad x \in (0, \ell) \tag{2.3}$$

$$\gamma\theta(0) = \gamma\theta(\ell) = 0 \tag{2.4}$$

where G is shear modulus, J is torsion constant [63], and T is applied torque.

For axial deformation, the boundary-value problem, in operator form, is given as

$$\bar{A}z \equiv -(EAz_x)_x = \tilde{f} \quad , \qquad x \in (0, \ell) \tag{2.5}$$

$$\gamma z(0) = \gamma z(\ell) = 0 \tag{2.6}$$

where $\tilde{f} \in C^1[0,\ell]$ is axial load and A is cross-sectional area of the beam.

For vibration, the formal operator eigenvalue problem for bending is

$$\bar{A}y \equiv (EIy_{xx})_{xx} = \zeta\rho Ay = \zeta\bar{B}y \quad , \qquad x \in (0,\ell) \tag{2.7}$$

$$\gamma y(0) = \gamma y(\ell) = 0 \tag{2.8}$$

where $\zeta = \omega^2$, ω is natural frequency and ρ is material density.

These boundary-value problems may be written in equivalent variational forms, essentially the principle of virtual work, by multiplying Eqs. 2.1, 2.3, and 2.5 by arbitrary virtual displacements that are consistent with the boundry conditions of Eqs. 2.2, 2.4, and 2.6, respectively, and integrating by parts to obtain the variational equations

$$a(z,\bar{z}) \equiv \int_0^\ell EIz_{xx}\bar{z}_{xx}dx = \int_0^\ell f\bar{z}dx \equiv \ell(\bar{z}) \tag{2.9}$$

for all $\bar{z} \in Z = \{z \in H^2(0,\ell)$:z satisfies kinematic boundary conditions$\}$ for bending,

$$a(\theta,\bar{\theta}) \equiv \int_0^\ell GJ\theta_x\bar{\theta}_x dx = T\bar{\theta}\,\Big|_0^\ell \equiv \ell(\bar{\theta}) \tag{2.10}$$

for all $\bar{\theta} \in Z = \{z \in H^1(0,\ell)$:z satisfies kinematic boundary conditions$\}$ for torsion [64], and

$$a(z,\bar{z}) \equiv \int_0^\ell EAz_x\bar{z}_x dx = \int_0^\ell \tilde{f}\bar{z}dx \equiv \ell(\bar{z}) \tag{2.11}$$

for all $\bar{z} \in Z = \{z \in H^1(0,\ell)$: z satisfies kinematic boundary conditions$\}$ for axial deformation.

Similarly, the variational form for the eigenvalue problem is

$$a(y,\bar{y}) \equiv \int_0^\ell EIy_{xx}\bar{y}_{xx}dx = \zeta\int_0^\ell \rho Ay\bar{y}dx = \zeta d(y,\bar{y}) \tag{2.12}$$

for all $\bar{y} \in Z = \{z \in H^2(0,\ell)$: z satisfies kinematic boundary conditions$\}$.

One can obtain the variational eigenvalue equations for torsion and axial deformation. Here, $H^i(\Omega)$ represents a Sobolev space. For a discussion of Sobolev spaces, the reader is referred to Refs. 5, 65, 66, and 67. In beam stiffened built-up structures, the torsional stiffness effect of beams is generally considered, making use of the terms presented here.

2.2.2 Plate

Bending and vibration of a plate of variable thickness $h(x) \geq h_0 > 0$ as shown in Fig. 2.1 are now considered. The operator form of the boundary-value problem is

$$\bar{A}z = f \ , \qquad x \in \Omega \tag{2.13}$$

$$\gamma z = 0 \ , \qquad x \in \Gamma \tag{2.14}$$

where the operator $\bar{A}$ is defined formally as

$$\bar{A}z = [D(u)(z_{11}+\nu z_{22})]_{11} + [D(u)(z_{22}+\nu z_{11})]_{22} + 2(1-\nu)[D(u)z_{12}]_{12} \tag{2.15}$$

where a subscript i denotes the operation $\frac{\partial}{\partial x_i}$, $D(u) = Eh^3/[12(1 - \nu^2)]$, E is Young's modulus, ν is Poisson's ratio, and γ is a boundary operator.

The variational equation for the plate is [5]

$$a(z,\bar{z}) \equiv \iint_\Omega D(u)[z_{11}\bar{z}_{11} + \nu z_{22}\bar{z}_{11} + z_{22}\bar{z}_{22} + \nu z_{11}\bar{z}_{22} + 2(1-\nu)z_{12}\bar{z}_{12}]d\Omega = \iint_\Omega f\bar{z}d\Omega \equiv \ell(\bar{z}) \tag{2.16}$$

for all $\bar{z} \in Z = \{Z \in H^2(\Omega)$: z satisfies kinematic boundary conditions$\}$ for static response. If the thickness h is constant, then the operator equation is simplified to

$$\bar{A}z \equiv D\nabla^4 z = f \quad , x \in \Omega \tag{2.17}$$

$$\gamma z = 0 \ , \ x \in \Gamma \tag{2.18}$$

where $f \in C^1(\bar{\Omega})$ and $\bar{\Omega}$ is the closure of Ω [66].

For vibration, the formal operator form of the eigenvalue problem is simplified to

$$\bar{A}y \equiv D\nabla^4 y = \zeta\rho h y \equiv \zeta\bar{B}y \quad , x \in \Omega \tag{2.19}$$

$$\gamma y = 0 \quad , x \in \Gamma \tag{2.20}$$

where $\zeta = \omega^2$, ω is natural frequency, and ρ is material density.

The variational equations are [5]

$$a(z,\bar{z}) \equiv D\iint_\Omega (\nabla^2 z)(\nabla^2\bar{z})d\Omega = \iint_\Omega f\bar{z}d\Omega \equiv \ell(\bar{z}) \tag{2.21}$$

for all $\bar{z} \in Z$, for static response, and

$$a(y,\bar{y}) = \zeta \iint_{\Omega} \rho h \bar{y} y d\Omega \equiv \zeta d(y,\bar{y}) \tag{2.22}$$

for all $\bar{y} \in Z$, for the eigenvalue problem.

2.2.3 Linear Elasticity

The three dimensional linear elasticity problem for a body of arbitrary shape, shown in Fig. 2.2, is considered. The strain tensor is defined as

$$\varepsilon^{ij}(z) = \frac{1}{2}(z^i_j + z^j_i) \quad , \; i,j = 1,2,3 \quad , \; x \in \Omega \tag{2.23}$$

where $z = [z^1, z^2, z^3]^T$ is displacement. The stress-strain relation (generalized Hook's law) is given as [68]

$$\sigma^{ij}(z) = \sum_{k,\ell=1}^{3} D^{ijk\ell}\varepsilon^{k\ell}(z) \quad , \quad i,j,k,\ell = 1,2,3 \quad , \; x \in \Omega \tag{2.24}$$

where D is the elastic modulus tensor, satisfying $D^{ijk\ell} = D^{jik\ell}$ and $D^{ijk\ell} = D^{ij\ell k}$, $i,j,k,\ell = 1,2,3$. The equilibrium equations are [68]

$$-\sum_{j=1}^{3} \sigma^{ij}_{j}(z) = F^i \quad , \; i = 1,2,3 \quad x \in \Omega \tag{2.25}$$

with boundary conditions

$$z^i = 0 \quad , \quad i = 1,2,3 \quad , \; x \in \Gamma^0 \tag{2.26}$$

$$T^{n^i}(z) \equiv \sum_{j=1}^{3} \sigma^{ij}(z) n^j = T^i, \quad i = 1,2,3, \quad x \in \Gamma^2 \tag{2.27}$$

and the boundary segment Γ^1 is traction free, where n^j is the jth

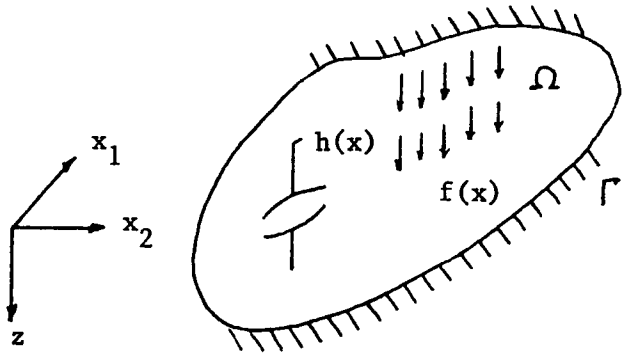

Figure 2.1 Clamped Plate of Variable Thickness h(x)

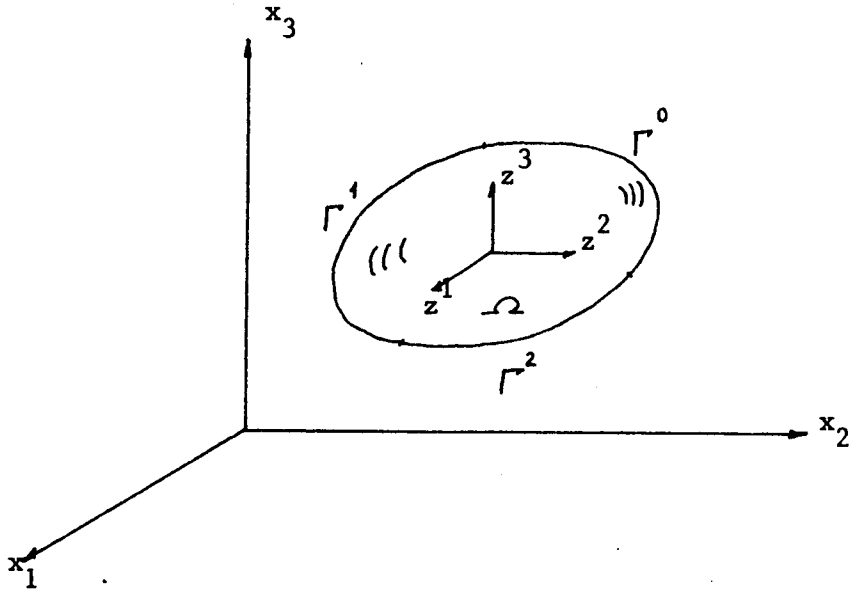

Figure 2.2 Three Dimensional Elastic Solid

component of the outward unit normal, $F = [F^1,F^2,F^3]^T \in [C^1(\bar{\Omega})]^3$, and $T = [T^1,T^2,T^3]^T \in [C^1(\Gamma)]^3$.

The variational equation for this problem is [5]

$$a(z,\bar{z}) \equiv \iiint_\Omega [\sum_{i,j=1}^{3} \sigma^{ij}(z)\varepsilon^{ij}(\bar{z})]d\Omega$$

$$= \iiint_\Omega [\sum_{i=1}^{3} F^i\bar{z}^i]d\Omega + \iint_\Gamma [\sum_{i=1}^{3} T^i\bar{z}^i]d\Gamma \equiv \ell(\bar{z}) \qquad (2.28)$$

which must hold for all $\bar{z} \in Z$, where Z is the space of kinematically admissible displacements; i.e.,

$$Z = \{z \in [H^1(\Omega)]^3 : z^i = 0,\ i = 1,2,3\ ,\quad x \in \Gamma^0\} \qquad (2.29)$$

For plane elasticity problems in which either all components of stress in the x_3-direction are zero or all components of strain in the x_3-direction are zero, Eq. 2.28 remains valid, with limits of summation running from 1 to 2 and an appropriate modification of the generalized Hook's law of Eq. 2.24.

2.3 Variational Equations of Built-Up Structures

Consider a general structure that is made up of a collection of structural components, for which each component, except truss elements, occupies a domain Ω^i with boundary Γ^i, i=1,2,..,r, and the components are interconnected by kinematic constraints at their boundaries. That is, structural components are interfaced by joints that connect them to adjacent components and constrain admissible displacement fields at the interfaces. Displacements in structural components are said to be

kinematically admissible if they satisfy kinematic constraints at the joints. The definition of kinematic constraints at each interface depends on the nature of the components connected by the joint. The axial displacement of the end of a truss component, for example, must be equal to the projection of the displacement of the point of attachment in an adjacent component, along the axis of the truss component. In the case of a beam component, kinematic boundary conditions at the ends of the element may involve both displacement and slope. In the case of plate components, kinematic interface conditions may likewise involve both displacement and slope. In the case of an elastic component of general shape, the kinematic interface conditions involve only displacement at the interface. This is the same set of boundary conditions imposed in the finite element model, since the compatibility condition in finite element analysis means that displacements within elements and across element boundaries are continuous.

In an abstract setting, let z denote a composite vector of displacement fields in the components that make up the built-up structure ; i.e., $z \equiv [z^1, z^2, \ldots, z^r, q]^T$, where $z^i \in [H^{m_i}(\Omega^i)]^{\ell_i}$ represent displacements for beam, plate, or elastic components and $q \in R^k$ represents displacements of truss components. The space of kinematically admissible displacement fields is defined as the set of displacement fields that satisfy homogeneous boundary conditions between the individual components and the ground reference frame and kinematic interface conditions between components. Symbolically, this is

$$Z = \{z \in W : \gamma z = 0 \text{ on } \Gamma, \quad \gamma^i z = \gamma^j z \text{ on } \Gamma^{ij}\} \tag{2.30}$$

where the product space $W = \prod_{i=1}^{r} [H^{m_i}(\Omega^i)]^{\ell_i} \times R^k$ is the space of displacement fields that satisfy the required degree of smoothness, γ is a boundary operator (the trace operator [66]) giving the projection of structural displacements and perhaps their derivatives onto the exterior boundary Γ, and γ^i and γ^j are interface operators that project displacement fields and perhaps their derivatives from within components i and j onto their common boundary Γ^{ij}. This space of functions is called the space of kinematically admissible displacement fields.

2.3.1 Hamilton's Principle

In order to state a general form of Hamilton's Principle, it is first necessary to define energy quantities associated with the structure. First, let the strain energy of the structural system be denoted by

$$\begin{aligned} U(z) &\equiv \frac{1}{2} a_{u,\Omega}(z,z) \\ &= \frac{1}{2} \left[\sum_{i=1}^{r} a_{u^i,\Omega^i}(z^i,z^i) + a_b(q,q) \right] \end{aligned} \tag{2.31}$$

where a_{u^i,Ω^i} is the strain energy of each component i and a_b is the strain energy of truss components. The design variable is $u = [u^1, u^2, \ldots u^r, b]^T$, where u^i is the design variable of component i and b is the design parameter vector of the trusses.

The dependence of the strain energy quadratic form on design variable u and shape Ω, which is to be parametrized later, of the

system is indicated. It is presumed that the quadratic strain energy in Eq. 2.31 is defined for all displacements in the space Z of kinematically admissible displacements. The strain energy quadratic form is defined as the sum of strain energies of the components that make up the built-up structure, each involving a matrix or integral quadratic form in its displacement field.

Next, define the kinetic energy of the system as

$$T(\frac{dz}{dt}) \equiv \frac{1}{2} d_{u,\Omega}(\frac{dz}{dt},\frac{dz}{dt})$$

$$= \frac{1}{2} [\sum_{i=1}^{r} d_{u^i,\Omega^i}(\frac{dz^i}{dt},\frac{dz^i}{dt}) + d_b(\frac{dq}{dt},\frac{dq}{dt})] \qquad (2.32)$$

where d_{u^i,Ω^i} is the kinetic energy of component i and d_b is the kinetic energy of the trusses. Here, dz/dt denotes time derivatives of the displacement z and the kinetic energy quadratic form depends on the design variable of the structure. As in the case of strain energy, kinetic energy is obtained by summing kinetic energies of each of the structural components, each involving its own matrix quadratic form or integral over the domain of the component. It is presumed that the kinetic energy in Eq. 2.32 is well defined for all kinematically admissible displacement fields.

Finally, let the virtual work of all externally applied forces be defined as

$$\bar{L}(\bar{z}) \equiv \ell_{u,\Omega}(\bar{z})$$

$$= \sum_{i=1}^{r} \ell_{u^i,\Omega^i}(\bar{z}^i) + f_b(\bar{q}) \qquad (2.33)$$

where ℓ_{u^i,Ω^i} is the virtual work of the applied forces for component i and f_b is the virtual work of the applied forces for the trusses, with time held constant, in undergoing a small virtual displacement $\bar{z}$ that satisfies the kinematic admissibility conditions; i.e., for all $\bar{z} \in Z$. The virtual work of applied forces acting on a built-up structure is obtained by summing the virtual work of external forces applied to each of the structural components. This virtual work functional is linear in the virtual displacement $\bar{z}$.

Since the displacement of a structural system will in general be time dependent, each of the functionals defined in Eqs. 2.31 through 2.33 is evaluated at a particular time t. In anticipation of employing Hamilton's Principle, it is helpful to define the first variation of the strain and kinetic energy quadratic forms of Eqs. 2.31 and 2.32. For any kinematically admissible virtual displacement $\bar{z}$, one defines these variations as

$$\bar{U} \equiv \frac{d}{d\tau} U(z + \tau\bar{z})\Big|_{\tau=0} \equiv a_{u,\Omega}(z,\bar{z}) \tag{2.34}$$

$$\bar{T} \equiv \frac{d}{d\tau} T(\frac{dz}{dt} + \tau \frac{d\bar{z}}{dt})\Big|_{\tau=0} \equiv d_{u,\Omega}(\frac{dz}{dt} \frac{d\bar{z}}{dt}) \tag{2.35}$$

where the strain energy and kinetic energy symmetric bilinear forms defined on the right sides of Eqs. 2.34 and 2.35 are obtained by calculating the first variation of the strain and kinetic energy quadratic forms of Eqs. 2.31 and 2.32.

With this notation, one is now in a position to state a general form of Hamilton's Principle that is suitable for design sensitivity analysis of built-up structures. Following the classical literature [69-71], the variational form of Hamilton's Principle requires that

$$\int_{t_0}^{t_1}(\bar{U} - \bar{T})dt = \int_{t_0}^{t_1} \bar{L}\, dt \tag{2.36}$$

for all times t_0 and t_1 and for all kinematically admissible virtual displacements $\bar{z}$ that satisfy the additional conditions

$$\bar{z}(t_0) = \bar{z}(t_1) = 0 \tag{2.37}$$

In terms of the virtual work linear form of Eq. 2.33 and the strain and kinetic energy bilinear forms of Eqs. 2.34 and 2.35, one may write Eq. 2.36 as

$$\int_{t_0}^{t_1} \{a_{u,\Omega}(z,\bar{z}) - d_{u,\Omega}\,(\frac{dz}{dt},\frac{d\bar{z}}{dt})\}dt = \int_{t_0}^{t_1} \ell_{u,\Omega}(\bar{z})dt \tag{2.38}$$

for all kinematically admissible virtual displacements $\bar{z}$ that satisfy Eq. 2.37.

This general formulation of Hamilton's Principle provides the variational equations of structural dynamics. The foregoing formulation directly specializes to the cases of static response and natural vibration of the built-up structure. Using the theorem of minimum total potential energy, one could similarly extend the variational formulation for buckling of a built-up structure, which is not pursued here.

2.3.2 The Principle of Virtual Work

Consider now the case of static response of a structure to load that does not depend on time. In this case, time is suppressed completely from the problem and Eq. 2.38 reduces to

$$a_{u,\Omega}(z,\bar{z}) = \ell_{u,\Omega}(\bar{z}) \tag{2.39}$$

for all $\bar{z} \in Z$, which may be viewed simply as a statement of the principle of virtual work. Note that this equation generalizes the variational formulation of boundary-value problems of individual structural components. Note also that if the load linear form on the right of Eq. 2.39 is continuous in the space Z and if the energy bilinear form on the left side of Eq. 2.39 is strongly elliptic on Z, then by Lax-Milgram theorem [66], Eq. 2.39 has a unique solution $z \in Z$.

2.3.3 Free Vibration

Consider next the special case in which there are no externally applied loads and in which one wishes to consider harmonic vibration of the built-up structure. Harmonic motion of the entire built-up structure is defined as a displacement field that can be written as the product of a time independent mode function $y \in Z$ and a harmonic function $\sin\omega t$; i.e.,

$$z = y\sin\omega t \tag{2.40}$$

where $y \in Z$.

Before substituting this harmonic displacement field into Eq. 2.38, it is helpful to transform Eq. 2.38, using an integration by parts.

Since the kinetic energy bilinear form is linear in its individual factors, one has

$$\frac{d}{dt}d_{u,\Omega}(\frac{dz}{dt},\bar{z}) = d_{u,\Omega}(\frac{d^2z}{dt^2},\bar{z}) + d_{u,\Omega}(\frac{dz}{dt},\frac{d\bar{z}}{dt}) \tag{2.41}$$

Integrating both sides of this equation from t_0 to t_1, recalling that $\bar{z}$ must satisfy Eq. 2.37, one has

$$0 = d_{u,\Omega}(\frac{dz}{dt},\bar{z})\Big|_{t_0}^{t_1} = \int_{t_0}^{t_1}\{d_{u,}(\frac{d^2z}{dt^2},\bar{z}) + d_{u,\Omega}(\frac{dz}{dt},\frac{d\bar{z}}{dt})\}dt \tag{2.42}$$

One may now substitute for the second term in the integrand on the right side of Eq. 2.42 into Eq. 2.38, with the load linear form equal to zero, to obtain

$$\int_{t_0}^{t_1}\{a_{u,\Omega}(z,\bar{z}) + d_{u,\Omega}(\frac{d^2z}{dt^2},\bar{z})\}dt = 0 \tag{2.43}$$

for all $\bar{z} \in Z$.

One may substitute z from Eq. 2.40 and $\bar{z}$ in the form $\bar{z} = \bar{y}f(t)$, where $\bar{y}$ is an arbitrary time independent displacement field in Z and f(t) is an arbitrary function of time that vanishes at t_0 and t_1, to obtain

$$\{a_{u,\Omega}(y,\bar{y}) - \omega^2 d_{u,\Omega}(y,\bar{y})\}\int_{t_0}^{t_1}\sin\omega t f(t)dt = 0 \tag{2.44}$$

for all $\bar{y} \in Z$. Since the integral in Eq. 2.44 is not zero for all functions f that vanish at t_0 and t_1, its coefficient must be zero. Defining $\zeta = \omega^2$, one has the variational eigenvalue equation

$$a_{u,\Omega}(y,\bar{y}) = \zeta d_{u,\Omega}(y,\bar{y}) \tag{2.45}$$

for all $\bar{y} \in Z$. Note that this is the form of the variational eigenvalue problem for individual structural components.

2.4 Material Derivative for Shape Variation

Structural design problems are considered in which the shape of a two or three dimensional structural element is to be optimized, subject to constraints on natural frequency, displacement, and stress in the structure. Since shape of the domain that a structural component occupies is treated as the design variable, it is convenient to think of the domain Ω as a continuous medium and to utilize the material derivative idea from continuum mechanics to find relationships between a variation in shape and the resulting variation in functionals that arise in shape optimal design problems. In this section, the material derivative is defined and basic material derivative formulas for structural response functionals are presented.

Consider a domain Ω in two or three dimensions, shown schematically in Fig. 2.3. Suppose that only one parameter τ defines the transformation T, as shown in Fig. 2.3. Then, the mapping $T : x \to x_\tau(x)$, $x \in \Omega$, is given by

$$\left.\begin{aligned} x_\tau &\equiv T(x,\tau) \\ \Omega_\tau &\equiv T(\Omega,\tau) \end{aligned}\right\} \tag{2.46}$$

where

$$T(x,\tau) = x + \tau V(x) \tag{2.47}$$

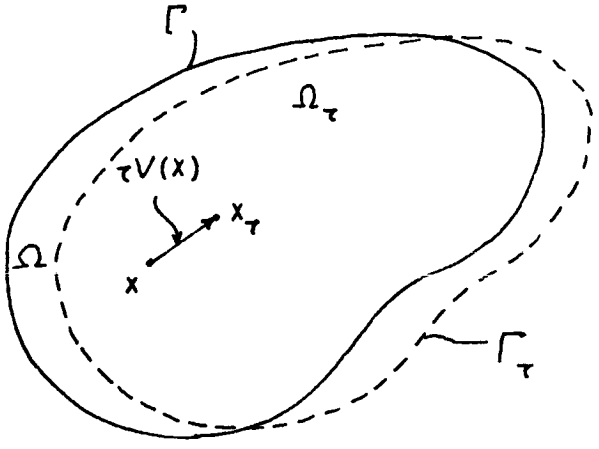

Figure 2.3 Variation of Domain

Variations of the domain Ω by the design velocity field $V(x)$ are denoted as $\Omega_\tau = T(\Omega,\tau)$ and the boundary of Ω_τ is denoted as Γ_τ.

Suppose $z_\tau(x_\tau)$ is a smooth classical solution of the formal operator equation on the deformed domain Ω_τ,

$$\left.\begin{aligned} \bar{A}z_\tau &= f \quad , \quad x \in \Omega_\tau \\ z_\tau &= 0 \quad , \quad x \in \Gamma_\tau \end{aligned}\right\} \tag{2.48}$$

Then, the mapping $z_\tau(x + \tau V(x))$ is defined on Ω and $z_\tau(x_\tau)$ in Ω_τ depends on τ in two ways. First, it is the solution of the boundary-value problem on Ω_τ. Second, it is evaluated at a point x_τ that moves with τ. The pointwise material derivative (if it exists) at $x \in \Omega$ is defined as

$$\dot{z}(x) = \frac{d}{d\tau} z_\tau(x+\tau V(x))\Big|_{\tau=0} = \lim_{\tau\to 0} \frac{z_\tau(x + \tau V(x)) - z(x)}{\tau} \tag{2.49}$$

If z_τ has a regular extension to a neighborhood U_τ of $\bar{\Omega}_\tau$, denoted as z_τ, then one has

$$\dot{z}(x) = z'(x) + \nabla z^T V(x) \tag{2.50}$$

where

$$z'(x) \equiv \lim_{\tau\to 0} \frac{z_\tau(x) - z(x)}{\tau}$$

is partial derivative.

Let $z_\tau(x_\tau)$ be the solution of the following variational equation on the deformed domain Ω_τ:

$$a_\tau(z_\tau, \bar{z}_\tau) = \iint_{\Omega_\tau} c(z_\tau, \bar{z}_\tau)d\Omega = \ell_\tau(\bar{z}_\tau) \tag{2.51}$$

for all $\bar{z}_\tau \in Z_\tau$, where $Z_\tau \subset H^m(\Omega_\tau)$ is the space of kinematically admissible displacements and $c(.,.)$ is a bilinear mapping that can be obtained by integration of the formal operator equation by parts. Then, $z_\tau \in Z_\tau \subset H^m(\Omega_\tau)$.

One attractive feature of the partial derivative is that, with smoothness assumptions, it commutes with derivatives with respect to x, because they are derivatives with respect to independent variables [5,72]; i.e.,

$$\left(\frac{\partial z}{\partial z_i}\right)' = \frac{\partial}{\partial x_i} z' \quad , \quad i = 1,2,3 \tag{2.52}$$

Consider now a general functional that is defined as an integration over Ω_τ,

$$\bar{\Psi} = \iint_{\Omega_\tau} F_\tau(x_\tau)d\Omega_\tau \tag{2.53}$$

where F_τ is a regular function defined on Ω_τ. The material derivative of Eq. 2.53 at Ω is [5]

$$\bar{\Psi}' = \iint_{\Omega} [F'(x) + \mathrm{div}(F(x)V(x))]d\Omega \tag{2.54}$$

Now, if Ω is C^k regular [5], one has

$$\bar{\Psi}' = \iint_{\Omega} F'(x)d\Omega + \int_{\Gamma} F(x)(V^T n)d\Gamma \tag{2.55}$$

It is shown in Ref. 5 that if a general domain functional $\bar{\Psi}$ has a gradient at Ω and Ω has C^{k+1} regularity, then one need consider only

the normal component ($V^T n$) of the velocity field on the boundary for derivative calculations. Similarly, one can obtain the material derivative calculations.

When one considers built-up structure shape optimization, the boundary movement of one structural component causes movement of the entire domain of an attached structural component at their interface. Special interest is directed to the material derivative of a general functional defined as an integration over a specific domain $\tilde{\Omega}$ (restricted to two-dimensional structures), where $\tilde{\Omega}$ moves in the normal direction to the plane (or line) on which $\tilde{\Omega}$ is defined. It is presumed that the normal to the plane (or line) where this specific domain $\tilde{\Omega}$ is defined is parallel to rectangular coordinate axes and the velocity field is $V = [V^x, V^y, V^z]^T$ at $\tilde{\Omega}$.

By the nature of the specific domain, one has $V^x_y = V^x_z = 0$ on the domain $\tilde{\Omega}$ that is on the y-z plane, $V^y_x = V^y_z = 0$ on the domain $\tilde{\Omega}$ that is on the x-z plane and $V^z_x = V^z_y = 0$ on the domain $\tilde{\Omega}$ that is on the x-y plane.

Consider now a general functional that is defined as an integration over $\tilde{\Omega}$,

$$\tilde{\Psi} = \iint_{\tilde{\Omega}} G d\Omega \tag{2.56}$$

where G is a regular function defined on $\tilde{\Omega}$. The material derivative is [5]

$$\tilde{\psi}' = \iint_{\tilde{\Omega}} (G' + G_N V^N) d\Omega + \int_{\tilde{\Gamma}} G(V^T n) d\Gamma \tag{2.57}$$

where N denotes the direction of domain movement.

Comparing the material derivative formula of Eq. 2.57 with the material derivative formula of Eq. 2.55, one can note that the second term in the domain integral of Eq. 2.57 is added to Eq. 2.55, which is regarded as the effect of domain movement normal to the plane (or line) on which $\tilde{\Omega}$ is defined.

2.5 Static Design Sensitivity Analysis

The variational method for design sensitivity analysis with respect to both design variable and shape changes is now considered, using the general variational formulation presented in Section 2.3, to obtain expressions for design sensitivity of functionals with respect to combined design variation. Differentiability of state with respect to design and existence of the material derivative $\dot{z}$ are presumed and are used in this section to derive an adjoint variable method for design sensitivity analysis of quite general functionals. An adjoint problem that is closely related to the original structural problem is obtained and explicit formulas for structural response design sensitivity are obtained.

2.5.1 Calculation of First Variations

Consider the variational form of the built-up structural equation in Eq. 2.39, repeated here as

$$a_{u,\Omega}(z,\bar{z}) = \ell_{u,\Omega}(\bar{z}) \tag{2.58}$$

for all $\bar{z} \in Z$. The objective is to use this variational equation to obtain a relationship between variations in design functions and shape and the resulting variation in state of the system.

To simplify notation, consider the deformed domain due to a velocity field V, written as

$$\Omega_\tau \equiv \{x_\tau \in R^n : x_\tau = x + \tau V(x),\ x \in \Omega\} \tag{2.59}$$

Assuming that the energy bilinear form is differentiable with respect to design functions and shape, the first variation with respect to both shape and design functions gives [5]

$$\begin{aligned}[a(z,\bar{z})]' \equiv\ & a'_{\delta u,\Omega}(z,\bar{z}) + a'_{u,V}(z,\bar{z}) + a_{u,\Omega}(\dot{z},\bar{z}) \\ =\ & \Big[\sum_{i=1}^{r} a'_{\delta u^i,\Omega^i}(z^i,\bar{z}^i) + a'_{\delta b}(q,\bar{q})\Big] + \sum_{i=1}^{r} a'_{u^i,V^i}(z^i,\bar{z}^i) \\ & + \sum_{i=1}^{r} a_{u^i,\Omega^i}(\dot{z}^i,\bar{z}^i)\end{aligned} \tag{2.60}$$

where V^i is the velocity field on Ω^i. Note here that the lengths of trusses are treated as design variables. The prime notation here plays the role of the first variation of the calculus of variations, with respect to explicit dependence of the energy form $a_{u,\Omega}$ on design and shape. This first variation is presumed to be linear in δu. Hence it is the Frechet derivative of $a_{u,\Omega}$ with respect to design and shape, evaluated in the direction δu. This notation is chosen to display clearly which variables are held fixed and which are varying in the terms that arise.

Similarly, one may take the first variation of the load linear form to obtain

$$[\ell(\bar{z})]' \equiv \ell'_{\delta u,\Omega}(\bar{z}) + \ell'_{u,V}(\bar{z})$$

$$= [\sum_{i=1}^{r} \ell'_{\delta u^i,\Omega^i}(\bar{z}^i) + f'_{\delta b}(\bar{q})] + \sum_{i=1}^{r} \ell'_{u^i,V^i}(\bar{z}^i) \qquad (2.61)$$

As in the case of the energy bilinear form, the variation of the load linear form is also presumed to be linear in δu.

With this notation, and denoting the solution of Eq. 2.58 on the deformed domain and varied design as $z(\tau)$, one may differentiate both sides of Eq. 2.58 with respect to τ and evaluate the result at $\tau = 0$, using the notation of Eqs. 2.60 and 2.61, to obtain

$$a_{u,\Omega}(\dot{z},\bar{z}) + a'_{\delta u,\Omega}(z,\bar{z}) + a'_{u,V}(z,\bar{z}) = \ell'_{\delta u,\Omega}(\bar{z}) + \ell'_{u,V}(\bar{z}) \qquad (2.62)$$

for all $\bar{z} \in Z$, where $\dot{z}$ is the sum of the first variations due to design and shape change and Z is the space of kinematically admissible displacements. Note that this equation is valid for arbitrary virtual displacements that are consistent with the constraints, so if the energy bilinear form is strongly elliptic, Eq. 2.62 uniquely determines $\dot{z}$, once δu and V are specified. Explicit solution of this equation for $\dot{z}$ as a function of δu and V, however, is not generally possible.

Consider a general functional that defines performance of a built-up structure, of the form

$$\Psi \equiv \Psi_{u,\Omega}(z)$$

$$= \sum_{i=1}^{r} \iint_{\Omega^i} g^i(z^i, \nabla z^i, z^i_{jk}, u^i) d\Omega + h(b,q) \tag{2.63}$$

where the function g is continuously differentiable with respect to its arguments, and $z_{jk} = \partial^2 z / \partial x_j \partial x_k$, j,k=1-3, denotes the second derivative of z. Note that in some structural components, arguments of the function g can be only first derivatives of z, in which the second derivative of z in Eq. 2.63 is presumed to be disregarded.

Taking the total variation of this functional for each component of a structure, one has

$$\Psi' = \frac{d}{d\tau} \Psi_{u+\tau\delta u, \Omega_\tau}(z(\tau))\Big|_{\tau=0}$$

$$= \sum_{i=1}^{r} \iint_{\Omega^i} [g^i_{z^i} \dot{z}^i + g_{\nabla z^i} \nabla \dot{z}^i + \sum_{j,k=n_1}^{n_2} (g^i_{z^i_{jk}} \dot{z}^i_{jk})$$

$$- g^i_{z^i} (\nabla z^{iT} V^i) - g^i_{\nabla z^i} \nabla (\nabla z^{iT} V^i)$$

$$- \sum_{j,k=n_1}^{n_2} g^i_{z^i_{jk}} (\nabla z^{iT} V^i)_{jk} - g^i_{z^i} (z^i_N V^{iN}) - g^i_{\nabla z^i} \nabla (z^i_N V^{iN})$$

$$- \sum_{j,k=n_1}^{n_2} g^i_{z^i_{jk}} (z^i_N V^{iN})_{jk} + g^i_N V^{iN} + g^i_{u^i} \delta u^i] d\Omega$$

$$+ \sum_{i=1}^{r} \int_{\Gamma^i} g^i (V^{iT} n^i) d\Gamma + \frac{\partial h}{\partial b} \delta b + \frac{\partial h}{\partial q} \dot{q} \tag{2.64}$$

where

$$\dot{z}^i = z^{i'} + \nabla z^{i^T} v^i + z_N^i v^{iN} \tag{2.65}$$

and n^i is the outward unit normal vector for each domain Ω^i. Note that terms including v^N in Eq. 2.65 are due to domain movement effects of a one- or two-dimensional structural component.

Rewriting the eighth and ninth terms in the domain integral of Eq. 2.64, one has

$$g^i_{\nabla z^i} \nabla(z_N^i v^{iN}) = g^i_{\nabla z^i} [(\nabla z_N^i) v^{iN} + z_N^i (\nabla v^{iN})] \tag{2.66}$$

and

$$\sum_{j,k=n_1}^{n_2} g^i_{z^i_{jk}} (z_N^i v^{iN})_{jk} = \sum_{j,k=n_1}^{n_2} g^i_{z^i_{jk}} [(z_N^i)_{jk} v^{iN} + z_N^i (v^{iN})_{jk}] \tag{2.67}$$

respectively.

The second terms on the right sides of Eqs. 2.66 and 2.67 vanish, since $\nabla v^{iN} = 0$ and $(v^{iN})_{jk} = 0$, respectively, due to the fact that v^{iN} is constant on Ω^i.

Four terms in the domain integral of Eq. 2.64 cancel; i.e.,

$$[-g^i_{z^i} z_N^i - g^i_{\nabla z^i} \nabla z_N^i - \sum_{j,k=n_1}^{n_2} g^i_{z^i_{jk}} (z_N^i)_{jk} + g^i_N] v^{iN} = 0 \tag{2.68}$$

Then, Eq. 2.64 becomes

$$\begin{aligned} \Psi' = \sum_{i=1}^{r} \iint_{\Omega^i} & [g^i_{z^i} \dot{z}^i + g^i_{\nabla z^i} \nabla \dot{z}^i + \sum_{j,k=n_1}^{n_2} (g^i_{z^i_{jk}} \dot{z}^i_{jk}) - g^i_{z^i} (\nabla z^{i^T} v^i) \\ & - g^i_{\nabla z^i} \nabla (\nabla z^{i^T} v^i) - \sum_{j,k=n_1}^{n_2} g^i_{z^i_{jk}} (\nabla z^{i^T} v^i)_{jk} + g^i_{u^i} \delta u^i] d\Omega \\ & + \sum_{i=1}^{r} \int_{\Gamma^i} g^i (v^{i^T} n^i) d\Gamma + \frac{\partial h}{\partial b} \delta b + \frac{\partial h}{\partial q} \dot{q} \end{aligned} \tag{2.69}$$

In order to take advantage of this result, one needs to write terms on the right of Eq. 2.69 explicitly in terms of δu and V. Since $\dot{z}$ cannot generally be determined explicitly from Eq. 2.62, one must resort to a technique such as the adjoint variable method to achieve the desired result.

2.5.2 Adjoint Variable Method

In order to treat terms on the right of Eq. 2.69, one may define an adjoint variational equation by replacing $\dot{z}$ in the term on the right of Eq. 2.69, by a virtual displacement $\bar{\lambda}$ and equate the result to the energy bilinear form, evaluated at the adjoint variable λ; i.e.,

$$a_{u,\Omega}(\lambda,\bar{\lambda}) = \sum_{i=1}^{r} \iint_{\Omega^i} [g^i_{z^i} \bar{\lambda}^i + g^i_{\nabla z^i} \nabla\bar{\lambda}^i + \sum_{j,k=n_1}^{n_2} g^i_{z^i_{jk}} \bar{\lambda}^i_{jk}]d\Omega + \frac{\partial h}{\partial q} \bar{p} \tag{2.70}$$

for all $\bar{\lambda} \in Z$, where $\lambda = [\lambda^1, \lambda^2, \ldots, \lambda^r, p]^T$. Presuming that the energy bilinear form is strongly elliptic, this equation uniquely determines λ, if the terms on the right are continuous linear forms in $\bar{\lambda}$.

Since $\dot{z}$ satisfies the kinematic admissibility conditions, one may evaluate Eq. 2.70 at $\bar{\lambda} = \dot{z}$ and Eq. 2.62 at $\bar{z} = \lambda$, to obtain

$$\sum_{i=1}^{r} \iint_{\Omega^i} [g^i_{z^i} \dot{z}^i + g^i_{\nabla z^i} \nabla\dot{z}^i + \sum_{j,k=n_1}^{n_2} g^i_{z^i_{jk}} \dot{z}^i_{jk}]d\Omega + \frac{\partial h}{\partial q} \dot{q}$$

$$= a_{u,\Omega}(\lambda,\dot{z}) = a_{u,\Omega}(\dot{z},\lambda) = \ell'_{\delta u,\Omega}(\lambda) + \ell'_{u,V}(\lambda)$$

$$- a'_{\delta u,\Omega}(z,\lambda) - a'_{u,V}(z,\lambda) \tag{2.71}$$

Substituting this result into Eq. 2.69 and collecting terms that are associated with variations in the design function and the velocity field, one has the total differential of the functional of Eq. 2.63, written explicitly in terms of design function variation and shape variation, as

$$\psi' = \{ \sum_{i=1}^{r} \iint_{\Omega_i} g^i_{u^i} \delta u^i d\Omega + \frac{\partial h}{\partial b} \delta b + \ell'_{\delta u, \Omega}(\lambda) - a'_{\delta u, \Omega}(z, \lambda) \}$$

$$+ \{ \sum_{i=1}^{r} \int_{\Gamma_i} g^i (V^i{}^T n^i) d\Gamma - \sum_{i=1}^{r} \iint_{\Omega_i} [g^i_{z^i} (\nabla z^i{}^T V^i)$$

$$+ g^i_{\nabla z^i} \nabla (\nabla z^i{}^T V^i) + \sum_{j,k=n_1}^{n_2} g^i_{z^i_{jk}} (\nabla z^i{}^T V^i)_{jk}] d\Omega$$

$$+ \ell'_{u,V}(\lambda) - a'_{u,V}(z, \lambda) \} \qquad (2.72)$$

The differentials of the linear and bilinear forms on the right side of Eq. 2.72 may be evaluated, using the expressions of Eqs. 2.60 and 2.61 and the results of each distributed component and truss, to get explicit formulas. Evaluating the terms in the second bracket of Eq. 2.72 requires manipulations to derive identities for transformation of the domain integral that involves velocity to a boundary integral, using integration by parts and boundary/interface conditions. This will be done in Chapter 3. Note that evaluation of the explicit design sensitivity formula requires solution of Eq. 2.70 for the adjoint variable and evaluation of functionals involving both the state z and adjoint variable λ. As will be seen in numerical examples, these

calculations are direct and take full advantage of the finite element method for solving both the state and adjoint equations, requiring only evaluation of the solution of the same set of finite element equations with different right sides.

2.6 Eigenvalue Design Sensitivity Analysis

One may now determine eigenvalue design sensitivity of a built-up structure, due to variation in both design variables and shape. No adjoint variable is required in eigenvalue design sensitivity calculation. Eigenvalue sensitivity can be expressed directly in terms of eigenvectors of the eigenvalue problem and variations in the eigenvalue bilinear forms. Differentiability of simple (non-repeated) eigenvalues is presumed to be used to obtain explicit formulas, utilizing the material derivative formulas for simple eigenvalue sensitivity analysis.

2.6.1 Calculation of First Variations

Consider the eigenvalue problems for vibration and buckling of a built-up structure that is described by a variational equation of the form of Eq. 2.45,

$$a_{u,\Omega}(y,\bar{y}) = \zeta d_{u,\Omega}(y,\bar{y}) \tag{2.73}$$

for all $\bar{y} \in Z$, where Z is the space of kinematically admissible displacements. Since Eq. 2.73 is homogeneous in y, a normalizing condition must be added to uniquely define the eigenfunction. The

normalizing condition employed is

$$d_{u,\Omega}(y,y) = 1 \tag{2.74}$$

The energy bilinear form on the left side of Eq. 2.73 is the same as the bilinear form in static problems treated in Section 2.5. Therefore, it has the same differentiability properties discussed there. The bilinear form $d_{u,\Omega}$ on the right side of Eq. 2.73 represents mass effects in vibration problems and geometric effects in buckling. In most cases, it is even more regular than the energy bilinear form in its dependence on design and eigenfunction. Since both bilinear forms in Eq. 2.73 depend on the design variable u and shape Ω, it is clear that the eigenvalue ζ also depends on these quantities. The objective here is to use this variational formulation to obtain design sensitivity of ζ to variations in the design function and shape. Using the notation of Eq. 2.59 for perturbation of the domain Ω, one may calculate the design variation of the bilinear form on the right side of Eq. 2.73 as [5]

$$\begin{aligned}[d(y,\bar{y})]' &\equiv d'_{\delta u,\Omega}(y,\bar{y}) + d'_{u,V}(y,\bar{y}) + d_{u,\Omega}(\dot{y},\bar{y}) \\ &= \Big[\sum_{i=1}^{r} d'_{\delta u^i,\Omega^i}(y^i,\bar{y}^i) + d'_{\delta b}(s,\bar{s})\Big] + \sum_{i=1}^{r} d'_{u^i,V^i}(y^i,\bar{y}^i) \\ &\quad + \sum_{i=1}^{r} d_{u^i,\Omega^i}(\dot{y}^i,\bar{y}^i)\end{aligned} \tag{2.75}$$

where $y = [y^1, y^2, \ldots, y^r, s]^T$. This notation parallels that of Eq. 2.60, which remains valid for design variation of the energy bilinear form on the left side of Eq. 2.73.

2.6.2 Eigenvalue Design Sensitivity

Presuming differentiability of the eigenvalue ζ and eigenfunction y with respect to design and shape, supported by the proofs presented in Ref. 5, one may take the total derivative of both sides of Eq. 2.73 to obtain the formal relationship

$$a_{u,\Omega}(\dot{y},\bar{y}) + a'_{\delta u,\Omega}(y,\bar{y}) + a'_{u,V}(y,\bar{y}) = \zeta' d_{u,\Omega}(y,\bar{y}) + \zeta d_{u,\Omega}(\dot{y},\bar{y}) + \zeta d'_{\delta u,\Omega}(y,\bar{y}) + \zeta d'_{u,V}(y,\bar{y}) \tag{2.76}$$

for all $\bar{y} \in Z$. One may evaluate this equation at $\bar{y} = y$, using Eq. 2.74, to obtain

$$\zeta' = [a'_{\delta u,\Omega}(y,y) - \zeta d'_{\delta u,\Omega}(y,y)] + [a'_{u,V}(y,y) - \zeta d'_{u,V}(y,y)] - [a_{u,\Omega}(\dot{y},y) - \zeta d_{u,\Omega}(\dot{y},y)] \tag{2.77}$$

Using symmetry of the two bilinear forms and $\dot{y} \in Z$, Eq. 2.73 implies that the third term on the right of Eq. 2.77 is zero, yielding the result

$$\zeta' = [a'_{\delta u,\Omega}(y,y) - \zeta d'_{\delta u,\Omega}(y,y)] + [a'_{u,V}(y,y) - \zeta d'_{u,V}(y,y)] \tag{2.78}$$

The differentials of the bilinear forms on the right side of Eq. 2.78 may be evaluated, using the expressions of Eqs. 2.60 and 2.75 and results for each distributed component and the truss, to get explicit design senstivity formulas. As in the static case, finding expressions in the second bracket of Eq. 2.78 for shape design sensitivity will be done in Chapter 3. Note that evaluation of the

design sensitivity of a simple eigenvalue given by Eq. 2.78 is explicit in terms of the eigenfunction y and does not require solution of a separate adjoint problem.

CHAPTER 3

A UNIFIED METHOD FOR SHAPE DESIGN SENSITIVITY ANALYSIS OF BUILT-UP STRUCTURES

3.1 Introduction

The technique employed in shape design sensitivity analysis of structural components [5] and built-up structures requires integrations by parts and manipulations to derive identities for transformation of domain integrals that involve velocity to boundary integrals. The integrations by parts that are required to achieve this objective depend on the nature of the terms arising in the integral, hence on the types of structural components involved. Furthermore, boundary and interface conditions are needed to obtain the final shape design sensitivities. In this chapter, standard formulas are derived for each structural component type (beam, plate, plane elastic solid, etc.) to obtain boundary integrals over the component boundary that involve only normal movement of the boundary of that component. Since built-up structures are defined as structures in which components intersect along common boundaries, contributions from each of the components that interface at the boundary may be accumulated to obtain the desired result for the built-up structure.

A guideline to be used in identifying types of components that may be interfaced and the specific character of the interface conditions will be the structural finite element technique. Standard finite

element interface conditions that are employed in analysis of built-up structures include definition of interfacing conditions that must be imposed in finite element modelling of a structure. The interface conditions that define the space of kinematically admissible displacement fields define the interface boundary conditions that are used in carrying out the integration by parts to obtain standard design sensitivity formulas for each structural component. Attention will be paid to this aspect of consistency of built-up structural shape design sensitivity analysis, with an eye toward unifying a practical analytical formulation that is consistent with the finite element modelling technique.

Basic shape design sensitivity forms for built-up structures that involve up to two dimensional structural components such as beams, plates and plane elastic solids are obtained in Section 3.2. In Section 3.3, analytical examples are used to obtain shape design sensitivity forms for typical built-up structural models. These examples demonstrate the unified method of shape design sensitivity analysis that applies to practical built-up structures and yield formulas that may be used in a variety of applications.

3.2 Basic Shape Design Sensitivity Forms for Built-Up Structures

The first bracket of Eq. 2.72 for static response and the first bracket of Eq. 2.78 for eigenvalues are simply explicit derivatives of structural response measures with respect to a conventional design variable u (cross-sectional area or thickness). In this chapter,

analytical design sensitivity analysis for shape variation is considered, to evaluate the remaining terms of Eqs. 2.72 and 2.78. Hence, the conventional design variable u is suppressed in this chapter. Further, even though there is self weight, in addition to externally applied load, and the self weight will depend explicitly on the design, the applied load is expressed only as f(x) in this chapter. Shape design sensitivity forms are obtained for built-up structures that involve beams, plates and plane elastic solids.

Rewriting shape design sensitivity terms in the second brackets of Eqs. 2.72 and 2.78, one obtains

$$\psi' = \sum_{i=1}^{r} \int_{\Gamma^i} g^i (V^{i^T} n^i) d\Gamma - \sum_{i=1}^{r} \iint_{\Omega^i} [g^i_{z^i} (\nabla z^{i^T} V^i) + g^i_{\nabla z^i} \nabla (\nabla z^{i^T} V^i) + \sum_{j,k=n_1}^{n_2} g^i_{z^i_{jk}} (\nabla z^{i^T} V^i)_{jk}] \, d\Omega + \ell'_{u,V}(\lambda) - a'_{u,V}(z,\lambda) \qquad (3.1)$$

for static response and

$$\zeta' = a'_{u,V}(y,y) - \zeta d_{u,V}(y,y) \qquad (3.2)$$

for the eigenvalue problem, respectively.

3.2.1 Static Shape Design Sensitivity Forms

Rewriting the variational equation of Eq. 2.51 on a deformed domain, one has

$$a_\tau(z_\tau, \bar{z}_\tau) \equiv \sum_{i=1}^{r} \iint_{\Omega_\tau^i} c(z_\tau^i, \bar{z}_\tau^i) d\Omega = \sum_{i=1}^{r} \iint_{\Omega_\tau^i} f^{i^T} \bar{z}_\tau^i d\Omega \equiv \ell_\tau(\bar{z}_\tau) \qquad (3.3)$$

for all $\bar{z}_\tau \in Z_\tau$. Suppose that the bilinear form in Eq. 3.3 is differentiable with respect to shape and note that the material derivative $\dot{z}$ depends on the direction V (velocity field).

Taking the material derivative of both sides of Eq. 3.3, with conventional design fixed, using Eq. 2.57, and noting that the partial derivatives with respect to τ and x commute with each other, one has

$$[a(z,\bar{z})]' \equiv a'_{u,V}(z,\bar{z}) + z(\dot{z},\bar{z}) = [\ell(\bar{z})]' \tag{3.4}$$

for all $\bar{z} \in Z$, where

$$[a(z,\bar{z})]' = \sum_{i=1}^{r} \iint_{\Omega^i} [c(z^{i'},\bar{z}^i) + c\,(z^i,z^{-i})' + (c(z^i,z^{-i}))_N V^{iN}]d\Omega$$

$$+ \sum_{i=1}^{r} \int_{\Gamma^i} c(z^i,\bar{z}^i)\,(V^{iT} n^i)d\Gamma \tag{3.5}$$

and

$$[\ell(\bar{z})]' = \sum_{i=1}^{r} \iint_{\Omega^i} [f^{iT}\bar{z}^{i'} + (f^{iT}\bar{z}^i)_N V^{iN}]d\Omega$$

$$+ \sum_{i=1}^{r} \int_{\Gamma^i} f^{iT}\bar{z}^i\,(V^{iT}_n i)d\Gamma \tag{3.6}$$

In Eqs. 3.5 and 3.6, terms involving V^N represent the effect of domain movement in the normal direction to each domain defined, as discussed in Section 2.4. The fact that the partial derivatives of the coefficients that depend on conventional design in the bilinear mapping c(.,.) are zero has been used in Eq. 3.5 and f' = 0 has been used in Eq. 3.6, because they do not depend explicitly on τ. For $\bar{z}_\tau$, one can take $\bar{z}_\tau(x+\tau V(x)) = \bar{z}(x)$; i.e., choose $\bar{z}$ as constant on the line

$x_\tau = x + \tau V(x)$. Then, $\bar{z}_\tau$ is an arbitrary element of $H^m(\Omega_\tau)$ that satisfies kinematic boundary conditions on Γ_τ. In this case, using Eq. 2.65, one has

$$\dot{\bar{z}}^i = \bar{z}^{i\prime} + \nabla \bar{z}^{i^T} V^i + \bar{z}^i_N V^{iN} = 0 \tag{3.7}$$

where ∇ is defined in the local coordinate system.

From Eqs. 3.4 to 3.6, one obtains, using Eqs. 2.65 and 3.7,

$$\begin{aligned} a'_{u,V}(z,\bar{z}) = - \sum_{i=1}^{r} \iint_{\Omega^i} [c(\nabla z^{i^T} V^i + z^i_N V^{iN}, \bar{z}^i) \\ + c(z^i, \nabla z^{i^T} V^i + \bar{z}^i_N V^{iN}) - (c(z^i, \bar{z}^i))_N V^{iN}] d\Omega \\ + \sum_{i=1}^{r} \int_{\Gamma^i} c(z^i, \bar{z}^i)(V^{i^T} n^i) d\Gamma \end{aligned} \tag{3.8}$$

and

$$\begin{aligned} \ell'_{u,V}(\bar{z}) = - \sum_{i=1}^{r} \iint_{\Omega^i} [f^{i^T}(\nabla \bar{z}^{i^T} V^i + \bar{z}^i_N V^{iN}) - (f^{i^T} \bar{z}^i)_N V^N] d\Omega \\ + \sum_{i=1}^{r} \int_{\Gamma} f^{i^T} \bar{z}^i (V^{i^T} n^i) d\Gamma \end{aligned} \tag{3.9}$$

respectively. As discussed in Chapter 2, $\nabla V^{iN} = 0$ is presumed to obtain Eqs. 3.8 and 3.9.

The final form of Eq. 3.1 becomes

$$\begin{aligned} \Psi' = \sum_{i=1}^{r} \iint_{\Omega^i} [c(\nabla z^{i^T} V^i, \lambda^i) + c(z^i, \nabla \lambda^{i^T} V^i) - f^{i^T}(\nabla \lambda^{i^T} V^i) \\ - g^i_{z^i}(\nabla z^{i^T} V^i) - g^i_{\nabla z^i} \nabla(\nabla z^{i^T} V^i) - \sum_{j,k=n_1}^{n_2} g^i_{z^i_{jk}} (\nabla z^{i^T} V^i)_{jk}] d\Omega \\ + \sum_{i=1}^{r} \int_{\Gamma^i} [g^i - c(z^i, \lambda^i) + f^{i^T} \lambda^i](V^{i^T} n^i) d\Gamma \end{aligned} \tag{3.10}$$

where it is assumed that $f_N^i = 0$, and the integrals over Ω^i can be transformed to boundary integrals by integrating by parts and using the formal operator equations. This is essential in shape design sensitivity analysis and remains to be done in the following section.

3.2.2 Eigenvalue Shape Design Sensitivity Forms

Writing the variational eigenvalue equation on a deformed domain, one has

$$a_\tau(y_\tau,\bar{y}_\tau) \equiv \sum_{i=1}^{r} \iint_{\Omega_\tau^i} c(y_\tau^i,\bar{y}_\tau^i)d\Omega = \zeta_\tau \sum_{i=1}^{r} \iint_{\Omega_\tau^i} y_\tau^{iT} M^i \bar{y}_\tau d\Omega$$

$$\equiv \zeta_\tau d(y_\tau,\bar{y}_\tau) \tag{3.11}$$

for all $\bar{y}_\tau \in Z_\tau$, with the normalizing condition of Eq. 2.74.

Taking the material derivative of both sides of Eq. 3.11, using Eq. 2.57, and noting that the partial derivatives with respect to τ and x commute with each other, one has

$$[a(y,\bar{y})]' = \zeta' d(y,\bar{y}) + \zeta[d(y,\bar{y})]' \tag{3.12}$$

for all $\bar{y} \in Z$, where

$$[a(y,\bar{y})]' = \sum_{i=1}^{r} \iint_{\Omega^i} [c(y^{i'},\bar{y}^i) + c(y^i,\bar{y}^{i'}) + (c(y^i,\bar{y}^i))_N V^{iN}]d\Omega$$

$$+ \sum_{i=1}^{r} \int_{\Gamma^i} c(y^i,\bar{y}^i)(V^{iT} n^i)d\Gamma \tag{3.13}$$

and

$$[d(y,\bar{y})]' = \sum_{i=1}^{r} \int_{\Omega^i} [y^{i'^T} M^i \bar{y}^i + y^{i^T} M^i \bar{y}^{i'} + (y^{i^T} M^i \bar{y}^i)_N V^{iN}] d\Omega$$

$$+ \sum_{i=1}^{r} \int_{\Gamma^i} y^{i^T} M^i y^i (V^{i^T} n^i) d\Gamma \qquad (3.14)$$

The third term in the domain integral of Eqs. 3.13 and 3.14, respectively, represents the effect of domain movement, as in static response. As in Eq. 3.5, the fact that the partial derivatives of the coefficients in the bilinear mapping $c(.,.)$ are zero has been used in Eq. 3.13. Also, $M' = 0$ has been used in Eq. 3.14. As in static response, for $\bar{y}_\tau$ one can take $\bar{y}(x_\tau + \tau V(x)) = \bar{y}(x)$. Hence, if $\bar{y} \in Z$ is arbitrary, then $\bar{y}_\tau$ is an arbitrary element of Z_τ. Also, from Eq. 3.7, one has

$$\dot{\bar{y}} = \bar{y}' + \nabla\bar{y}^T V + \bar{y}^i_N V^{iN} = 0 \qquad (3.15)$$

Now Eqs. 3.13 and 3.14, using Eqs. 2.65 and 3.15, become

$$a'_{u,V}(y,\bar{y}) = [a(y,y)]' - a(\dot{y},\bar{y})$$

$$= - \sum_{i=1}^{r} \iint_{\Omega^i} [c(\nabla y^{i^T} V^i + y^i_N V^{iN}, \bar{y}^i) + c(y^i, \nabla\bar{y}^{i^T} V^i + \bar{y}^i_N V^{iN})$$

$$- (c(y^i, \bar{y}^i))_N V^{iN}] d\Omega$$

$$+ \sum_{i=1}^{r} \int_{\Gamma^i} c(y^i, \bar{y}^i)(V^{i^T} n^i) d\Gamma \qquad (3.16)$$

and

$$d'_{u,V}(y,\bar{y}) = [d(y,\bar{y})]' - d(\dot{y},\bar{y})$$

$$= -\sum_{i=1}^{r} \iint_{\Omega^i} [(\nabla y^{i^T} V^i + y_N^i V^{iN})^T M^i \bar{y}^i + y^{i^T} M^i (\nabla \bar{y}^{i^T} V^i + \bar{y}^i{}_N V^{iN})$$

$$- (y^{i^T} M^i \bar{y}^i)_N V^{iN}] d\Omega$$

$$+ \sum_{i=1}^{r} \int_{\Gamma^i} y^{i^T} M^i \bar{y}^i (V^{i^T} n^i) d\Gamma \qquad (3.17)$$

respectively, where it is assumed that $M_N^i = 0$.

Equation 3.12 can now be written as

$$a'_{u,V}(y,\bar{y}) + a(\dot{y},\bar{y}) = \zeta' d(y,\bar{y}) + \zeta d'_{u,V}(y,\bar{y}) + \zeta d(\dot{y},\bar{y}) \qquad (3.18)$$

for all $\bar{y} \in Z$. Since $\bar{y} \in Z$, one may evaluate Eq. 3.18 with $\bar{y} = y$, using symmetry of the bilinear forms, to obtain

$$\zeta' d(y,y) = a'_{u,V}(y,\bar{y}) - \zeta d'_{u,V}(y,\bar{y}) + [a(y,\dot{y}) - \zeta d(y,\dot{y})] \qquad (3.19)$$

Noting that $\dot{y} \in Z$, the term in the bracket on the right of Eq. 3.19 is zero. Furthermore, due to the normalizing condition of Eq. 2.74, one has the simplified equation

$$\zeta' = a'_{u,V}(y,y) - \zeta d'_{u,V}(y,y)$$

$$= \sum_{i=1}^{r} \iint_{\Omega^i} [-2c(y^i, \nabla y^{i^T} V^i) + 2\zeta y^{i^T} M^i (\nabla y^{i^T} V^i)] d\Omega$$

$$+ \sum_{i=1}^{r} \int_{\Gamma^i} [c(y^i,y^i) - \zeta(y^{i^T} M^i y^i)](V^{i^T} n^i) d\Gamma \qquad (3.20)$$

where, as in the static response case, integrals over Ω^i can be transformed to boundary integrals by integrating by parts and using formal eigenvalue differential equations, which remains to be done in the following section.

3.3 Analytical Examples of the Unified Method for Shape Design Sensitivity Analysis

From the basic shape design sensitivity forms in Section 3.2, shape design sensitivity forms for built-up structures that involve beams, plates and plane elastic solids in a variety of configurations are derived in this section by applying the boundary conditions (outside and interface) to the standard forms for structural components of each built-up structural model encountered. Typical outside boundary conditions for structural components are summarized in Table 3.1. Symbols used in Table 3.1 and their physical interpretations are defined in Table 3.2. Final shape design sensitivity forms for static response are obtained for the built-up structural models listed in Fig. 3.1. Throughout the procedure, a general displacement or stress functional that is defined on certain structural component in each built-up structural model is considered to show the unified method for shape design sensitivity analysis. One can notice that the final shape design sensitivity forms are identical, regardless of constraints, with only different right sides of the adjoint equations. Similarly, shape design sensitivity forms can be obtained for the eigenvalue problem, which is not pursued in this section, but is treated in Chapter 5.

Table 3.1 Outside Boundary Conditions for Structural Components

Structural Component		Boundary Conditions	
		Kinematic	Natural
Beam (Bending)	SS	$z = 0$ (3.21)	$\tilde{M}_x = 0$ (3.22)
	C	$z = z_x = 0$ (3.23)	
	Fr		$\tilde{M}_x = \tilde{V}_x = 0$ (3.24)
Beam (Axial)	Fx	$z = 0$ (3.25)	
	Fr		$\tilde{F} = 0$ (3.26)
Plate	SS	$z = 0$ (3.27)	$M_x = M_y = 0$ (3.28)
	C	$z = \nabla z.n = 0$ (3.29)	
	Fr		$M_x = M_y = V_x = V_y = 0$ (3.30)
Plane Elastic Solid	Fx	$z = 0$ (3.31)	
	Fr		$T^i = 0$ (3.32)

* SS: Simply Supported, C: Clamped, Fr: Free, Fx: Fixed

Table 3.2 Definitions of Symbols and Physical Interpretations for Structural Components

Structural Component	Definition of Symbol	Physical Interpretation
Beam (Bending)	$\tilde{M}_x = EIz_{xx}$	Bending moment
	$\tilde{M}_y = EIz_{yy}$	Bending moment
	$\tilde{M}_{xy} = GJz_{xy}$	Twisting moment
	$\tilde{V}_x = (EIz_{xx})_x$	Shear force
	$\tilde{V}_y = (EIz_{yy})_y$	Shear force
Beam (Axial)	$\tilde{F} = EAz_x$	Axial force
Plate	$M_x = -D(z_{xx} + \nu z_{yy})$	Bending moment
	$M_y = -D(z_{yy} + \nu z_{xx})$	Bending moment
	$M_{xy} = -D(1-\nu)z_{xy}$	Corner force, Torsional moment
	$V_x = -D(z_{xxx} + (2-\nu)z_{xyy})$	Effective shear force
	$V_y = -D(z_{yyy} + (2-\nu)z_{xxy})$	Effective shear force
Plane Elastic Solid	$T^i = \sum_{j=x,y} \sigma^{ij}(z)n^j,\ i=x,y$	Traction

3.3.1 Description of Basic Built-Up Structural Models

Figure 3.1 shows basic built-up structural models that consist of trusses, beams, plates, and plane elastic solids, interconnected at the interior or edge (or corner) position. Most real engineering built-up structures can be related to these models. Structural components in each built-up structural model are specified by a, b,.... The domains and outside boundaries of structural components in each built-up structural model are denoted as Ω^i (Ω for a single component) and Γ^i (Γ for a single component), i= a,b,..., respectively. The interfaces are specified as γ for a single interface and γ^i, i=1,2,... for multiple interfaces. For the models listed in Fig. 3.1, it is presumed that all the outside boundaries are fixed and that dimensions and material properties of structural components are given. Interface conditions (kinematic and natural) are defined in Table 3.3 for each model listed in Fig. 3.1. The symbols used in Table 3.3 and their physical interpretations are defined in Table 3.2. The space of kinematically admissible displacement fields Z is then defined as displacements that satisfy all kinematic boundary conditions (outside and interface) for each model encountered.

3.3.1a Beam-Truss Built-Up Structure with Interior Interface

Bending of a clamped beam under lateral load, supported by a pin-jointed truss, shown in Fig. 3.1a, is considered. Effects of torsion and axial deformation of the beam are neglected. Truss length is also presumed to be fixed. This means that the ground supporting position of the truss can move together with the position γ.

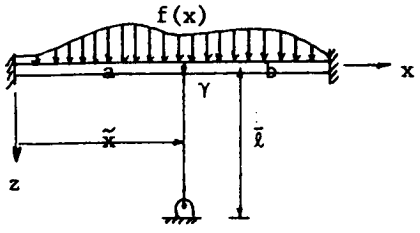

(a) Beam-Truss Built-Up Structure with Interior Interface

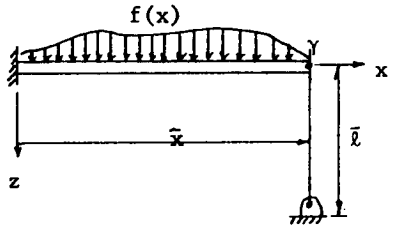

(b) Beam-Truss Built-Up Structure with Edge Interface

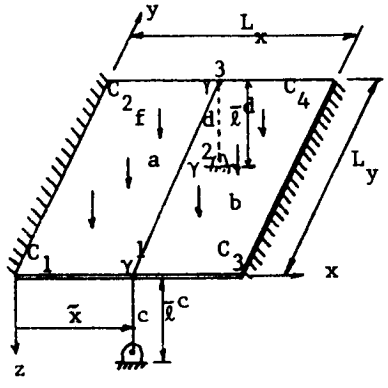

(c) Plate-Truss Built-Up Structure with Edge Interface

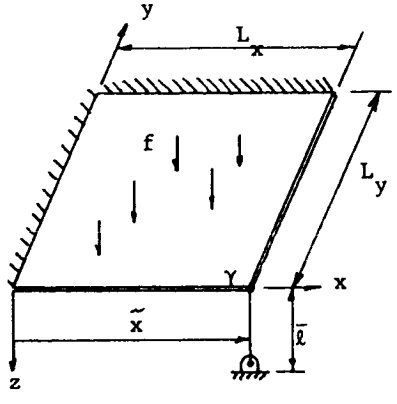

(d) Plate-Truss Built-Up Structure with Corner Interface

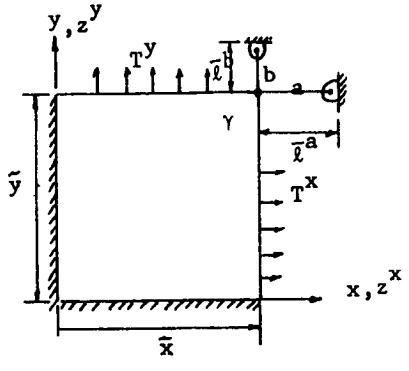

(e) Plane Elastic Solid-Truss Built-Up Structure with Corner Interface

Figure 3.1 Basic Built-Up Structural Model

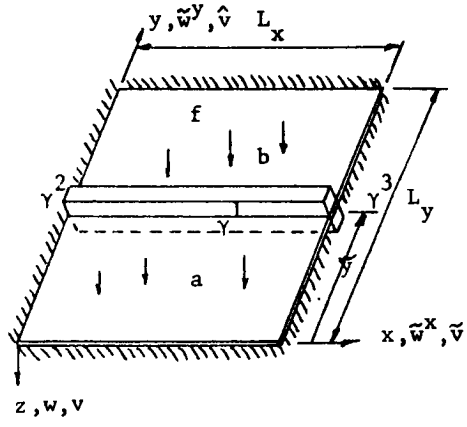

(f) Beam-Plate Built-Up Structure with Interior Interface

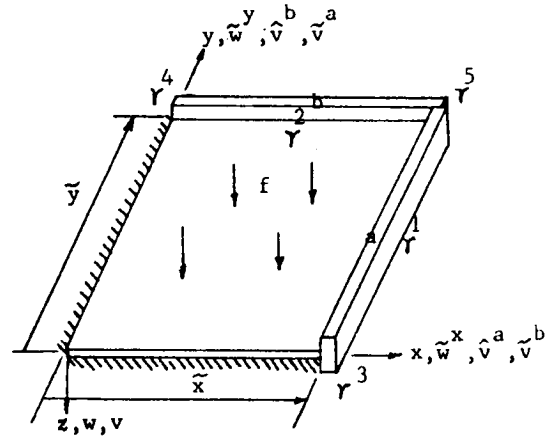

(g) Beam-Plate Built-Up Structure with Edge Interface

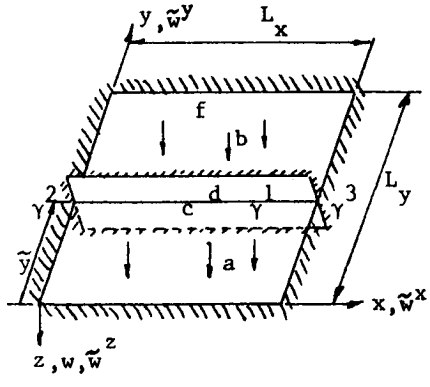

(h) Plane Elastic Solid-Plate Built-Up Structure with Interior Interface

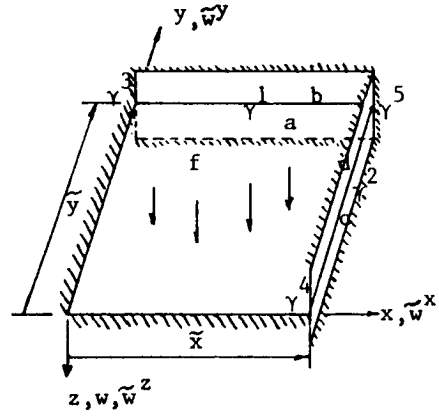

(i) Plane Elastic Solid-Plate Built-Up Structure with Edge Interface

Table 3.3 Interface Conditions between Structural Components for the Built-Up Structural Model

Structural Model	Kinematic		Natural	
Fig. 3.1a	$z^a = z^b = q$ $z_x^a = z_x^b$	$x \in \gamma$ (3.33)	$\tilde{M}^a = \tilde{M}^b$ $\tilde{V}_x^a - \tilde{V}_x^b = -\frac{EA}{\bar{\ell}} q$	$x \in \gamma$ (3.34)
Fig. 3.1b	$z = q$,	$x \in \gamma$ (3.35)	$\tilde{M}_x = 0$ $\tilde{V}_x = -\frac{EA}{\bar{\ell}} q_x$	$x \in \gamma$ (3.36)
Fig. 3.1c	$z^a = z^b$ $z_x^a = z_x^b$	$x \in \gamma^p$, $p = 1\text{-}3$ (3.37)	$M_x^a = M_x^b$ $V_x^a = V_x^b$	$x \in \gamma^2$ (3.40)
	$z^a = z^b = q^c$,	$x \in \gamma^1$ (3.38)	$2M_{xy}^a + 2M_{xy}^b = \frac{EA^c}{\bar{\ell}^c} q^c$,	$x \in \gamma^1$ (3.41)
	$z^a = z^b = q^d$,	$x \in \gamma^3$ (3.39)	$2M_{xy}^a + 2M_{xy}^b = -\frac{EA^d}{\bar{\ell}^d} q^d$,	$x \in \gamma^3$ (3.42)

Table 3.3 Continued

Fig. 3.1d	$z = q \quad , \quad x \in \gamma$	(3.43)	$2M_{xy} = \frac{EA}{\bar{\ell}} q \quad , \quad x \in \gamma$	(3.44)
Fig. 3.1e	$z^x = q^a \ , \quad z^y = q^b \ , \quad x \in \gamma$	(3.45)	$\left.\begin{aligned} T^x(z) &= \frac{EA^a}{\bar{\ell}^a} q^a \\ T^y(z) &= \frac{EA^b}{\bar{\ell}^b} q^b \end{aligned}\right\} \quad x \in \gamma$	(3.46)
Fig. 3.1f	$\left.\begin{aligned} w^a &= w_b = v \\ w_y^a &= w_y^b = \theta \end{aligned}\right\} \quad x \in \gamma^p \ , \quad p = 1\text{-}3$	(3.47)	$\left.\begin{aligned} M_y^a - M_y^b &= -GJv_{xxy} \\ V_y^a - V_y^b &= -(EIv_{xx})_{xx} \end{aligned}\right\} \quad x \in \gamma^1$	(3.49)
			$2M_{xy}^a + 2M_{xy}^b + \tilde{V}_x = 0 \ , \quad x \in \gamma^2$	(3.50)
			$2M_{xy}^a + 2M_{xy}^b + \tilde{V}_x = 0 \ , \quad x \in \gamma^3$	(3.51)

Table 3.3 Continued

Fig. 3.1f Cont	$\left.\begin{aligned} \tilde{w}^{ax} = \tilde{w}^{bx} &= \tilde{v} \\ \tilde{w}^{ay} = \tilde{w}^{by} &= \hat{v} \end{aligned}\right\}$	$x \in \gamma^p$, $p = 1\text{-}3$ (3.48)	$\left.\begin{aligned} T^x(\tilde{w}^a) - T^x(\tilde{w}^b) &= (EA\tilde{v}_x)_x \\ T^y(\tilde{w}^a) - T^y(\tilde{w}^b) &= -(EA\hat{v}_{xx})_{xx} \end{aligned}\right\}$ $x \in \gamma^1$ (3.52)
			$\left.\begin{aligned} T^x(\tilde{w}^a) - T^x(\tilde{w}^b) &= \tilde{F} \\ T^y(\tilde{w}^a) - T^y(\tilde{w}^b) &= -\hat{V}_x \end{aligned}\right\}$ $x \in \gamma^2$ (3.53)
			$\left.\begin{aligned} T^x(\tilde{w}^a) = -T^x(\tilde{w}^b) &= -\tilde{F} \\ T^y(\tilde{w}^a) - T^y(\tilde{w}^b) &= \hat{V}_x \end{aligned}\right\}$ $x \in \gamma^3$ (3.54)
Fig. 3.1g	$\left.\begin{aligned} w &= v^a \\ w_x &= \theta^a \end{aligned}\right\}$	$x \in \bar{\gamma}^p$, $p = 1,3,5$ (3.55)	$\left.\begin{aligned} M_x &= -GJ^a v^a_{xyy} \\ V_x &= -(EI^a v^a_{yy})_{yy} \end{aligned}\right\}$ $x \in \gamma'$ (3.61)

Table 3.3 Continued

Fig. 3.1g Cont

$$\left.\begin{aligned} w &= v^b \\ w_y &= \theta^b \end{aligned}\right\} \quad x \in \gamma^p, \quad p = 2,4,5 \qquad (3.56)$$

$$\left.\begin{aligned} w &= v^a = v^b \\ w_x &= \theta^a = v^b_x \\ w_y &= v^a_y = \theta^b \end{aligned}\right\} \quad x \in \gamma^5$$

$$\tilde{w}^x = \hat{v}^a, \quad \tilde{w}^y = \tilde{v}^a, \quad x \in \gamma^p, \quad p = 1,2,5 \qquad (3.58)$$

$$\left.\begin{aligned} M_y &= -GJ^b v^b_{xxy} \\ V_y &= -(EI^b v^b_{xx})_{xx} \end{aligned}\right\} \quad x \in \gamma^2 \qquad (3.62)$$

$$2M_{xy} + \tilde{V}^a_y = 0, \quad x \in \gamma^3 \qquad (3.63)$$

$$2M_{xy} + \tilde{V}^b_x = 0, \quad x \in \gamma^4 \qquad (3.64)$$

$$\left.\begin{aligned} 2M_{xy} + \tilde{V}^a_y + \tilde{V}^b_x &= 0 \\ \tilde{M}^b_x + \tilde{M}^a_{xy} &= 0 \\ \tilde{M}^a_y + \tilde{M}^b_{xy} &= 0 \end{aligned}\right\} \quad x \in \gamma^5 \qquad (3.65)$$

$$\left.\begin{aligned} T^x(\tilde{w}) &= -(EI^a \hat{v}^a_{yy})_{yy} \\ T^y(\tilde{w}) &= (EA^a \tilde{v}^a_y)_y \end{aligned}\right\} \quad x \in \gamma^1 \qquad (3.66)$$

Table 3.3 Continued

Fig. 3.1g Cont	$\tilde{w}^a = \tilde{v}^b, \quad \tilde{w}^y = \hat{v}^p, \quad x \in \gamma^p \quad p = 2,4,5$	(3.59)	
	$\tilde{v}^a = \hat{v}^b, \quad \hat{v}^a = \tilde{v}^b, \quad x \in \gamma^5$	(3.60)	
	$T^x(\tilde{w}) = (EA^b \tilde{v}^b_x)_x$ $T^y(\tilde{w}) = -(EI^b_{xx} v^b_{xx})$	$x \in \gamma^2$	(3.67)
	$T^x(\tilde{w}) = -\hat{V}^a_y$ $T^y(\tilde{w}) = \tilde{F}^a$	$x \in \gamma^3$	(3.68)
	$T^x(\tilde{w}) = \tilde{F}^b$ $T^y(\tilde{w}) = -\hat{V}^b_x$	$x \in \gamma^4$	(3.69)
	$T^x(\tilde{w}) - \hat{V}^a_y + \tilde{F}^b = 0$ $T^y(\tilde{w}) - \hat{V}^b_x + \tilde{F}^a = 0$	$x \in \gamma^5$	(3.70)

Table 3.3 Continued

Fig. 3.1h	$w^a = w^b = \tilde{w}^{cz} = \tilde{w}^{dz}$ $w_y^a = w_y^b$ } $x \in \gamma^p$, $p = 1\text{-}3$ (3.71) $\tilde{w}^{ax} = \tilde{w}^{bx} = \tilde{w}^{cx} = \tilde{w}^{dx}$ $\tilde{w}^{ay} = \tilde{w}^{by}$ } $x \in \gamma^p$, $p = 1\text{-}3$ (3.72)	$M_y^a = M_y^b$ $V_y^a - V_y^b + T^z(\tilde{w}^c) - T^z(\tilde{w}^d) = 0$ } $x \in \gamma^1$ (3.73) $2M_{xy}^a + 2M_{xy}^b + T^z(\tilde{w}^c) - T^z(\tilde{w}^d) = 0$, $x \in \gamma^2$ (3.74) $-2M_{xy}^a - 2M_{xy}^b + T^z(\tilde{w}^c) - T^z(\tilde{w}^d) = 0$, $x \in \gamma^3$ (3.75) $T^x(\tilde{w}^a) - T^x(\tilde{w}^b) + T^x(\tilde{w}^c) - T^x(\tilde{w}^d) = 0$ $T^y(\tilde{w}^a) = T^y(\tilde{w}^b)$ } $x \in \gamma^p$, $p = 1\text{-}3$ (3.76)
Fig. 3.1i	$w = \tilde{w}^{az} = \tilde{w}^{bx}$ $\tilde{w}^x = \tilde{w}^{ax} = \tilde{w}^{bx}$ } $x \in \gamma^p$, $p = 1,3,5$ (3.77)	$M_y = 0$ $V_y + T^z(\tilde{w}^a) - T^z(\tilde{w}^b) = 0$ } $x \in \gamma^1$ (3.79)

Table 3.3 Continued

Fig. 3.1i Cont	$w = \tilde{w}^{cz} = \tilde{w}^{dz}$ $\tilde{w}^{y} = \tilde{w}^{cy} = \tilde{w}^{dy}$ $\Big\}$ $x \in \gamma^p, \quad p = 2,4,5$ (3.78)	$M_x = 0$ $V_x + T^z(\tilde{w}^c) - T^z(\tilde{w}^d) = 0$ $\Big\}$ $x \in \gamma^2$ (3.80) $2M_{xy} + T^z(\tilde{w}^a) - T^z(\tilde{w}^b) = 0, \quad x \in \gamma^3$ (3.81) $2M_{xy} + T^z(\tilde{w}^c) - T^z(\tilde{w}^d) = 0, \quad x \in \gamma^4$ (3.82) $2M_{xy} + T^z(\tilde{w}^a) - T^z(\tilde{w}^b) + T^z(\tilde{w}^c) - T^z(\tilde{w}^d) = 0,$ $x \in \gamma^5$ (3.83)

The design variable is the position $\tilde{x}$ of the supporting truss, as shown in Fig. 3.1a. The state variable consists of the displacement functions z^i, i=a,b of the beam components and the displacement vector q of the truss components.

Interface conditions are obtained in Table 3.3; i.e., at the interface γ, displacement and slope are continuous (Eq. 3.33), bending moment is continuous and the shear force difference between beam components acts as the load on the supporting truss (Eq. 3.34).

3.3.1b Beam-Truss Built-Up Structure with Edge Interface

Bending of a beam under lateral load with one end clamped and the other end supported by a pin-jointed truss, as shown in Fig. 3.1b, is considered. The same assumptions made in Subsection 3.3.1a are applied to this model.

The design variable is the position $\tilde{x}$ of the supporting truss as shown in Fig. 3.1b, and the state variable is the displacement function z of the beam component and the displacement q of the truss component.

Interface conditions similar to those for Fig. 3.1a are obtained in Table 3.3 (Eqs. 3.35 and 3.36).

3.3.1c Plate-Truss Built-Up Structure with Edge Interface

Bending of a rectangular plate of constant thickness under lateral load with two sides clamped and the other two sides free, supported by pin-jointed trusses at the free edges shown in Fig. 3.1c, is considered. It is presumed that truss lengths are fixed and the boundaries of the plate components are parallel to the coordinate axes.

The design variable is the position $\tilde{x}$ of the supporting trusses as shown in Fig. 3.1c. The state variable consists of displacement functions z^i, i=a,b of the plate components and displacement vectors q^i, i=c,d of the truss components.

The interface conditions are obtained in Table 3.3; i.e., the displacement and slope at the interface γ^i, i=1-3 are continuous (Eqs. 3.37 to 3.39), the bending moment and shear force are continuous at γ^2 (Eq. 3.40), and the difference of corner forces at γ^1 and γ^3 acts as the load on the truss components c and d, respectively (Eqs. 3.41 and 3.42).

3.3.1d Plate-Truss Built-Up Structure with Corner Interface

Bending of a rectangular plate of constant thickness under lateral load with two sides clamped and the other two sides free, supported by a pin-jointed truss at the plate corner as shown in Fig. 3.1d, is considered. The same assumptions made in Subsection 3.3.1c are applied to this model.

The design variable is the position $\tilde{x}$ of the supporting truss as shown in Fig. 3.1d, and the state variable is the displacement function z of the plate component and the displacement q of the truss component.

Interface conditions similar to those for Fig. 3.1c are obtained in Table 3.3 (Eqs. 3.43 and 3.44).

3.3.1e Plane Elastic Solid-Truss Built-Up Structure with Corner Interface

In-plane deformation of a rectangular plane elastic solid under traction with two sides fixed and the other two sides free interconnected by trusses at the corner of plane elastic solid, as shown

in Fig. 3.1e, is considered. It is presumed that the truss lengths are fixed.

The design variables are $\tilde{x}$ and $\tilde{y}$ of the intersecting position as shown in Fig. 3.1e. The state variable consists of displacement functions z^j, j=x,y of the plane elastic solid and displacement vectors q^i, i=a,b of the truss components.

Interface conditions are obtained in Table 3.3; i.e., displacement and traction are continuous at γ (Eqs. 3.45 and 3.46).

3.3.1f Beam-Plate Built-Up Structure with Interior Interface

Bending and in-plane deformation of a clamped beam-plate built-up structure under lateral load, as shown in Fig. 3.1f, are considered. Effects of torsion and axial deformation of the beam component are also considered. In this case, a part of the plate boundaries is the domain of the beam, denoted as γ^1 as shown in Fig. 3.1f. Hence boundary movement of the plate component causes movement of the entire domain of the beam component. It is presumed that the boundaries of plate components are parallel to the coordinate axes.

The design variable is the location $\tilde{y}$ of the beam component. The state variable consists of bending displacements w^i, i=a,b, in-plane displacements $\tilde{w}^{ij}$, i=a,b, j=x,y of the plate components where j is used to specify the direction in in-plane displacement, bending displacements v and $\hat{v}$ of the beam in the z- and y-directions, respectively, and axial displacement $\tilde{v}$ of the beam component. For the corresponding adjoint variable, a bar(-) is employed on top of the state variable as $\bar{w}$, $\bar{\tilde{w}}$, $\bar{v}$, $\bar{\hat{v}}$, and $\bar{\tilde{v}}$ for design sensitivity analysis, which will be used in the following section.

Interface conditions are obtained in Table 3.3; i.e., bending displacements and normal slopes (torsion angle for the beam) are continuous at γ^i, i=1-3 (Eq. 3.47), in-plane displacements of the plates and axial displacements of the beam are continuous at γ^i, i=1-3 (Eq. 3.48), differences of the bending moments and shear forces between the plates act as the twisting moment and load on the beam at γ^1 (Eq. 3.49), corner forces from the plates and shear forces from the beam should be in equilibrium at γ^i, i=2,3 (Eqs. 3.50 and 3.51), difference of tractions between plates (plane elastic solids) acts as the load on the beam at γ^1 (Eq. 3.52), and forces at the interfaces γ^2 and γ^3 should also be in equilibrium (Eqs. 3.53 and 3.54), where in Eqs. 3.53 and 3.54 $\hat{V}_x$ represents the shear force of the beam in the y-direction.

3.3.1g Beam-Plate Built-Up Structure with Edge Interface

Bending and in-plane deformation of a beam-plate built-up structure under lateral load with two sides of the plate clamped and the other two sides of the plate with beams free, as shown in Fig. 3.1g, are considered. The same assumptions made in Subsection 3.3.1f are applied to this model.

The design variables are the positions $\tilde{x}$ and $\tilde{y}$ of the beam components a and b, respectively, as shown in Fig. 3.1g. The state variable is the bending displacement w, the in-plane displacements $\tilde{w}^j$, j = x,y, of the plate component, and the bending displacements v^i and $\hat{v}^i$, i=a,b, the axial deformations $\tilde{v}^i$, i = a,b, of the beam components.

Interface conditions similar to those of Fig. 3.1f are obtained in Table 3.3 (Eqs. 3.55 to 3.70).

3.3.1h Plane Elastic Solid-Plate Built-Up Structure with Interior Interface

Bending and in-plane deformation of clamped plates under lateral load connected by plane elastic solids with fixed boundaries, as shown in Fig. 3.1h, are considered. Boundary movements of the plate components a and b cause movements of the entire domains of the plane elastic solids c and d. It is presumed that the plane elastic solids c and d do not bend in the y-direction during shape variation.

The design variable is the location $\tilde{y}$ of the plane elastic solids c and d. The state variable is the same as defined in Subsection 3.3.1f for plate components a and b and in-plane displacements $\tilde{w}^{ij}$, i=c,d, j=x,z of the plane elastic solids c and d. The same notations are used to identify the corresponding adjoint variable, as defined in Subsection 3.3.1f.

Interface conditions are obtained in Table 3.3; i.e., the displacement (bending and in-plane) and normal slope are continuous at γ^1, i=1-3 (Eqs. 3.71 and 3.72), bending moment (shear force) is continuous (in equilibrium in force system) at γ^1 (Eq. 3.73), corner forces and tractions are in equilibrium at γ^i, i=2,3 (Eqs. 3.74 and 3.75), and the in-plane forces are in equilibrium at γ^i, i=1-3 (Eq. 3.76).

3.3.1i Plane Elastic Solid-Plate Built-Up Structure with Edge Interface

Bending and in-plane deformation of a plate under lateral load with two sides clamped and the other two sides connected by plane elastic

solids a, b, c, and d, with fixed boundaries, as shown in Fig. 3.1i, are considered. Boundary movement of the plate component causes movement of entire domains of the plane elastic solids a, b, c, and d.

The design variables are locations $\tilde{x}$ and $\tilde{y}$ of plane elastic solids c and d, and a and b, respectively as shown in Fig. 3.1i. The state variable is the bending (in-plane) displacement w ($\tilde{w}^i$, i = x,y) of the plate components and the in-plane displacements $\tilde{w}^{ij}$, i=a,b,c,d, j=x,z for i=a,b and j=y,z for i=c,d of the plane elastic solids. The same notations are used to identify the corresponding adjoint variable, as defined in Subsection 3.3.1f.

Interface conditions are obtained in Table 3.3 (Eqs. 3.77 to 3.83).

3.3.2 Shape Design Sensitivity Forms

3.3.2a Beam-Truss Built-Up Structure with Interior Interface

Consider a displacement response functional defined in Ω^a as

$$\Psi_a = \int_{\Omega^a} \hat{\delta}(x-\hat{x}) z d\Omega \tag{3.84}$$

where $\hat{x} \in \Omega^a$ is presumed to be a fixed point and $\hat{\delta}(x)$ is the dirac measure. Since $\hat{\delta}(x-\hat{x})$ in Eq. 3.84 is defined on a neighborhood of $\bar{\Omega}^a$ by zero extension and $\hat{x}$ is fixed, $\hat{\delta}'(x-\hat{x}) = 0$. Thus Eq. 3.84 can be treated as the functional form of Eq. 2.63 and the adjoint equation is, from Eq. 2.70,

$$a(\lambda,\bar{\lambda}) = \int_{\Omega^a} \hat{\delta}(x-\hat{x}) \bar{\lambda} d\Omega \tag{3.85}$$

for all $\bar{\lambda} \in Z$. Equation 3.85 has a unique solution λ, which is the displacement due to a unit load at $\hat{x}$. That is, with smoothness

assumptions, the variational equation of Eq. 3.85 is equivalent to the formal operator equation

$$\left.\begin{aligned} (EI^a\lambda^a_{xx})_{xx} &= \hat{\delta}(x-\hat{x}) \quad , \quad x \in \Omega^a \\ (EI^b\lambda^b_{xx})_{xx} &= 0 \qquad\quad , \quad x \in \Omega^b \end{aligned}\right\} \tag{3.86}$$

where λ satisfies all the boundary conditions of Eqs. 3.23, 3.33 and 3.34 in Tables 3.1 and 3.3.

One can write the shape design sensitivity form of Eq. 3.10 as

$$\begin{aligned} \psi'_a = \sum_{i=a,b} \int_{\Omega^i} &\{EI^i[(z^i_x V^i)_{xx}\lambda^i_{xx} + z^i_{xx}(\lambda^i_x V^i)_{xx}] \\ &- f^i(\lambda^i_x V^i) - \hat{\delta}(x-\hat{x})(z^a_x V^a)\}d\Omega \\ + \sum_{i=a,b} &(f^i\lambda^i - EI^i z^i_{xx}\lambda^i_{xx})V^i\Big|_{\Gamma^i \cup \gamma} \end{aligned} \tag{3.87}$$

Integrating terms in the domain integral of Eq. 3.87 by parts, one has

$$\begin{aligned} \psi'_a = \sum_{i=a,b} \int_{\Omega^i} &[(EI^i\lambda^i_{xx})_{xx}(z^i_x V^i) + (EI^i z^i_{xx})_{xx}(\lambda^i_x V^i) \\ &- f^i(\lambda^i_x V^i) - \delta(x-\hat{x})(z^a_x V^a)]d\Omega \\ + \sum_{i=a,b} &[EI^i(z^i_x V^i)_x\lambda^i_{xx} + EI^i z^i_{xx}(\lambda^i_x V^i)_x - (EI^i\lambda^i_{xx})_x(z^i_x V^i) \\ &- (EI^i z^i_{xx})_x(\lambda^i_x V^i) + (f^i\lambda^i - EI^i z^i_{xx}\lambda^i_{xx})V^i]\Big|_{\Gamma^i \gamma} \end{aligned} \tag{3.88}$$

Then, from the formal operator equations of Eqs. 2.1 and 3.86, one obtains the final shape design sensitivity form, by imposing the interface conditions of Eqs. 3.33 and 3.34 in Table 3.3, as

$$\psi_a' = \sum_{i=a,b} \left[EI^i z^i_{xx} \lambda^i_{xx} - (EI^i \lambda^i_{xx})_x z^i_x - (EI^i z^i_{xx})_x \lambda^i_x + f^i \lambda^i \right] V^i \Big|_\gamma \tag{3.89}$$

at the interface γ.

If the outside boundary Γ^i is not fixed, one obtains the shape design sensitivity form as

$$\psi_a' = \sum_{i=a,b} (EI^i z^i_{xx} \lambda^i_{xx}) V^i \Big|_{\Gamma^i} \tag{3.90}$$

at the clamped boundary Γ^i, i=a,b from Eq. 3.23 in Table 3.1,

$$\psi_a' = \sum_{i=a,b} \left[- (EI^i \lambda^i_{xx})_x z^i_x - (EI^i z^i_{xx})_x \lambda^i_x \right] V^i \Big|_{\Gamma^i} \tag{3.91}$$

at the simply supported boundary Γ^i, i=a,b from Eqs. 3.21 and 3.22 in Table 3.1, and

$$\psi_a' = \sum_{i=a,b} (f^i \lambda^i) V^i \Big|_{\Gamma^i} \tag{3.92}$$

at the free boundary Γ^i, i=a,b from Eq. 3.24 in Table 3.1.

3.3.2b Beam-Truss Built-Up Structure with Edge Interface

The same procedure presented in Subsection 3.3.2a is applied to the problem in Subsection 3.3.1b to yield the final shape design sensitivity form at interface γ , by using the interface conditions of Eqs. 3.35 and 3.36 in Table 3.3, as

$$\psi_b' = \left[f\lambda - (EI\lambda_{xx})_x z_x - (EIz_{xx})_x \lambda_x \right] V \Big|_\gamma \tag{3.93}$$

If the outside boundary Γ is not fixed, one can obtain the same shape design sensitivity forms at Γ as in Eqs. 3.90 to 3.92 depending on the outside boundary conditions.

3.3.2c Plate-Truss Built-Up Structure with Edge Interface

Consider a stress response functional defined in Ω^a instead of a displacement response functional for the present model. The maximum bending stress for a plate occurs on the surface of the plate and is given in the form

$$\sigma_x = -\frac{Eh}{2(1-\nu^2)}(z_{xx} + \nu z_{yy}) \tag{3.94}$$

where σ_x is taken as a strength constraint. One can extend the idea to the Von-Mises failure criteria, which will be treated in Chapter 5. As will be discussed in Section 4.3, one may use a characteristic function $M_p(x)$ defined on a small open subset of Ω_p of Ω^a to treat the pointwise stress constraint. Then, the averaged value of σ_x over this small region is

$$\begin{aligned} \Psi_c &= \iint_{\Omega^a} \sigma_x M_p d\Omega \\ &= -\frac{Eh}{2(1-\nu^2)} \iint_{\Omega^a} (z_{xx} + \nu z_{yy}) M_p d\Omega \end{aligned} \tag{3.95}$$

Thus, Eq. 3.95 can be treated as the functional form of Eq. 2.63 and the adjoint equation is, from Eq. 2.70,

$$a(\lambda,\bar{\lambda}) = -\frac{Eh}{2(1-\nu^2)} \iint_{\Omega^a} (\bar{\lambda}_{xx} + \nu\bar{\lambda}_{yy}) M_p d\Omega \tag{3.96}$$

for all $\bar{\lambda} \in Z$. Equation 3.96 has a unique solution λ [5]. With smoothness assumptions, the variational equation of Eq. 3.96 is equivalent to the formal operator equation

$$\left.\begin{aligned} D\nabla^4\lambda^a &= -\frac{Eh}{2(1-\nu^2)}(M_{p_{xx}} + \nu M_{p_{yy}}), \quad x \in \Omega^a \\ D\nabla^4\lambda^b &= 0 \qquad\qquad\qquad\qquad\quad , \quad x \in \Omega^b \end{aligned}\right\} \tag{3.97}$$

where λ satisfies all boundary conditions of Eqs. 3.29, 3.30 and 3.37 to 3.42 in Tables 3.1 and 3.3.

One can write the shape design sensitivity form of Eq. 3.10 as

$$\begin{aligned}\psi_c' = \sum_{i=a,b} \iint_{\Omega^i} \{ & D^i[\lambda^i_{xx}((\nabla z^{i^T} V^i)_{xx} + \nu(\nabla z^{i^T} V^i)_{yy}) + \lambda^i_{yy} \\ & \times ((\nabla z^{i^T} V^i)_{yy} + \nu(\nabla z^{i^T} V^i)_{xx}) \\ & + 2(1-\nu) z^i_{xy} (\nabla z^{i^T} V^i)_{xy} + (\nabla \lambda^{i^T} V^i)_{xx} (z^i_{xx} + \nu z^i_{yy}) \\ & + (\nabla \lambda^{i^T} V^i)_{yy} (z^i_{yy} + \nu z^i_{xx}) + 2(1-\nu)(\nabla \lambda^{i^T} V^i)_{xy} z^i_{xy}] \\ & - f^i(\nabla \lambda^{i^T} V^i) + \frac{Eh}{2(1-\nu^2)} (M_{p_{xx}} + \nu M_{p_{yy}})(\nabla z^{a^T} V^a)\} d\Omega \\ & + \sum_{i=a,b} \int_{\Gamma^i \cup \gamma^2} \{f^i \lambda^i - D^i[\lambda^i_{xx}(z^i_{xx} + \nu z^i_{yy}) + \lambda^i_{yy}(z^i_{yy} + \nu z^i_{xx}) \\ & + 2(1-\nu)\lambda^i_{xy} z^i_{xy}]\} (V^{i^T} n^i) d\Gamma \end{aligned} \tag{3.98}$$

Integrating terms in the domain integral of Eq. 3.98 by parts, one has

$$\begin{aligned}\psi_c' = \sum_{i=a,b} \iint_{\Omega^i} \{ & D^i[\nabla^4 \lambda^i (\nabla z^{i^T} V^i) + \nabla^4 z^i (\nabla \lambda^{i^T} V^i)] \\ & - f^i(\nabla \lambda^{i^T} V^i) + \frac{Eh}{2(1-\nu^2)} (M_{p_{xx}} + \nu M_{p_{yy}})(\nabla z^{a^T} V^a)\} d\Omega \\ & + \sum_{i=a,b} \int_{\Gamma^i \cup \gamma^2} D^i[(\lambda^i_{xx} + \nu\lambda^i_{yy})(\nabla z^{i^T} V^i)_x + (z^i_{xx} + \nu z^i_{yy})(\nabla \lambda^{i^T} V^i)_x \end{aligned}$$

$$- (\lambda^i_{xxx} + (2-\nu)\lambda^i_{xyy})(\nabla z^{i^T} V^i) - (z^i_{xxx} + (2-\nu) z^i_{xyy})(\nabla \lambda^{i^T} V^i)] dy$$

$$+ \sum_{i=a,b} \int_{\Gamma^i} D^i [(\lambda^i_{yy} + \nu \lambda^i_{xx})(\nabla z^{i^T} V^i)_y + (z^i_{yy} + \nu z^i_{xx})(\nabla \lambda^{i^T} V^i)_y$$

$$- (\lambda^i_{yyy} + (2-\nu)\lambda^i_{xxy})(\nabla z^{i^T} V^i) - (z^i_{yyy} + (2-\nu) z^i_{xxy})(\nabla \lambda^{i^T} V^i)] dx$$

$$+ \{ 2(1-\nu) D^a [\lambda^a_{xy} (\nabla z^{a^T} V^a) + z^a_{xy} (\nabla \lambda^{a^T} V^a)] \Big|_{C_1}$$

$$+ 2(1-\nu) D^b [\lambda^b_{xy} (\nabla z^{b^T} V^b) + z^b_{xy} (\nabla \lambda^{b^T} V^b)] \Big|_{\gamma^1}$$

$$- 2(1-\nu) D^a [\lambda^a_{xy} (\nabla z^{a^T} V^a) + z^a_{xy} (\nabla \lambda^{a^T} V^a)] \Big|_{C_2}$$

$$- 2(1-\nu) D^b [\lambda^b_{xy} (\nabla z^{b^T} V^b) + z^b_{xy} (\nabla \lambda^{b^T} V^b)] \Big|_{\gamma^3}$$

$$- 2(1-\nu) D^a [\lambda^a_{xy} (\nabla z^{a^T} V^a) + z^a_{xy} (\nabla \lambda^{a^T} V^a)] \Big|_{\gamma^1}$$

$$- 2(1-\nu) D^b [\lambda^b_{xy} (\nabla z^{b^T} V^b) + z^b_{xy} (\nabla \lambda^{b^T} V^b)] \Big|_{C_3}$$

$$+ 2(1-\nu) D^a [\lambda^a_{xy} (\nabla z^{a^T} V^a) + z^a_{xy} (\Delta \lambda^{a^T} V^a)] \Big|_{\gamma^3}$$

$$+ 2(1-\nu) D^b [\lambda^b_{xy} (\nabla z^{b^T} V^b) + z^b_{xy} (\nabla \lambda^{b^T} V^b)] \Big|_{C_4} \}$$

$$+ \sum_{i=a,b} \int_{\Gamma^i \gamma^2} \{ f^i \lambda^i - D^i [\lambda^i_{xx} (z^i_{xx} + \nu z^i_{yy}) + \lambda^i_{yy} (z^i_{yy} + \nu z^i_{xx})$$

$$+ 2(1-\nu) \lambda^i_{xy} z^i_{xy}] \} (V^{i^T} n^i) d\Gamma \qquad (3.99)$$

where C_1, C_2, C_3, and C_4 are corner points of the rectangular plate components as shown in Fig. 3.1c.

From the formal operator equations of Eqs. 2.17 and 3.97, one obtains the shape design sensitivity form, by imposing the interface conditions of Eqs. 3.37 to 3.42 in Table 3.3, as

$$\begin{aligned}\psi_c' = & \int_{\gamma^2} [(f^a\lambda^a + D^a\lambda^a_{xx}z^a_{xx})V^a + (f^b\lambda^b + D^b\lambda^b_{xx}z^b_{xx})V^b]dy \\ & + \{[f^a\lambda^a - 2(1-\nu)D^a(\lambda^a_{xy}z^a_x + z^a_{xy}\lambda^a_x)]V^a \\ & + [f^b\lambda^b + 2(1-\nu)D^b(\lambda^b_{xy}z^b_x + z^b_{xy}\lambda^b_x)]V^b\}\Big|_{\gamma^1} \\ & + \{[f^a\lambda^a + 2(1-\nu)D^a(\lambda^a_{xy}z^a_x + z^a_{xy}\lambda^a_x)]V^a \\ & + [f^b\lambda^b - 2(1-\nu)D^b(\lambda^b_{xy}z^b_x + z^b_{xy}\lambda^b_x)]V^b\}\Big|_{\gamma^3} \end{aligned} \tag{3.100}$$

at the interfaces γ^i, i = 1-3.

If the outside boundary Γ^i is not fixed, one may obtain the shape design sensitivity forms as

$$\psi_c' = \sum_{i=a,b} \int_{\Gamma^i} (D^i(\lambda^i_{xx}z^i_{xx})V^{xi}dy + \sum_{i=a,b} \int_{\Gamma^i} (D^i\lambda^i_{yy}z^i_{yy})V^{yi}dx \tag{3.101}$$

at the clamped boundary Γ^i from Eq. 3.29 in Table 3.1,

$$\begin{aligned}\psi_c' = & -\sum_{i=a,b} \int_{\Gamma^i} D^i[(\lambda^i_{xxx} + \nu\lambda^i_{xyy})z^i_x + (z^i_{xxx} + \nu z^i_{xyy})\lambda^i_x]V^{xi}dy \\ & - \sum_{i=a,b} \int_{\Gamma^i} D^i[(\lambda^i_{yyy} + \nu\lambda^i_{xxy})z^i_y + (z^i_{yyy} + \nu z^i_{xxy})\lambda^i_y]V^{yi}dx \end{aligned} \tag{3.102}$$

at the simply supported boundary Γ^i from Eqs. 3.27 and 3.28 in

Table 3.1, and

$$\psi_c' = \sum_{i=a,b} \int_{\Gamma^i} (f^i \lambda^i)(V^{i^T} n^i) d\Gamma \tag{3.103}$$

at the free boundary Γ^i from Eq. 3.30 in Table 3.1.

3.3.2d Plate-Truss Built-Up Structure with Corner Interface

The same procedure presented in Subsection 3.3.2c is applied to the problem in Subsection 3.3.1d, to yield the shape design sensitivity form at the interface γ, by using the interface conditions of Eqs. 3.43 and 3.44 in Table 3.3, as

$$\psi_d' = [f\lambda - 2(1-\nu)D(\lambda_{xy} z_x + z_{xy} \lambda_x)]V \Big|_\gamma \tag{3.104}$$

3.3.2e Plane Elastic Solid-Truss Built-Up Structure with Corner Interface

The same procedure presented in Subsection 3.3.2c can be applied to the problem in Subsection 3.3.1e to yield the shape design sensitivity form at the interface γ, by using the interface conditions of Eqs. 3.45 and 3.46 in Table 3.3, as

$$\psi_e' = \{ \sum_{i=x,y} F^i \lambda^i - \sum_{i,j=x,y} [\sigma^{ij}(z)\varepsilon^{ij}(\lambda)] \}(V^T n) + \sum_{i,j=x,y} [\sigma^{ij}(\lambda) n^j (\nabla z^T V) + \sigma^{ij}(z) n^j (\nabla \lambda^T V)] \Big|_\gamma \tag{3.105}$$

If the outside boundary Γ is not fixed, one may obtain the shape design sensitivity forms as

$$\psi_e' = - \sum_{i,j=x,y} [\sigma^{ij}(z)\varepsilon^{ij}(\lambda)](V^T n) + \sum_{i,j=x,y} [\sigma^{ij}(\lambda) n^j (\nabla z^T V) + \sigma^{ij}(z) n^j (\nabla \lambda^T V)] \Big|_\Gamma \tag{3.106}$$

at the fixed boundary Γ from Eq. 3.31 in Table 3.1 and

$$\psi'_e = \sum_{i=x,y} (F^i \lambda^i)(V^T n)\Big|_\Gamma \tag{3.107}$$

at the free boundary Γ from Eq. 3.32 in Table 3.1.

3.3.2f Beam-Plate Built-Up Structure with Interior Interface

Consider a displacement response functional defined in Ω^a as

$$\psi_f = \iint_{\Omega^a} \hat{\delta}(x-\hat{x}) w \, d\Omega \tag{3.108}$$

With the same procedure described in Subsection 3.3.2c, the adjoint equation is, from Eq. 2.70,

$$a(\lambda,\bar{\lambda}) = \iint_{\Omega^a} \hat{\delta}(x-\hat{x}) \bar{w} \, d\Omega \tag{3.109}$$

for all $\bar{\lambda} \in Z$, which is equivalent to the formal operator equation

$$\left.\begin{aligned} D^a \nabla^{4-a} w &= \hat{\delta}(x-\hat{x}) \quad , \quad x \in \Omega^a \\ D^b \nabla^{4-b} w &= 0 \qquad\quad , \quad x \in \Omega^b \\ -\sum_{i=x,y} \sigma_j^{ij}(\bar{w}) &= 0, \quad i = x,y \ , \ x \in \Omega^k \ , \ k = a,b \end{aligned}\right\} \tag{3.110}$$

where λ satisfies all the boundary conditions of Eqs. 3.23, 3.25, 3.29, 3.31, and 3.47 to 3.54 in Tables 3.1 and 3.3.

The shape design sensitivity form of Eq. 3.10 is obtained, by using the state and adjoint variables defined in Subsection 3.3.1f, as

$$
\begin{aligned}
\Psi_f' = \int_{\gamma_1} \{ & EI[(v_x V^x)_{xx} \bar{v}_{xx} + v_{xx}(\bar{v}_x V^x)_{xx}] \\
& + GJ[(v_x V^x)_{xy} \bar{v}_{xy} + v_{xy}(\bar{v}_x V^x)_{xy}] \\
& + EA[(\tilde{v}_x V^x)_x \bar{\tilde{v}}_x + \tilde{v}_x(\bar{\tilde{v}}_x V^x)_x] \} dx \\
+ \sum_{k=a,b} \iint_{\Omega^k} \{ & D^k[\bar{w}^k_{xx}((\nabla w^{k^T} V^k)_{xx} + \nu(\nabla w^{k^T} V^k)_{yy}) \\
& + \bar{w}^k_{yy}((\nabla w^{k^T} V^k)_{yy} + \nu(\nabla w^{k^T} V^k)_{xx}) \\
& + 2(1-\nu) w^k_{xy}(\nabla w^{k^T} V^k)_{xy} + (\nabla \bar{w}^{k^T} V^k)_{xx}(w^k_{xx} + \nu w^k_{yy}) \\
& + (\nabla \bar{w}^{k^T} V^k)_{yy}(w^k_{yy} + \nu w^k_{xx}) + 2(1-\nu)(\nabla \bar{w}^{k^T} V^k)_{xy} w^k_{xy}] \\
+ \sum_{i,j=x,y} & [\sigma^{ij}(\bar{\tilde{w}}^k)\varepsilon^{ij}(\nabla \tilde{w}^{k^T} V^k) + \sigma^{ij}(\tilde{w}^k)\varepsilon^{ij}(\nabla \bar{\tilde{w}}^{k^T} V^k)] \\
& - f^k(\nabla \bar{w}^{k^T} V^k) - \sum_{i=x,y} F^{ki}(\nabla \bar{\tilde{w}}^{k^T} V^k) - \hat{\delta}(x-\hat{x})(\nabla w^{a^T} V^a) \} d\Omega \\
+ \sum_{k=a,b} \int_{\gamma_1} \{ & f^k \bar{w}^k - D^k[\bar{w}^k_{xx}(w^k_{xx} + \nu w^k_{yy}) + \bar{w}^k_{yy}(w^k_{yy} + \nu w^k_{xx}) \\
& + 2(1-\nu)\bar{w}^k_{xy} w^k_{xy}] + \sum_{i=x,y} F^{ki} \bar{\tilde{w}}^k \\
& - \sum_{i,j=x,y} [\sigma^{ij}(\tilde{w}^k)\varepsilon^{ij}(\bar{\tilde{w}}^k)] \} (V^{k^T} n^k) d\Gamma
\end{aligned}
\tag{3.111}
$$

Since the outside boundary Γ^i is presumed to be fixed, boundary terms at Γ^i are omitted in Eq. 3.111. Integrating terms in the domain integral of Eq. 3.111 by parts, one has

$$
\begin{aligned}
\Psi_f' = \int_{\gamma^1} & [(EI\bar{v}_{xx})_{xx}(v_x V^x) + (EIv_{xx})_{xx}(\bar{v}_x V^x) \\
& -GJ(\bar{v}_{xxy} v_{xy} V^x + v_{xxy}\bar{v}_{xy} V^x) \\
& -(EA\tilde{\bar{v}}_x)_x(\tilde{v}_x V^x) - (EA\tilde{v}_x)_x(\tilde{\bar{v}}_x V^x)]dx \\
+ \sum_{k=a,b} \iint_{\Omega^k} & \{D^k[\nabla^4 \bar{w}^k(\nabla w^{kT} V^k) + \nabla^4 w^k(\nabla \bar{w}^{kT} V^k)] \\
& - \sum_{i,j=x,y} [\sigma_j^{ij}(\tilde{\bar{w}}^k)(\nabla \tilde{w}^{kT} V^k) + \sigma_j^{ij}(\tilde{w}^k)(\nabla \tilde{\bar{w}}^{kT} V^k)] \\
& - f^k(\nabla \bar{w}^{kT} V^k) - \sum_{i=x,y} F^{ki}(\nabla \tilde{\bar{w}}^{kT} V^k) - \hat{\delta}(x-\hat{x})(\nabla w^{aT} V^a)\}d\Omega \\
+ \sum_{k=a,b} \int_{\gamma^1} & D^k[(\bar{w}^k_{yy} + \nu \bar{w}^k_{xx})(\nabla w^{kT} V^k)_y + (w^k_{yy} + \nu w^k_{xx})(\nabla \bar{w}^{kT} V^k)_y \\
& - (\bar{w}^k_{yyy} + (2-\nu)\bar{w}^k_{xxy})(\nabla w^{kT} V^k) - (w^k_{yyy} + (2-\nu)w^k_{xxy})(\nabla \bar{w}^{kT} V^k)]dx \\
& + \{2(1-\nu)D^b[\bar{w}^b_{xy}(\nabla w^{bT} V^b) + w^b_{xy}(\nabla \bar{w}^{bT} V^b)]\Big|_{\gamma^2} \\
& - 2(1-\nu)D^a[\bar{w}^a_{xy}(\nabla w^{aT} V^a) + w^a_{xy}(\nabla \bar{w}^{aT} V^a)]\Big|_{\gamma^2} \\
& - 2(1-\nu)D^b[\bar{w}^b_{xy}(\nabla w^{bT} V^b) + w^b_{xy}(\nabla \bar{w}^{bT} V^b)]\Big|_{\gamma^3}
\end{aligned}
$$

$$+ 2(1-\nu)D^a[\bar{w}^a_{xy}(\nabla w^{a^T} V^a) + w^a_{xy}(\nabla \bar{w}^{a^T} V^a)]\Big|_{\gamma^3} \}$$

$$+ \sum_{k=a,b} \int_{\gamma^1} \{(f^k \bar{w}^k + \sum_{i=x,y} F^{ki} \tilde{\bar{w}}^{ki})(V^{k^T} n^k)$$

$$- D^k[\bar{w}^k_{xx}(w^k_{xx} + \nu w^k_{yy}) + \bar{w}^k_{yy}(w^k_{yy} + \nu w^k_{xx}) + 2(1-\nu)\bar{w}^k_{xy} w^k_{xy}](V^{k^T} n^k)$$

$$+ \sum_{i,j=x,y} [\sigma^{ij}(\tilde{\bar{w}}^k) n^j (\nabla \tilde{w}^{k^T} V^k) + \sigma^{ij}(\tilde{w}^k) n^j (\nabla \tilde{\bar{w}}^{k^T} V^k)]$$

$$- \sum_{i,j=x,y} [\sigma^{ij}(\tilde{\bar{w}}^k) \varepsilon^{ij}(\tilde{\bar{w}}^k)](V^{k^T} n^k)\} dx \qquad (3.112)$$

Boundary terms at the outside boundary Γ^i are omitted in Eq. 3.112, since the outside boundary Γ^i is presumed to be fixed.

From the formal operator equations of Eqs. 2.17, 2.25 and 3.110, one obtains the shape design sensitivity form at the interface γ^1, by imposing the interface conditions of Eqs. 3.47 to 3.54 in Table 3.3, as

$$\psi'_f = \sum_{k=a,b} \int_{\gamma^1} \{[f^k \bar{w}^k + D^k(w^k_{yy} \bar{w}^k_{yy} - w^k_{xx} \bar{w}^k_{xx} - (\bar{w}^k_{yyy} + \nu \bar{w}^k_{xxy}) w^k_y$$

$$- (w^k_{yyy} + \nu w^k_{xxy}) \bar{w}^k_y)] V^{ky}$$

$$+ \sum_{j=x,y} [{}^{yj}(\tilde{\bar{w}}^k) n^j ({}^{\tilde{w}^k_y}{}^T V^{ky}) + {}^{yj}(\tilde{w}^k) n^j ({}^{\tilde{\bar{w}}^k_y}{}^T V^{ky})]$$

$$+ [F^{ky} \bar{w}^{ky} - (\sum_{j=x,y} {}^{yj}(w^k) \varepsilon^{yj}(\bar{w}^k))] V^{ky}\} dx \qquad (3.113)$$

3.3.2g Beam-Plate Built-Up Structure with Edge Interface

The same procedure presented in Subsection 3.3.2f is applied to the problem in Subsection 3.3.1g to yield the shape design sensitivity form at the interface γ^i, i=1,2, by imposing the interface conditions of

Eqs. 3.55 to 3.70 in Table 3.3, as

$$\begin{aligned}
\Psi_g' = \int_{\gamma_1} \{ & [f\bar{w} + D(w_{xx}\bar{w}_{xx} - w_{yy}\bar{w}_{yy} - (\bar{w}_{xxx} + \nu\bar{w}_{xyy})w_x \\
& - (w_{xxx} + \nu w_{xyy})\bar{w}_x)]V^x \\
& + \sum_{j=x,y} [\sigma^{xj}(\bar{\tilde{w}})n^j(\tilde{w}_x V^x) + \sigma^{xj}(\tilde{w})n^j(\bar{\tilde{w}}_x V^x)] \\
& + [F^x \bar{\tilde{w}}^x - (\sum_{j=x,y} \sigma^{xj}(\tilde{w})\varepsilon^{xj}(\bar{\tilde{w}}))]V^x \}dy \\
& + \int_{\gamma_2} \{f\bar{w} + D(w_{yy}\bar{w}_{yy} - w_{xx}\bar{w}_{xx} - (\bar{w}_{yyy} + \nu\bar{w}_{xxy})w_y \\
& - (w_{yyy} + \nu w_{xxy})\bar{w}_y)]V^y \\
& + \sum_{j=x,y} [\sigma^{yj}(\bar{\tilde{w}})n^j(\tilde{w}_y V^y) + \sigma^{yj}(\tilde{w})n^j(\bar{\tilde{w}}_y V^y)] \\
& + [F^y \bar{\tilde{w}}^y - (\sum_{j=x,y} \sigma^{yj}(\tilde{w})\varepsilon^{yj}(\bar{\tilde{w}}))]V^y \}dx
\end{aligned} \tag{3.114}$$

3.3.2h Plane Elastic Solid-Plate Built-Up Structure with Interior Interface

Consider a displacement response functional defined in Ω^a as

$$\Psi_h = \iint_{\Omega^a} \hat{\delta}(x-\hat{x})w\,d\Omega \tag{3.115}$$

With the same procedure discussed in Subsection 3.3.2c, the adjoint equation is, from Eq. 2.70,

$$a(\lambda,\bar{\lambda}) = \iint_{\Omega^a} \hat{\delta}(x-\hat{x})\bar{\bar{w}}\,d\Omega \tag{3.116}$$

for all $\bar{\lambda} \in Z$, which is equivalent to the formal operator equation

$$\left.\begin{aligned} D\nabla^4 \bar{w}^a &= \hat{\delta}(x-\hat{x}) \quad , \qquad x \in \Omega^a \\ D\nabla^4 \bar{w}^b &= 0 \qquad , \qquad x^b \in \Omega \\ -\sum_{j=x,y} \sigma_j^{ij}(\tilde{\bar{w}}^k) &= 0 \ , \quad i=x,y \ , \quad x \in \Omega^k \ , \quad k=a,b \\ -\sum_{j=x,z} \sigma_j^{ij}(\tilde{\bar{w}}^k) &= 0 \ , \quad i=x,z \ , \quad x \in \Omega^k \ , \quad k=c,d \end{aligned}\right\} \tag{3.117}$$

where λ satisfies all the boundary conditions of Eqs. 3.29, 3.31, and 3.71 to 3.76 in Tables 3.1 and 3.3.

The shape design sensitivity form of Eq. 3.10 is obtained, by using the state and adjoint variables defined in Subsection 3.3.1h, as

$$\begin{aligned} \psi_h' = \sum_{k=a,b} \iint_{\Omega^k} \{ & D^k [\bar{w}^k_{xx}((\nabla w^{k^T} V^k)_{xx} + \nu(\nabla w^{k^T} V^k)_{yy}) \\ & + \bar{w}^k_{yy}((\nabla w^{k^T} V^k)_{yy} + \nu(\nabla w^{k^T} V^k)_{xx}) + 2(1-\nu) w^k_{xy}(\nabla w^{k^T} V^k)_{xy} \\ & + (\nabla \bar{w}^{k^T} V^k)_{xx}(w^k_{xx} + \nu w^k_{yy}) + (\nabla \bar{w}^{k^T} V^k)_{yy}(w^k_{yy} + \nu w^k_{xx}) \\ & + 2(1-\nu)(\nabla \bar{w}^{k^T} V^k)_{xy} w^k_{xy}] \\ & + \sum_{i,j=x,y} [\sigma^{ij}(\tilde{\bar{w}}^k)\varepsilon^{ij}(\nabla \tilde{w}^{k^T} V^k) + \sigma^{ij}(\tilde{w}^k)\varepsilon^{ij}(\nabla \tilde{\bar{w}}^{k^T} V^k)] \\ & - f^k(\nabla \bar{w}^{k^T} V^k) - \sum_{i=x,y} F^{ki}(\nabla \tilde{\bar{w}}^{k^T} V^k) - \hat{\delta}(x-\hat{x})(\nabla w^{a^T} V^a)\} d\Omega \\ + \sum_{k=a,b} \int_{\gamma^1} \{ & f^k \bar{w}^k - D^k [\bar{w}^k_{xx}(w^k_{xx} + \nu w^k_{yy}) + \bar{w}^k_{yy}(w^k_{yy} + \nu w^k_{xx}) \end{aligned}$$

$$+ 2(1-\nu)\bar{w}^k_{xy} w^k_{xy} + \sum_{i=x,y} F^{ki}\bar{\tilde{w}}^{ki}$$

$$- \sum_{i,j=x,y} [\sigma^{ij}(\tilde{w}^k)\varepsilon^{ij}(\bar{\tilde{w}}^k)]\}(v^{k^T} n^k)dx$$

$$+ \sum_{k=x,d} \iint_{\Omega^k} \{ \sum_{i,j=x,z} [\sigma^{ij}(\bar{\tilde{w}}^k)\varepsilon^{ij}(\nabla\tilde{w}^{k^T} v^k) + \sigma^{ij}(\tilde{w}^k)\varepsilon^{ij}(\nabla\bar{\tilde{w}}^{k^T} v^k)]$$

$$- \sum_{i=x,z} F^{ki}(\nabla\bar{\tilde{w}}^{k^T} v^k)\}d\Omega \qquad (3.118)$$

Since the outside boundary Γ^i is fixed, boundary terms at Γ^i, i=a-d, are omitted. Integrating the remaining terms in the domain integrals of Eq. 3.118 by parts, one has

$$\Psi'_h = \sum_{k=a,b} \iint_{\Omega^k} \{D^k[\nabla^{4-k}(\nabla w^{k^T} v^k) + \nabla^4 w^k(\nabla\bar{w}^{k^T} v^k)]$$

$$- \sum_{i,j=x,y} [\sigma^{ij}_j(\bar{\tilde{w}}^k)(\nabla\tilde{w}^{k^T} v^k) + \sigma^{ij}_j(\tilde{w}^k)(\nabla\bar{\tilde{w}}^{k^T} v^k)]$$

$$- f^k(\nabla\bar{w}^{k^T} v^k) - \sum_{i=x,y} F^{ki}(\nabla\bar{\tilde{w}}^{k^T} v^k) - \hat{\delta}(x-\hat{x})(\nabla w^{a^T} v^a)\}d\Omega$$

$$+ \sum_{k=a,b} \int_{\gamma^1} D^k[(\bar{w}^k_{yy} + \nu\bar{w}^k_{xx})(\nabla w^{k^T} v^k)_y + (w^k_{yy} + \nu w^k_{xx})(\nabla\tilde{w}^{k^T} v^k)_y$$

$$- (\bar{w}^k_{yyy} + (2-\nu)\bar{w}^k_{xxy})(\nabla w^{k^T} v^k)$$

$$- (w^k_{yyy} + (2-\nu)w^k_{xxy})(\nabla\bar{w}^{k^T} v^k)]dx$$

$$+ \{2(1-\nu)D^b[\bar{w}^b_{xy}(\nabla w^{b^T} v^b) + w^b_{xy}(\nabla\bar{w}^{b^T} v^b)]\Big|_{\gamma^2}$$

$$- 2(1-\nu)D^a[\bar{w}^a_{xy}(\nabla w^{a^T} V^a) + w^a_{xy}(\nabla \bar{w}^{a^T} V^a)]\Big|_{\gamma^2}$$

$$- 2(1-\nu)D^b[\bar{w}^b_{xy}(\nabla w^{b^T} V^b) + w^b_{xy}(\nabla \bar{w}^{b^T} V^b)]\Big|_{\gamma^3}$$

$$+ 2(1-\nu)D^a[\bar{w}^a_{xy}(\nabla w^{a^T} V^a) + w^a_{xy}(\nabla \bar{w}^{a^T} V^a)]\Big|_{\gamma^3}\}$$

$$+ \sum_{k=a,b} \int_{\gamma^1} \{(f^k \bar{w}^k + \sum_{i=x,y} F^{ki} \bar{\tilde{w}}^{ki})(V^{k^T} n^k)$$

$$- D^k[\bar{w}^k_{xx}(w^k_{xx} + \nu w^k_{yy}) + \bar{w}^k_{yy}(w^k_{yy} + \nu w^k_{xx})$$

$$+ 2(1-\nu)\bar{w}^k_{xy} w^k_{xy}](V^{k^T} n^k)$$

$$+ \sum_{i,j=x,y} [\sigma^{ij}(\bar{\tilde{w}}^k) n^j (\nabla \tilde{w}^{k^T} V^k) + \sigma^{ij}(\tilde{w}^k) n^j (\nabla \bar{\tilde{w}}^{k^T} V^k)]$$

$$- \sum_{i,j=x,y} [\sigma^{ij}(\tilde{w}^k) \varepsilon^{ij}(\bar{\tilde{w}}^k)](V^{k^T} n^k)\} dx$$

$$+ \sum_{k=c,d} \iint_{\Omega^k} \{- \sum_{i,j=x,z} [\sigma^{ij}_j(\bar{\tilde{w}}^k)(\nabla \tilde{w}^{k^T} V^k) + \sigma^{ij}_j(\bar{\tilde{w}}^k)(\nabla \bar{\tilde{w}}^{k^T} V^k)]$$

$$- \sum_{i=x,z} F^{ki}(\nabla \bar{\tilde{w}}^{k^T} V^k)\} d\Omega \qquad (3.119)$$

Boundary terms at Γ^i, i=a-d, are omitted, since the outside boundary is fixed.

From the formal operator equations of Eqs. 2.17, 2.25 and 3.117, one obtains the shape design sensitivity form at the interface γ^1, by imposing the interface conditions of Eqs. 3.71 to 3.76 in Table 3.3, as

$$\psi_h' = \sum_{k=a,b} \int_{\gamma^1} \{[f^{k-k}\bar{w} - D^k((\bar{w}^k_{yyy} + \nu\bar{w}^k_{xxy})w^k_y + (w^k_{yyy} + \nu w^k_{xxy})\bar{w}^k_y)]V^k$$

$$+ \sum_{j=x,y} [\sigma^{yj}(\tilde{\bar{w}}^k)n^j(\tilde{w}^{kT}_y V^k) + \sigma^{yj}(\tilde{w}^k)n^j(\tilde{\bar{w}}^{kT}_y V^k)]$$

$$+ [F^{ky}\tilde{\bar{w}}^{ky} - \sum_{j=x,y} \sigma^{yj}(\tilde{w}^k)\varepsilon^{yj}(\tilde{\bar{w}}^k)]V^k\}dx \qquad (3.120)$$

3.3.2i Plane Elastic Solid-Plate Built-Up Structure with Edge Interface

The same procedure presented in Subsection 3.3.2h is applied to the problem in Subsection 3.3.1i to yield the shape design sensitivity form at the interfaces γ^i, i=1,2, by imposing the interface conditions of Eqs. 3.77 to 3.83 in Table 3.3, as

$$\psi_i' = \int_{\gamma^2} \{[f\bar{w} + D(w_{xx}\bar{w}_{xx} - (\bar{w}_{xxx} + \nu\bar{w}_{xyy})w_x - (w_{xxx} + \nu w_{xyy})\bar{w}_x)]V^x$$

$$+ \sum_{j=x,y} [\sigma^{xj}(\tilde{\bar{w}})n^j(\tilde{w}_x V^x) + \sigma^{xj}(\tilde{w})n^j(\tilde{\bar{w}}_x V^x)]$$

$$+ [F^x\tilde{\bar{w}}^x - \sum_{j=x,y} \sigma^{xj}(\tilde{w})\varepsilon^{xj}(\tilde{\bar{w}})]V^x\}dy$$

$$+ \int_{\gamma^1} \{[f\bar{w} + D(w_{yy}\bar{w}_{yy} - (\bar{w}_{yyy} + \bar{w}_{xxy})w_y - (w_{yyy} + w_{xxy})\bar{w}_y)]V^y$$

$$+ \sum_{j=x,y} [\sigma^{yj}(\tilde{\bar{w}})n^j(\tilde{w}_y V^y) + \sigma^{yj}(\tilde{w})n^j(\tilde{\bar{w}}_y V^y)]$$

$$+ [F^y\tilde{\bar{w}}^y - \sum_{j=x,y} \sigma^{yj}(\tilde{w})\varepsilon^{yj}(\tilde{\bar{w}})]V^y\}dx \qquad (3.121)$$

CHAPTER 4

NUMERICAL CONSIDERATIONS IN DESIGN SENSITIVITY CALCULATIONS

4.1 Introduction

The formulation presented in Chapters 2 and 3, using distributed parameter theory for design sensitivity analysis and the finite element method for structural analysis, provides a tool to check for numerical errors in finite element analysis. One can predict the effect of a design change that is to be implemented with the design sensitivity analysis method. When reanalysis is carried out, one can compare the predicted change in structural response with the change realized. If a disagreement arises, then error has crept in the numerical approximation. If one carries out design sensitivity analysis directly with the matrix/finite element method, in which the structure is discretized and the design variables built into the global stiffness matrix, then any error that is inherent in the finite element model is consistently parametrized. Therefore, one obtains precise design sensitivity coefficients of the matrix model of the structure, without realizing that there is substantial inherent error in the original model. In fact, as optimization is carried out, the optimization algorithm may feed on this error and lead to erroneous designs. In the current formulation, one can use the design sensitivity formulas derived from distributed parameter structural theory and the finite element

model to obtain a warning that approximation error is creeping into the calculation.

Before going to numerical calculations of structural analysis and design sensitivity analysis of complex built-up structures, it is helpful for the designer to investigate inherent numerical aspects involved in finite element analysis and design sensitivity analysis of structural components.

Finite element analysis and the associated characteristics of simple beams and plates are presented in Section 4.2, to gain insights for design sensitivity calculations of a beam-plate built-up structure. Gauss quadrature and accurate stress computations are also discussed in Section 4.2. A characteristic function is introduced to treat stress constraints in Section 4.3. Element boundary movement effects for shape variations, using the material derivative idea are considered in Section 4.4. In Section 4.5, a sparse matrix symbolic factorization method for iterative analysis is outlined. Finally, numerical calculation of design sensitivities for a beam-truss built-up structure is carried out and results are tabulated in Section 4.6.

4.2 Accuracy and Characteristics of the Finite Element Method

In structural optimization, the state and adjoint equations are solved numerically using the finite element method, which is regarded as a versatile tool to solve these equations. The importance of maintaining acceptable accuracy in finite element analysis cannot be

overstated, since design sensitivity coefficients are evaluated from the finite element analysis results.

For fourth order boundary-value problems that arise in the case of beam and plate bending, the design sensitivity coefficients include up to third derivatives of displacement functions, as shown in Chapter 3. Hence, it is important to employ appropriate finite elements and the associated shape functions to get accurate values of displacements and their derivatives needed in calculating design sensitivities. Particularly in shape design sensitivity analysis, good approximate values related to the design sensitivity coefficients that are evaluated at the boundary or interface are required, since they can be significantly in error, depending on the shape functions employed.

In this section, accuracy and the associated characteristics of the finite element method for simple beam and plate bending problems are discussed, based on the displacement method, since the displacement method formulation of the finite elements matches the theory of design sensitivity analysis presented in the preceding chapters. Some remarks on Gauss quadratures and stress computations are also discussed in this section.

4.2.1 Finite Element Analysis of a Beam

Beams serve as structures in their own right and also serve as ribs and edge stiffners for plates and shells. Many researchers have tested new optimization methods with a simple beam bending problem. In most cases, cubic shape functions are employed with successful results.

However, for shape design sensitivity analysis, it is worth while to investigate the finite element method and its characteristics for a simple beam bending problem.

Consider a simply supported beam subject only to bending, as shown in Fig. 4.1. The finite element method with cubic shape functions allows the displacement function and its first derivative to be continuous between elements. In a normalized interval connecting points i and j, with coordinate $\xi = x/L$, as shown in Fig. 4.2, one seeks to construct a function v(x) that will satisfy conditions on displacement and its first derivative at the end points. This function can be written in cubic form as

$$v = \alpha_1 + \alpha_2 x + \alpha_3 x^2 + \alpha_4 x^3 \tag{4.1}$$

This will define the shape functions corresponding to v_i and v_i' by taking for each a cubic with unit value at the appropriate points ($x = 0;L$) and zero at other points. The shape function in this case is of the form

$$\left.\begin{aligned} N_i &= [1 - 3\xi^2 + 2\xi^3, \quad x(\xi - 1)^2] \\ N_j &= [3\xi^2 - 2\xi^3, \quad x(\xi^2 - \xi)] \end{aligned}\right\} \tag{4.2}$$

If the displacement function has to satisfy up to second derivative continuity at the nodal points, it can be written as a quintic,

$$v = \beta_1 + \beta_2 x + \beta_3 x^2 + \beta_4 x^3 + \beta_5 x^4 + \beta_6 x^5 \tag{4.3}$$

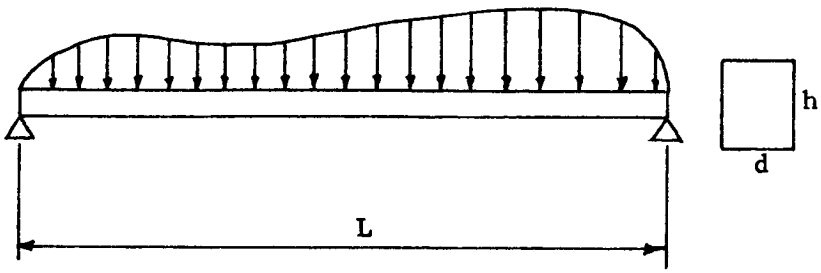

Figure 4.1 A Simply Supported Beam

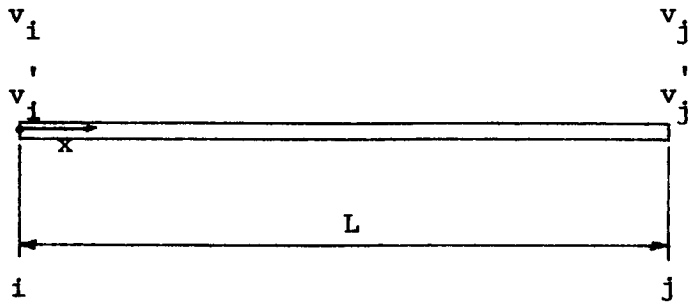

Figure 4.2 Degree of Freedom for Cubic Shape Function in One Dimensional Beam

The shape functions in this case are fifth order polynomials that can be written in a normalized interval with coordinate $\eta = x/L$, as shown in Fig. 4.3, as

$$\left.\begin{aligned} N_i &= \left[1-10\eta^3+15\eta^4-6\eta^5,\ L(\eta-6\eta^3+8\eta^4-3\eta^5),\ \frac{L^2}{2}(\eta^2-3\eta^3+3\eta^4-\eta^5)\right] \\ N_j &= \left[10\eta^3-15\eta^4+6\eta^5\ ,\ L(-4\eta^3+7\eta^4-3\eta^5)\ ,\ \frac{L^2}{2}(\eta^3-2\eta^4+\eta^5)\right] \end{aligned}\right\} \quad (4.4)$$

To test accuracy of the finite element method using cubic and quintic shape functions, a simply supported beam with rectangular cross section of Fig. 4.1, with the finite element model of Fig. 4.4, is used to illustrate how approximate solutions of the finite element method compare with analytical solutions.

Three different loading conditions are applied, to compare numerical results of up to third derivatives of displacement functions with those of the analytical solution, since the loading conditions (either static or adjoint load) in design sensitivity calculations are one of the following loads: point load, distributed load, point moment, or some combination of these.

Numerical data for this problem are as follows: beam length $L = 100$ in., beam height $h = 1$ in., beam width $d = 0.4$ in., Young's Modulus $E = 3\times10^7$ psi, the uniformly distributed load $f = 0.1$ lb/in. for Case 1, point load at center $P = 5$ lb for Case 2, and point moment at center $M = -5$ in.-lb for Case 3.

Numerical results are tabulated in Table 4.1, where A denotes the analytical solution, C denotes the numerical solution using cubic shape functions, and Q denotes results with quintic shape functions.

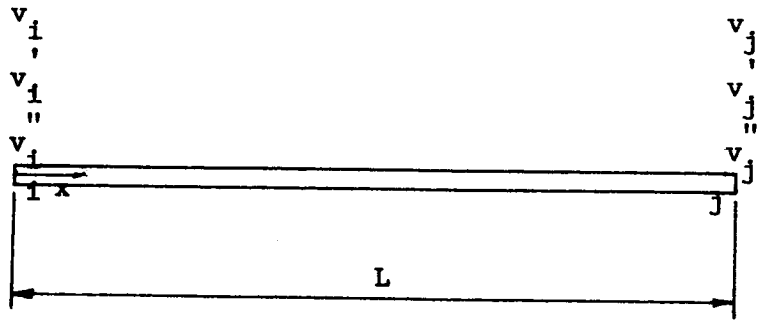

Figure 4.3 Degree of Freedom for Quintic Shape Function in One Dimensional Beam

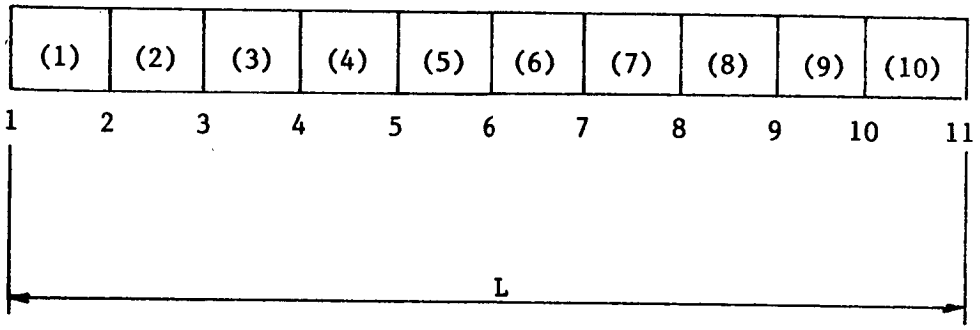

Figure 4.4 Finite Element Model of a Simply Supported Beam

Table 4.1 Comparison of Analysis Results for Simply Supported Beam

Case 1

Elmnt No.	X		Vxx	Vxxx	X		Vxx	Vxxx
(1)	0.	C	0.833E-06	-0.450E-05	10.	C	-0.458E-04	-0.450E-05
				-0.500E-05*				-0.400E-05*
		Q	0.000E 00	-0.500E-05		Q	-0.450E-04	-0.400E-05
		A	0.000E 00	-0.500E-05		A	-0.450E-04	-0.400E-05
(2)	10.	C	-0.458E-04	-0.350E-05	20.	C	-0.808E-04	-0.350E-05
				-0.400E-05*				-0.300E-05*
		Q	-0.450E-04	-0.400E-05		Q	-0.800E-04	-0.300E-05
		A	-0.450E-04	-0.400E-05		A	-0.800E-04	-0.300E-05
(3)	20.	C	-0.808E-04	-0.250E-05	30.	C	-0.106E-03	-0.250E-05
				-0.300E-05*				-0.200E-05*
		Q	-0.800E-04	-0.300E-05		Q	-0.105E-03	-0.200E-05
		A	-0.800E-04	-0.300E-05		A	-0.105E-03	-0.200E-05
(4)	30.	C	-0.106E-03	-0.150E-05	40.	C	-0.121E-03	-0.150E-05
				-0.200E-05*				-0.100E-05*
		Q	-0.105E-03	-0.200E-05		Q	-0.120E-03	-0.100E-05
		A	-0.105E-03	-0.200E-05		A	-0.120E-03	-0.100E-05
(5)	40.	C	-0.121E-03	-0.500E-06	50.	C	-0.126E-03	-0.500E-06
				-0.100E-05*				0.000E 00*
		Q	-0.120E-03	-0.100E-05		Q	-0.125E-03	-0.740E-15
		A	-0.120E-03	-0.100E-05		A	-0.125E-03	0.000E 00

Case 2

Elmnt No.	X		Vxx	Vxxx	X		Vxx	Vxxx
(1)	0.	C	-0.486E-16	-0.250E-05	10.	C	-0.250E-04	-0.250E-05
		Q	0.000E 00	-0.250E-05		Q	-0.250E-04	-0.250E-05
		A	0.000E 00	-0.250E-05		A	-0.250E-04	-0.250E-05
(2)	10.	C	-0.250E-04	-0.250E-05	20.	C	-0.500E-04	-0.250E-05
		Q	-0.250E-04	-0.250E-05		Q	-0.500E-04	-0.250E-05
		A	-0.250E-04	-0.250E-05		A	-0.500E-04	-0.250E-05
(3)	20.	C	-0.500E-04	-0.250E-05	30.	C	-0.750E-04	-0.250E-05
		Q	-0.500E-04	-0.250E-05		Q	-0.750E-04	-0.250E-05
		A	-0.500E-04	-0.250E-05		A	-0.750E-04	-0.250E-05
(4)	30.	C	-0.750E-04	-0.250E-05	40.	C	-0.100E-03	-0.250E-05
		Q	-0.750E-04	-0.250E-05		Q	-0.100E-03	-0.250E-05
		A	-0.750E-04	-0.250E-05		A	-0.100E-03	-0.250E-05
(5)	40.	C	-0.100E-03	-0.250E-05	50.	C	-0.125E-03	-0.250E-05
		Q	-0.100E-03	-0.250E-05		Q	-0.125E-03	-0.250E-05
		A	-0.100E-03	-0.250E-05		A	-0.125E-03	-0.250E-05

Table 4.1 Continued

Case 3

Elmnt No.	X		Vxx	Vxxx	X		Vxx	Vxxx
(1)	0.	C	-0.298E-18	-0.500E-07	10.	C	-0.500E-06	-0.500E-07
		Q	0.000E 00	-0.499E-07		Q	-0.499E-06	-0.496E-07
		A	0.000E 00	-0.500E-07		A	-0.500E-06	-0.500E-07
(2)	10.	C	-0.500E-06	-0.500E-07	20.	C	-0.100E-05	-0.500E-07
		Q	-0.499E-06	-0.515E-07		Q	-0.101E-05	-0.537E-07
		A	-0.500E-06	-0.500E-07		A	-0.100E-05	-0.500E-07
(3)	20.	C	-0.100E-05	-0.500E-07	30.	C	-0.150E-05	-0.500E-07
		Q	-0.101E-05	-0.383E-07		Q	-0.146E-05	-0.207E-07
		A	-0.100E-05	-0.500E-07		A	-0.150E-05	-0.500E-07
(4)	30.	C	-0.150E-05	-0.500E-07	40.	C	-0.200E-05	-0.500E-07
		Q	-0.146E-05	-0.142E-06		Q	-0.232E-05	-0.280E-06
		A	-0.150E-05	-0.500E-07		A	-0.200E-05	-0.500E-07
(5)	40.	C	-0.200E-05	-0.500E-07	50.	C	-0.250E-05	-0.500E-07
		Q	-0.232E-05	0.672E-06		Q	0.369E-17	0.176E-05
		A	-0.200E-05	-0.500E-07		A	-0.250E-05	-0.500E-07

Vxx : Second derivative of displacement function V
Vxxx : Third derivative of displacement function V
* : Extrapolated values

Table 4.1 shows that the finite element results are in reasonably good agreement with analytical solutions, except the following features.

When a cubic shape function is employed for a uniformly distributed loading condition, third derivatives of displacement have constant values throughout finite elements, since the order of shape functions is 3. Considering that the shear force of a beam varies linearly, one can extrapolate these constant (average) values at the nodal points for uniformly distributed load. Then, these extrapolated values can be the same as those of the analytical solution. Another feature to note is that when a quintic shape function is employed for a point moment loading condition, the second derivatives of displacement at the nodal points are continuous in adjacent finite elements, which contradicts the existence of external applied moment.

4.2.2 Finite Element Analysis of a Plate

As in the case of beams, plates serve as structures in their own right. They also serve as structural components for complex built-up structures. In plate bending problems, one is required to choose a method among various existing finite element methods in analysis, since characteristics of plate are much more complicated than in the case of beam. A large number of conforming and non-conforming elements have been used to solve thin flat plate bending problems. In most cases, the simplest nodal degrees of freedom are used; i.e., only displacements and their first derivatives, as in the case of a beam, and such elements are admirably suited for an extension to shell problems and indeed to other situations demanding C^1 continuity.

Figure 4.5 [73] shows convergence of rectangular and triangular elements for the case of a simply supported plate under a concentrated, central load. A process, leading to a necessary condition for convergence, has been proposed. This process, known as the "patch test" developed by Irons [83], has first been studied from a mathematical standpoint by Strang [84], Ciarlet [6], and others.

Consider a simply supported plate subject to bending only, as shown in Fig. 4.6. A non-conforming rectangular element [73], with sign convention and nodal order specified in Fig. 4.7, is employed.

The displacement function for a plate, under usual thin plate theory, is uniquely specified once the deflection w is known at all node points and can be written in general form as

$$w = Na^e \tag{4.5}$$

where a^e contains the element(nodal) parameters $a^e = [a_i, a_j, a_k, a_l]^T$, where

$$a_i = \begin{Bmatrix} w_i \\ \theta_{xi} \\ \theta_{yi} \end{Bmatrix} = \begin{Bmatrix} w_i \\ -\left(\frac{\partial w}{\partial y}\right)_i \\ \left(\frac{\partial w}{\partial x}\right)_i \end{Bmatrix} \tag{4.6}$$

The nodal 'forces' corresponding to displacement can be interpreted as a direct force and two couples, as shown in Fig. 4.7.

It is impossible to specify simple polynomial expressions for shape functions that ensure full compatibility, when only w and its slopes are prescribed at nodes. If any functions satisfying compatibility are

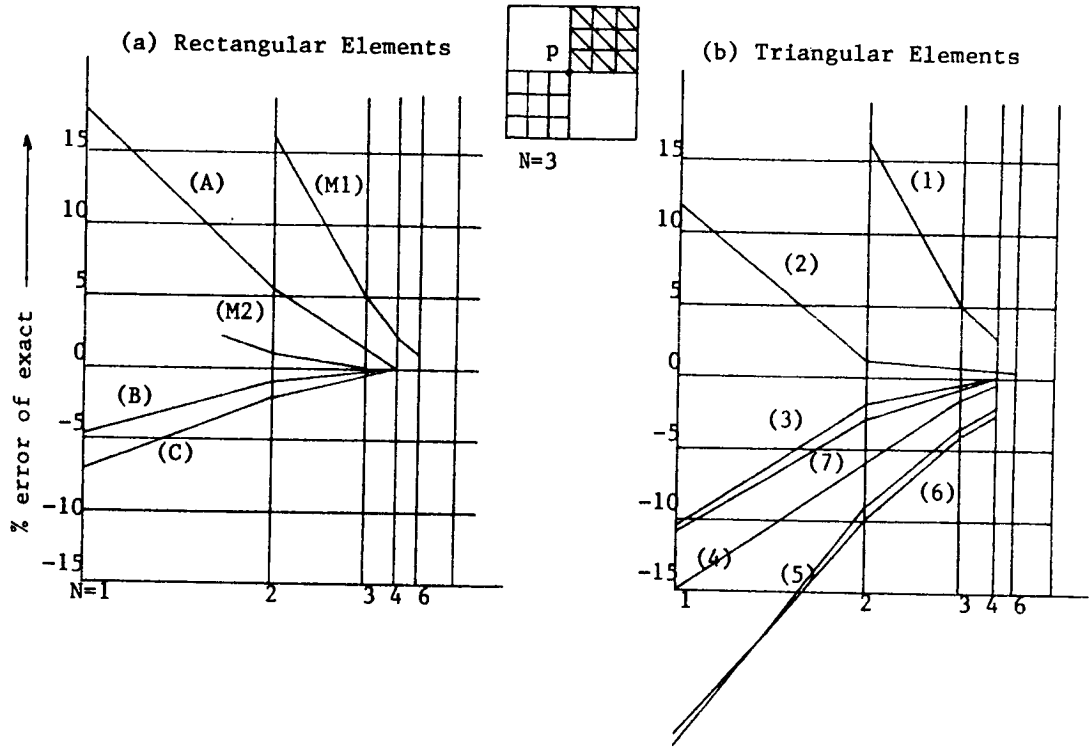

(A) 12 DOF Non-conforming [74,75]
(B) 16 DOF Hermitian-conforming [76]
(c) 16 DOF Conforming [77]
(M1) Mixed Linear M/w [78]
(M2) Mixed quadratic m/w [78]

(1) 6 DOF Non-conforming [79]
(2) 9 DOF Non-conforming [80]
(3) 9 DOF Non-conforming [81]
(4) 12 DOF Non-conforming [81]
(5) 9 DOF Conforming [80]
(6) 9 DOF Conforming [81]
(7) 12 DOF Conforming [82]

Figure 4.5 Comparative Errors-Thin Plate, Simply Supported, Central Load

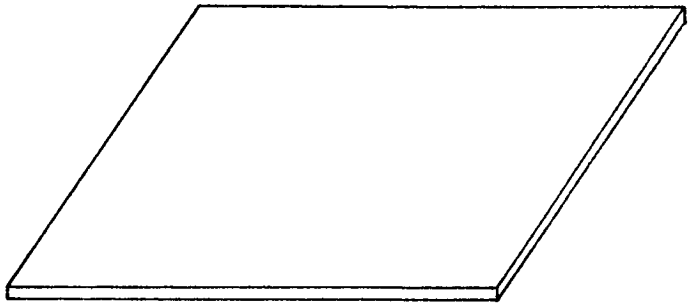

Figure 4.6 A Simply Supported Plate

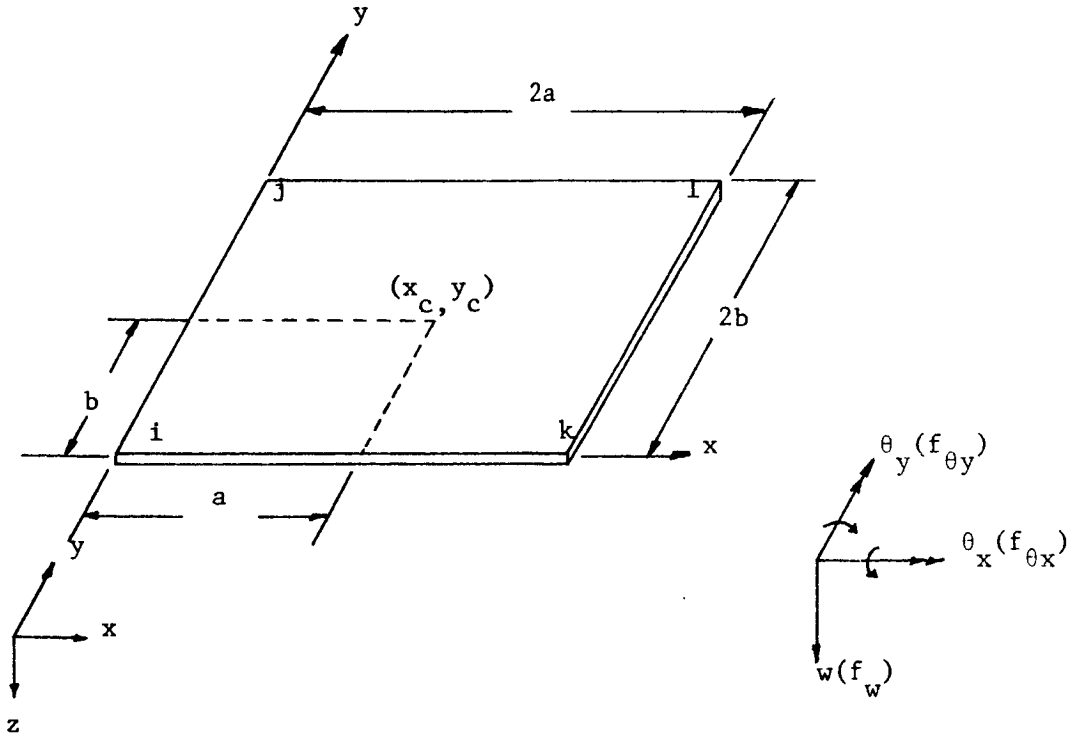

Figure 4.7 A Rectangular Plate Element

found with the three nodal variables, they must be such that at corner nodes they are not continuously differentiable and the cross derivative is not unique. This fact is important in calculating shape design sensitivity of built-up structure that involve plate components. A way out of this difficulty is to specify the cross derivative as one of the nodal parameters, regarded as a conforming element suggested by Bogner et al. [76].

A polynomial expression is conveniently used to define shape functions in terms of 12 parameters, in which certain terms must be omitted from a complete fourth order polynomial, as

$$w = \alpha_1 + \alpha_2 x + \alpha_3 y + \alpha_4 x^2 + \alpha_5 xy + \alpha_6 y^2 + \alpha_7 x^3 + \alpha_8 x^2 y + \alpha_9 xy^2 + \alpha_{10} y^3 + \alpha_{11} x^3 y + \alpha_{12} xy^3 \qquad (4.7)$$

In particular, along lines x = constant or y = constant, the displacement w varies as a cubic. The element boundaries are composed of such lines. This characteristic can give complete information to the ribs (beams) as in the case of a beam-plate built-up structure. Hence, by taking advantage of cubic shape function over higher order shape function as in the case of simple beam, one can apply the Hermite cubic shape function to the plate and related built-up structure problems. One should note that slope continuity is satisfied only at the nodal points, not at the element boundaries. This property is important when cubic shape functions are employed, since one must resort to a technique such as averaging of slopes at the element boundaries of the plate.

It is interesting to investigate the behaviour of derivatives of the displacement function, which are related to the design sensitivities of built-up structures involving plate components when a cubic shape function is employed. Taking derivatives of Eq. 4.7 with respect to x and y, successively, one obtains

$$w_x = \alpha_2+2\alpha_4 x+\alpha_5 y+3\alpha_7 x^2+2\alpha_8 xy+\alpha_9 y^2+3\alpha_{11} x^2 y+\alpha_{12} y^3 \tag{4.8}$$

$$w_y = \alpha_3+\alpha_5 x+2\alpha_6 y+\alpha_8 x^2+2\alpha_9 xy+3\alpha_{10} y^2+\alpha_{11} x^3+3\alpha_{12} xy^2 \tag{4.9}$$

$$w_{xx} = 2\alpha_4 + 6\alpha_7 x + 2\alpha_8 y + 6\alpha_{11} xy \tag{4.10}$$

$$w_{xy} = \alpha_5 + 2\alpha_8 x + 2\alpha_9 y + 3\alpha_{11} x^2 + 3\alpha_{12} y^2 \tag{4.11}$$

$$w_{yy} = 2\alpha_6 + 2\alpha_9 x + 6\alpha_{10} y + 6\alpha_{12} xy \tag{4.12}$$

$$w_{xxx} = 6\alpha_7 + 6\alpha_{11} y \tag{4.13}$$

$$w_{xxy} = 2\alpha_8 + 6\alpha_{11} x \tag{4.14}$$

$$w_{xyy} = 2\alpha_9 + 6\alpha_{12} y \tag{4.15}$$

$$w_{yyy} = 6\alpha_{10} + 6\alpha_{12} x \tag{4.16}$$

Note that along lines x = constant in finite element, the bending monent $\tilde{M}_x$ and shear force $\tilde{V}_x$ defined in Table 3.2 vary linearly. The same argument can be applied along lines y = constant. This linearity allows one to take numerical advantage discussed for the beam in previous section. The mixed derivative w_{xy} varies in a quadratic way, which is generally evaluated at a plate corner, and needs special

attention for more accurate evaluations. It is required to use an appropriate numerical integration scheme to evaluate those values for design sensitivities, using derivatives of displacement functions of Eqs. 4.8 to 4.16. This will be discussed in the following sections.

The shape function can be obtained in terms of normalized coordinates (see Fig. 4.7) as [73]

$$N_i = \frac{1}{8}\,[(\xi_0 + 1)(\eta_0 + 1)(2 + \xi_0 + \eta_0 - \xi^2 - \eta^2),$$

$$a\xi_i(\xi_0 + 1)^2(\xi_0 - 1)(\eta_0 + 1),$$

$$b\eta_i(\xi_0 + 1)(\eta_0 + 1)^2(\eta_0 - 1)]$$

with $\xi = (x - x_c)/a, \quad \eta = (y - y_c)/b$

$$\xi_0 = \xi \cdot \xi_i , \quad \eta_0 = \eta \cdot \eta_i \tag{4.17}$$

As mentioned earlier in this section, it is impossible to devise a simple polynomial function with only three degrees of nodal freedom that will be able to satisfy slope continuity requirements. The alternative of imposing curvature parameters at nodes has the disadvantage, however, of imposing excessive conditions of continuity. Furthermore, it is desirable to limit the nodal variables to three quantities only. These, with a simple physical interpretation, allow the generalization of plate elements to shells to be easily interpreted. Also computational advantages arise. The simple alternative is to provide additional shape functions, for which second order derivatives have non-unique values at nodes. Providing no singularities occur, convergence is assured. The

21 degree of freedom triangular element is described by Argyris [85], Bell [86], Bosshard [87], Irons [88], and Visser [89]. The reduced 18 degree of freedom version is developed by Argyris [85], Bell [86], and Cowper et al. [90]. An essentially similar, but more complicated formulation has been developed by Butlin and Ford [91] and mention of the element shape functions is made earlier by Withum [92] and Fellipa [82].

It is clear that many more elements of this type could be developed and indeed some are suggested in the above references. A full study is included in the work of Zenisek [93]. However, it should always be borne in mind that they involve an inconsistency when discontinuous variation of material properties occurs. Further, the existence of higher order derivatives makes it difficult to impose boundary conditions and indeed the simple interpretation of energy derivatives as 'nodal forces' disappears.

4.2.3 Remarks on Gauss Quadrature and Stress Computation

In design sensitivity analysis, one source of poor design sensitivity stems from numerical integration error in evaluation of stresses. A definite integral can be evaluated numerically by any of several methods. Here only the Gauss method [94,95] is described, since it has proved most useful in finite element work.

To approximate the integral

$$I = \int_{-1}^{1} \phi(\xi)\, d\xi \tag{4.18}$$

one can sample (evaluate) ϕ at the midpoint of the interval and

multiply by the length of the interval, as shown in Fig. 4.8a. Thus, one finds $I \approx 2\phi_1$. This result is exact if the function happens to be a straight line of any slope.

Generalization of Eq. 4.18 leads to the formula

$$I = \int_{-1}^{1} \phi d\xi \approx W_1\phi_1 + W_2\phi_2 + \cdots + W_n\phi_n \tag{4.19}$$

Thus, to approximate I, one evaluates $\phi = \phi(\xi)$ at each of several locations ξ_i, multiplies the resulting ϕ_i by an appropriate weight W_i, and adds. Gauss's method locates the sampling points so that for a given number of them, the greatest accuracy is achieved. Sampling points are located symmetrically with respect to the center of the interval. Symmetrically paired points have the same weight W_i. Table 4.2 gives data for Gauss rules of order n = 1 through n = 3. Data for higher orders can be obtained from most numerical methods textbooks. In computer work, numerical data for the ξ_i and W_i should be written with as many digits as the machine allows. In general, a polynomial of degree 2n-1 is integrated exactly by n-point Gauss quadrature.

In two dimensions, one finds the quadrature formula for $\phi = \phi(\xi,\eta)$ by integrating with respect to ξ and then with respect to η

$$I = \int_{-1}^{1}\int_{-1}^{1} \phi(\xi,\eta)d\xi d\eta \approx \int_{-1}^{1} \left[\sum_i W_i\phi(\xi,\eta)\right]d\eta$$

$$\approx \sum_j W_j \left[\sum_i W_i\phi(\xi_i,\eta_j)\right] = \sum_i \sum_j W_iW_j\phi(\xi_i,\eta_j) \tag{4.20}$$

In three dimensions, one has

$$I = \int_{-1}^{1} \int_{-1}^{1} \int_{-1}^{1} \phi(\xi\ \eta,\zeta)d\xi d\eta d\zeta \approx \sum_{ijk}\sum\sum W_iW_jW_k\phi(\xi_i,\eta_j,\zeta_k) \tag{4.21}$$

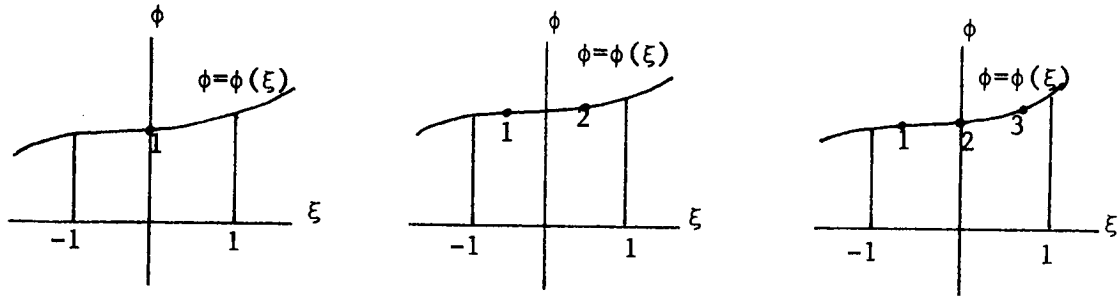

(a) one sampling point

(b) two sampling points

(c) three sampling points

Figure 4.8 Gauss Quadrature Using One, Two, and Three Sampling Points

Table 4.2 Sampling Points and Weights for Gauss Quadrature

Order n	Location ξ_i	Weight W_i
1	0.	2.
2	±0.57735 02691 89626	1.00000 00000 00000
3	±0.77459 66692 41483	0.55555 55555 55556
	0.00000 00000 00000	0.88888 88888 88889

One need not use the same number of Gauss points in each direction, but this is most common.

It has been shown [96-99] that finite element stress predictions are least accurate at element corners, more accurate at midsides (or midface in solid elements), and most accurate at certain interior points. These interior points can be used to define a stress field that can be extrapolated to yield stress at element boundaries. A procedure to obtain optimum points where stresses are most accurate is presented in Ref. 99.

Table 4.3 lists optimal points for stress evaluation [100]. Figure 4.9 shows an example of their benefit [96]. In Fig. 4.9, the dashed line denotes correct transverse shear stress under uniformly distributed load, while the solid line denotes computed shear stress. Optimal (Gauss) points are denoted by * symbols, at $\xi = P = + 0.57735$ ..... One sees that stresses away from the optimal points define a parabola that is grossly in error. But optimal points define a straight line that is essentially exact and is a least squares fit to the parabola. It is suggested that stresses will be most accurate when the element stiffness matrix is generated using the same Gauss points recommended in Table 4.3 for stress calculation. To extrapolate stresses from Gauss points, consider a one-dimensional situation, the upper part of Fig. 4.9. In the span $-P < \xi < P$ one interpolates linearly between the known stresses σ_1 and σ_2 at stations 1 and 2.

$$\sigma = \begin{bmatrix} \frac{1-s}{2} & \frac{1+s}{2} \end{bmatrix} \begin{Bmatrix} \sigma_1 \\ \sigma_2 \end{Bmatrix} \tag{4.22}$$

Table 4.3 Location of Optimal Points for Stress Calculation

Element	Locations: Gauss Rule and/or Coordinates
Beam (Fig. 4.2)	2 point ($\pm pL/2$ from center)
Linear Plane (Fig. 4.10a)	1 point ($\xi = \eta = 0$)
Quadratic Lagrange (Fig. 4.10b)	2x2 ($\xi = \pm p$, $\eta = \pm p$)
Quadratic Plane (Fig. 4.10c)	2x2 ($\xi = \pm p$, $\eta = \pm p$)
Cubic Plane (Fig. 4.10d)	3x3 (9 points; see Table 4.2)

p = 0.55735 02691 89626

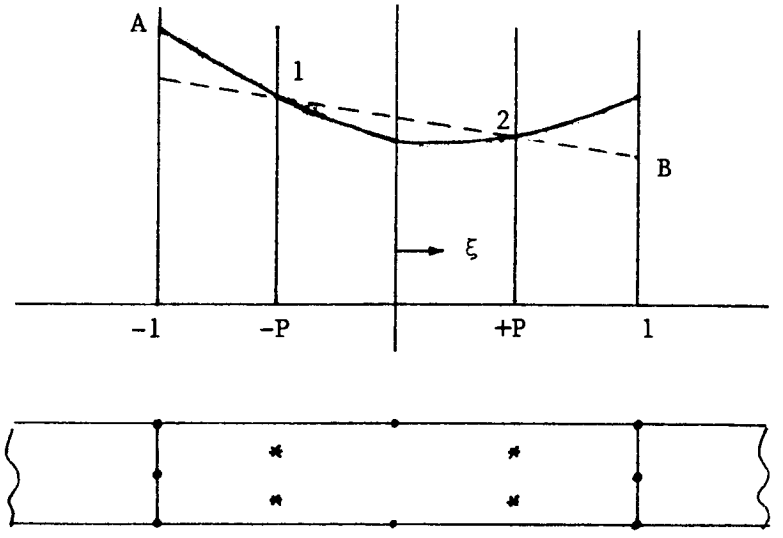

Figure 4.9 Portion of a Beam Modeled a Single Layer of Plane Quadratic Elements

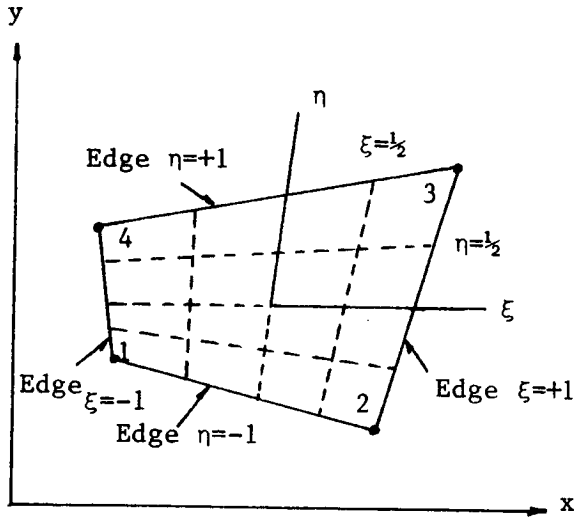

(a) Linear Plane

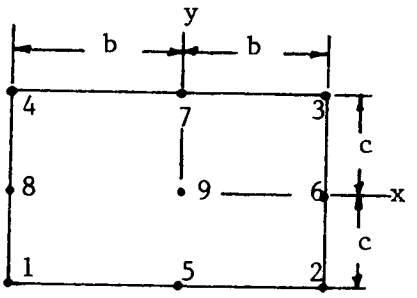

(b) Quadratic Lagrange

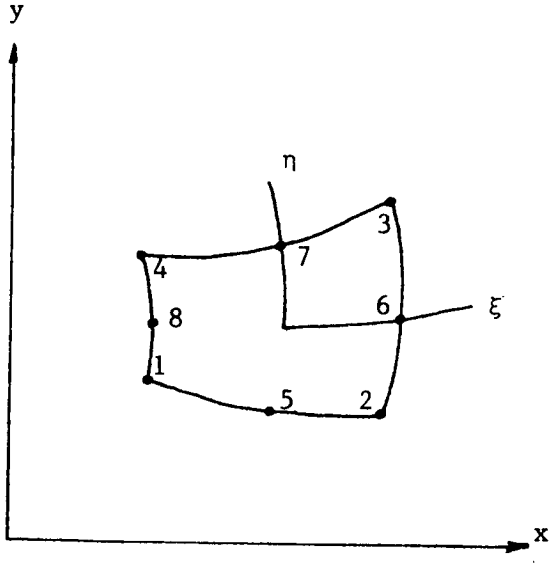

(c) Quadratic Plane

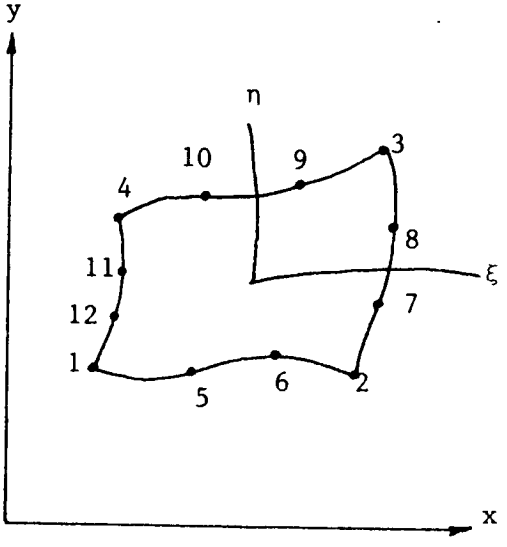

(d) Cubic Plane

Figure 4.10 Plane Elements

where s is the natural coordinate $s = \xi/P$, so that $s = -1$ at $\xi = -P$ and $s = +1$ at $\xi = +P$. Again, $P = 0.57735....$ To extrapolate to points A and B, at $\xi = \pm 1$ one sets $s = \pm 1/P$. Thus, with $\sigma = \sigma_A$ and then $\sigma = \sigma_B$ in Eq. 4.22,

$$\begin{Bmatrix} \sigma_A \\ \sigma_B \end{Bmatrix} = \frac{1}{2} \begin{bmatrix} 1 + \frac{1}{P} & 1 - \frac{1}{P} \\ 1 - \frac{1}{P} & 1 + \frac{1}{P} \end{bmatrix} \begin{Bmatrix} \sigma_1 \\ \sigma_2 \end{Bmatrix} \tag{4.23}$$

Stresses σ_A, σ_B, σ_1, and σ_2 each represent one stress component (σ_x, σ_y, or τ_{xy}). The extrapolation scheme can be applied to the two-dimensional case, which is presented in Ref. 100. This scheme will contribute to improving accuracy of design sensitivity in the next chapter.

4.3 Formulation of Constraints with Characteristic Functions

In design sensitivity analysis and optimization, stress constraints are among the most important and difficult to deal with. It is not easy to handle stress constraint as pointwise constraints. In this section, an equivalent functional form of stress constraints with a characteristic function [5] is presented.

Suppose one has pointwise constraints

$$\phi_\beta(x,u,z,b) \leq 0 \ , \ \beta = 1,2, \ ..,q, \ x \in \Omega \tag{4.24}$$

These pointwise constraints can be replaced by the equivalent functional constraints [101]

$$\Psi_\beta = \int_\Omega (\phi_\beta + |\phi_\beta|) d\Omega = 0 \ , \ \beta = 1,2,\cdots,q \tag{4.25}$$

so that one can reduce the difficulty of handling pointwise constraints in numerical calculations.

One may get poor sensitivities of the constraints of Eq. 4.25 during design iterations, particularly when violations of constraints of Eq. 4.24 are small and occur only in some local area of the domain, due to smearing characteristics of the constraints of Eq. 4.25. This phenomenon causes much difficulty when design iterations approach an optimum design, for which violations of constraints are usually small and occur only in some local area of the domain.

A characteristic function is introduced to cope with the problem, with the idea that it can be used to reduce the smearing characteristics described above. A characteristic function is a positive, constant function, defined in a local region Ω_p of Ω and is zero outside Ω_p, with the property

$$\int_{\Omega_p} M_p d\Omega = 1 = \int_{\Omega} M_p d\Omega \tag{4.26}$$

where M_p denotes the characteristic function defined in Ω_p. As the area of Ω_p approaches zero, M_p approaches the Dirac-δ distribution.

One can transform the constraints of Eq. 4.24 to integral form over small test cells by weighting $\phi_\beta(x,z)$, $\beta = 1,\cdots,q$, with a characteristic function defined in that region,

$$\Psi_{\beta k} = \int_{\Omega_k} \phi_\beta M_k d\Omega \leq 0, \quad \beta = 1,\cdots,q, \quad k = 1,\cdots,m \tag{4.27}$$

where Ω_k denotes the domain of test cell k and $\Omega = \Omega_1 \cup \Omega_2 \cup \cdots \cup \Omega_m$. With this formulation, one can isolate the areas in which violations

occur and hence reduce the smearing characteristics significantly by suitable choice of characteristic functions defined in the test cells. The scheme is quite useful when one employs the finite element method for analysis of the system. In that case, each element is treated as a test cell and the characteristic function is approximated by a step function that is defined inside the element and equal to zero outside the element. The magnitudes of violations in the elements are weighted properly and, therefore, give reasonable values of sensitivities.

4.4 Element Boundary Movement Effect for Shape Variation

In the continuous shape optimization method [72], the normal boundary movement $V^T n$ is obtained as the result of an optimization iteration. After each iteration, one can directly move the boundary by the amount $V^T n$ to construct a new boundary. However, in the finite dimensional shape optimization method, the velocity field V at the boundary is represented by a design parameter vector b and its variation δb. In this method, δb is determined as the result of an optimization iteration and, after the iteration, one generates a new design parameter vector and constructs a new boundary. Considering that the domain of a structural component consists of several finite elements, one may presume that the boundary movement of the structural component causes element boundary movement. This section introduces development of the element boundary movement effect that will be tested and used in shape design sensitivity analysis of built-up structures in later sections.

Let $M(x)$ be a characteristic function on an open region $\Omega_i \subset \Omega$ with smooth boundary Γ_i such that $\int_\Omega M(x) d\Omega = 1$, where $M = 1/\int_{\Omega_i} d\Omega$ on Ω_i and

$M = 0$ on $\Omega \backslash \Omega_i$. Then one has, on domain Ω_i,

$$\dot{M}(x) = \lim_{\tau \to 0} \frac{\frac{1}{\int_{\Omega_i(\tau)} d\Omega} - \frac{1}{\int_{\Omega_i} d\Omega}}{\tau}$$

$$= - \lim_{\tau \to 0} \left(\frac{\int_{\Omega_i(\tau)} d\Omega - \int_{\Omega_i} d\Omega}{\tau} \right) \left(\frac{1}{\int_{\Omega_{i(\tau)}} d\Omega \int_{\Omega_i} d\Omega} \right)$$

$$= - M^2 \int_{\Gamma_i} V^T n \, d\Gamma$$

$$= M'(x) + \nabla M(x)^T V = M'(x) \qquad (4.28)$$

since M is constant on Ω_i.

Now consider the stress constraint

$$\phi(\sigma) \leq 0 \qquad (4.29)$$

The functional form with the characteristic function M is

$$\Psi = \int_\Omega \phi M d\Omega = \int_{\Omega_i} \phi M d\Omega \leq 0 \qquad (4.30)$$

Taking material derivative of Eq. 4.30, using Eq. 4.28, yields

$$\Psi' = \int_{\Omega_i} \phi' M d\Omega + \int_{\Omega_i} \phi M' d\Omega + \int_{\Gamma_i} \phi M V^T n \, d\Gamma$$

$$= \int_\Omega \phi' M d\Omega - M^2 \int_{\Gamma_i} V^T n \, d\Gamma \int_{\Omega_i} \phi d\Omega + \int_{\Gamma_i} \phi M V^T n \, d\Gamma \qquad (4.31)$$

4.5 A Sparse Matrix Symbolic Factorization Technique for Iterative Analysis

In built-up structure optimization, one must solve the state equation of the system and adjoint equations that have exactly the same form, with different loads, repeatedly with the finite element method to calculate design sensitivities in each design iteration. This procedure is continued until one obtains an optimum design. In each design iteration, one constructs the global stiffness matrix, factors the matrix, saves the factors, and solves the equation with different load vectors, using forward-backward substitutions.

Since factorization of the matrix takes a major portion of the computation time, it is necessary to employ techniques to reduce this factorization time in each design iteration or to generate and store data that can be used in all design iterations and eliminate several steps of factorization in each design iteration. For the former, the bandwidth technique, the skyline technique, or various large matrix handling techniques [102] are conveniently employed. For the latter, a sparse matrix symbolic factorization technique [103] is highly desirable, because it does not require selection of the best node numbering sequence for minimum bandwidth of the global stiffness matrix. When this technique is combined with an iterative optimization algorithm, data generated by the symbolic factorization process can be used in all design iterations, which results in a substantial reduction of factorization time, provided that one maintains the same pattern of the global stiffness matrix during design iterations. This technique, which is used extensively in numerical calculations for optimal design

of built-up structure in Chapter 5, is briefly discussed in this section.

Consider a structure that is partitioned into n finite elements and a matrix equation for the entire structure, of the form

$$Kz = f \tag{4.32}$$

where z is a vector of independent generalized displacements, obtained by elimination of degrees of freedom specified by boundary conditions of the structure, f is a corresponding vector of equivalent nodal forces, and K is symmetric, positive definite, sparse structural stiffness matrix that is to be constructed from element stiffness matrices K^i, $i = 1,2,3,\cdots,n$. If the local coordinate systems are parallel to the global coordinate system, one has

$$K = \sum_{i=1}^{n} C^{i^T} K^i C^i \tag{4.33}$$

where C^i are boolean matrices, each of which has only unit element per row and the rotation matrices are presumed to be identity matrices. In Eq. 4.33, one sees that a nonzero entry in K is equal to a sum of nonzero entries in K^i.

The sparse matrix symbolic factorization technique starts from a preprocessing step to define pointer arrays that will be used in structural analysis to construct the matrix K from K^i, reorder the array containing the nonzero entries in the lower triangular part of K, and numerically factor a symmetric permutation of the matrix. Generation of these pointer arrays is considered as a symbolic factorization, since it

is equivalent to choosing a permutation matrix P and reordering the matrix elements for storage by columns in L, where L is a lower triangular matrix that is obtained from factorization of K to the form LDL^T, with D a diagonal matrix. It allows one to factor PKP^T into LDL^T, given only the zero/nonzero pattern of the matrix K and not the numerical values of the nonzero entries in K.

It is worth noting that, by virtue of the pointer arrays, one does not have to select the best node numbering sequence for minimum bandwidth of K. It is also worth noting that if the zero/nonzero pattern of K is not changed during design iterations, only one preprocessing step is necessary and the pointer arrays can be used repeatedly in every design iteration, which results in substantial reduction in computation time for the iterations.

After the preprocessing step, one can supply numerical values of the nonzero entries in K for numerical factorization. This is done, upon generation of each K^i and elimination of degrees of freedom specified by the boundary conditions of the structures, by supplying only nonzero entries in the lower triangular part of K^i. One then performs a numerical factorization of the symmetric permutation of K into the form LDL^T. For a given load vector f, one can perform forward and backward substitutions to calculate $K^{-1}f$. With the factored form of K saved, one can continue solving equations with a different load vector f.

The sparse matrix symbolic factorization technique explained above can easily be adapted to iterative optimization algorithms, as shown in

Fig. 4.11. The preprocessing step, which requires large storage, is executed just once as long as the pattern of K is not changed; i.e., as long as the connectivity of the finite elements is preserved. For optimization problems in which design changes affect only a few elements, one can further save computation time and store space.

The method presented in this section has been succesfully applied to optimal design of a built-up structure problem in Chapter 5. For the preprocessing step, numerical factorization, and forward and backward substitutions, various subroutines of the Harwell Subroutine Library [104] are called. For detailed information of the method and usage of the subroutines, the reader is referred to Ref. 103.

4.6 Design Sensitivity Analysis of a Beam-Truss Built-Up Structure

Numerical results of design sensitivity analysis for the beam-truss built-up structure of Fig. 3.1a is obtained, based on the analytical formulas of design sensitivity analysis derived in Chapters 2 and 3 for fixed or variable domain.

The finite element method, using cubic shape functions with an extrapolation scheme for accurate evaluation of the third derivatives of displacement function at the nodal points for uniformly distributed load has been employed. Conventional and shape design sensitivity forms are obtained separately. In shape design sensitivity calculations, it is presumed that the conventional design u (widths and heights of the beam elements) is suppressed and the outside boundaries are fixed; i.e., only the position of the truss can move with velocity V. Simultaneous

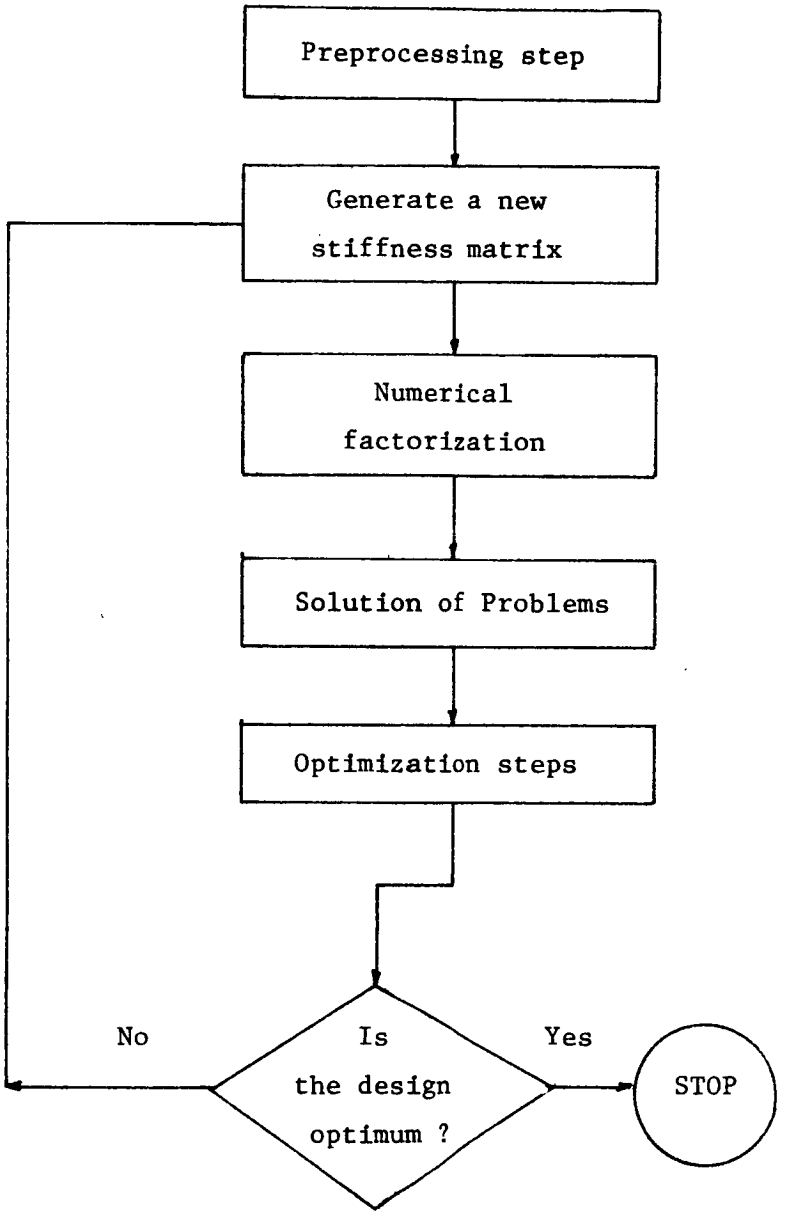

Figure 4.11 Optimization Loop

changes of conventional design and shape can be applied as a simple combination of the two separate cases.

Consider a stress constraint functional defined in Ω^a

$$\psi = \int_{\Omega^a} \sigma M d\Omega \tag{4.34}$$

where σ is bending stress, defined as

$$\sigma = -\frac{Eh}{2} z_{xx} \tag{4.35}$$

and M is a characteristic function defined on each finite element in Ω^a.

One can treat Eq. 4.34 as the functional form of Eq. 2.63 and the adjoint equation is, from Eq. 2.70,

$$a(\lambda,\bar{\lambda}) = -\int_{\Omega^a} \frac{Eh}{2} \bar{\lambda}_{xx} M d\Omega \tag{4.36}$$

for all $\bar{\lambda} \in Z$, where Z is the space of kinematically admissible displacement fields. Equation 4.36 has a unique solution λ, which is the displacement due to load $-(EhM/2)_{xx}$ in the region where the constraint functional is defined. That is, with smoothness assumptions, the variational equation of Eq. 4.36 is equivalent to the formal operator equation

$$\left.\begin{aligned} (EI^a \lambda^a_{xx})_{xx} &= -\left(\frac{Eh}{2} M\right)_{xx}, \quad x \in \Omega^a \\ (EI^b \lambda^b_{xx})_{xx} &= 0, \quad x \in \Omega^b \end{aligned}\right\} \tag{4.37}$$

where λ satisfies all the boundary and interface conditions of Eqs. 3.23, 3.33 and 3.34 in Tables 3.1 and 3.3. Therefore, the

conventional design sensitivity is, from Eq. 2.72,

$$\psi_c' = -\int_{\Omega^a} \frac{E}{2} z_{xx} M d\Omega - a'_{\delta u,\Omega}(z,\lambda) \tag{4.38}$$

where

$$a'_{\delta u,\Omega}(z,\lambda) = \int_{\Omega^a} (EI^a_{e^a} z^a_{xx} \lambda^a_{xx}) d\Omega + \int_{\Omega^b} (EI^b_{e^b} z^b_{xx} \lambda^b_{xx}) d\Omega \tag{4.39}$$

where $e = [d,h]^T$ and d(h) is width (height) of the beam. The shape design sensitivity is, from Eq. 3.89 with $f^a = f^b$,

$$\psi_s' = [EI^a(z^a_{xx}\lambda^a_{xx} - z^a_{xxx}\lambda^a_x - \lambda^a_{xxx} z^a_x)$$

$$- EI^b(z^b_{xx}\lambda^b_{xx} - z^b_{xxx}\lambda^b_x - \lambda^b_{xxx} z^b_x)]V\big|_\gamma \tag{4.40}$$

Considering the element boundary movement effect of Eq. 4.31, one may write the shape design sensitivity of Eq. 4.40 as

$$\psi_s' = [EI^a(z^a_{xx}\lambda^a_{xx} - z^a_{xxx}\lambda^a_x - \lambda^a_{xxx} z^a_x)$$

$$-EI^b(z^b_{xx}\lambda^b_{xx} - z^b_{xxx}\lambda^b_x - \lambda^b_{xxx} z^b_x)]V\Big|_\gamma$$

$$+ (M^2 \int_{\Omega^a} \frac{Eh}{2} z_{xx} d\Omega - \frac{Eh}{2} z_{xx} M) V^e\Big|_{\Gamma^e_M} \tag{4.41}$$

where V^e is the velocity of the element boundary that is presumed to be proportional to the velocity V of the component boundary, depending on the position, and Γ^e_M denotes the boundary of the element where the characteristic function M is applied.

Special attention is required for the case in which the element boundary Γ_M^e coincides with the interface γ, where Eq. 4.41 needs to be modified.

Rewriting the adjoint equation of Eq. 4.36, one has

$$\sum_{i=a,b} \int_{\Omega^i} EI^i \lambda^i_{xx} \bar{\lambda}^i_{xx} \, d\Omega = - \int_{\Omega^a} \frac{Eh}{2} \bar{\lambda}^a_{xx} M d\Omega \tag{4.42}$$

for all $\bar{\lambda} \in Z$. Integrating terms in Eq. 4.42 by parts yields

$$\sum_{i=a,b} \{ \int_{\Omega^i} (EI^i \lambda^i_{xx})_{xx} \bar{\lambda}^i d\Omega + [EI^i \lambda^i_{xx} \bar{\lambda}^i_x - (EI^i \lambda^i_{xx})_x \bar{\lambda}^i] \Big|_{\Gamma^i \cup \gamma} \}$$
$$= - \int_{\Omega^a} (\frac{Eh}{2} M)_{xx} \bar{\lambda}^a d\Omega + [- \frac{Eh}{2} M \bar{\lambda}^a_x + (\frac{Eh}{2} M)_x \bar{\lambda}^a] \Big|_{\gamma} \tag{4.43}$$

where Γ^i is the outside boundary of the beam component i. With smoothness assumptions, the variational equation of Eq. 4.42 is equivalent to the formal operator equation.

$$\left.\begin{aligned} (EI^a \lambda^a_{xx})_{xx} &= - (\frac{Eh}{2} M)_{xx} \quad , \quad x \in \Omega^a \\ (EI^b \lambda^b_{xx})_{xx} &= 0 \quad , \quad x \in \Omega^b \end{aligned}\right\} \tag{4.44}$$

$$z^i = z^i_x = \lambda^i = \lambda^i_x = 0 \quad , \quad x \in \Gamma^i, \quad i = a,b \tag{4.45}$$

$$\left.\begin{aligned} z^a &= z^b \\ z^a_x &= z^b_x \\ \lambda^a &= \lambda^b \\ \lambda^a_x &= \lambda^b_x \end{aligned}\right\} \quad , \quad x \in \gamma \tag{4.46}$$

$$\left.\begin{aligned} EI^a z^a_{xx} &= EI^b z^b_{xx} \\ (EI^a z^a_{xx})_x - (EI^b z^b_{xx})_x &= -\frac{EA}{\ell} q \end{aligned}\right\} \quad x \in \gamma \tag{4.47}$$

$$\left.\begin{aligned} EI^a \lambda^a_{xx} - EI^b \lambda^b_{xx} &= -\frac{Eh}{2} M \\ (EI^a \lambda^a_{xx})_x - (EI^b \lambda^b_{xx})_x &= -\frac{EA}{\ell} s - (\frac{Eh}{2} M)_x \end{aligned}\right\} \quad x \in \gamma \tag{4.48}$$

Note that the conditions of Eqs. 4.45 to 4.47 are the same as those of Eqs. 3.23, 3.33, and 3.34, respectively. In Eq. 4.48, another set of jump conditions for the adjoint variables, which are different from those of Eq 3.34, are obtained, due to coincidence of the element boundary with the interface γ. Then, with the element boundary movement effect and coincidence of the element boundary with the interface γ, Eq. 3.10 becomes

$$\begin{aligned} \psi'_a = & \sum_{i=a,b} \int_{\Omega^i} \{EI^i[(z^i_x V^i)_{xx} \lambda^i_{xx} + z^i_{xx}(\lambda^i_x V^i)_{xx}] \\ & - f^i(\lambda^i_x V^i) + \frac{Eh}{2}(z^a_x V^a)_{xx} M\} d\Omega \\ & + \sum_{i=a,b} (f^i \lambda^i - EI^i z^i_{xx} \lambda^i_{xx}) V^i \Big|_{\Gamma^i \cup \gamma} \\ & + (M^2 \int_{\Omega^a} \frac{Eh}{2} z^a_{xx} d\Omega - \frac{Eh}{2} z^a_{xx} M) V^e \Big|_{\Gamma^e_M} \end{aligned} \tag{4.49}$$

Integrating terms in the domain integral of Eq. 4.49 by parts, one has

$$\begin{aligned} \psi'_a = & \sum_{i=a,b} \int_{\Omega^i} [(EI^i \lambda^i_{xx})_{xx}(z^i_x V^i) + (EI^i \tfrac{i}{z}_{xx})_{xx}(\lambda^i_x V^i) \\ & - f^i(\lambda^i_x V^i) + (\frac{Eh}{2} M)_{xx}(z^a_x V^a)] d\Omega \\ & + \sum_{i=a,b} [EI^i(z^i_x V^i)_x \lambda^i_{xx} + EI^i z^i_{xx}(\lambda^i_x V^i)_x - (EI^i \lambda^i_{xx})_x (z^i_x V^i) \end{aligned}$$

$$- (EI^i z^i_{xx})_x(\lambda^i_x V^i) + (f^i\lambda^i - EI^i z^i_{xx}\lambda^i_{xx})V^i]$$

$$+ \frac{Eh}{2}(z^a_x V^a)_x M - (\frac{Eh}{2}M)_x(z^a_x V^a)$$

$$+ (M^2 \int_{\Omega^a} \frac{Eh}{2} z^a_{xx} d\Omega - \frac{Eh}{2} z^a_{xx} M)V^e \Big|_{\Gamma^e_M} \qquad (4.50)$$

From the formal operator equations of Eqs. 2.1 and 4.44, one obtains the shape design sensitivity by imposing the interface conditions of Eqs. 4.46 to 4.48, with $f^a = f^b$, as

$$\psi'_a = [EI^a(z^a_{xx}\lambda^a_{xx} - z^a_{xxx}\lambda^a_x - \lambda^a_{xxx}z^a_x)$$

$$- EI^b(z^b_{xx}\lambda^b_{xx} - z^b_{xxx}\lambda^b_x - \lambda^b_{xxx}z^b_x)]V\Big|_\gamma$$

$$+ \frac{Eh}{2} z^a_{xx} V^a M + (M^2 \int_{\Omega^a} \frac{Eh}{2} z^a_{xx} d\Omega - \frac{Eh}{2} z^a_{xx} M)V^e \Big|_{\Gamma^e_M} \qquad (4.51)$$

Noting that the velocity V^e is the same as the velocity V^a at the interface γ, one can obtain the final shape design sensitivity as

$$\psi'_a = [EI^a(z^a_{xx}\lambda^a_{xx} - z^a_{xxx}\lambda^a_x - \lambda^a_{xxx}z^a_x)$$

$$- EI^b(z^b_{xx}\lambda^b_{xx} - z^b_{xxx}\lambda^b_x - \lambda^b_{xxx}z^b_x)]V\Big|_\gamma$$

$$+ (M^2 \int_{\Omega^a} \frac{Eh}{2} z^a_{xx} d\Omega)V^e \Big|_{\Gamma^e_M} - (\frac{Eh}{2} z^a_{xx} M)V^e \Big|_{\Gamma^e_M \setminus \gamma} \qquad (4.52)$$

Comparing Eq. 4.52 with Eq. 4.41, one notes that coincidence of the element boundary with the interface γ causes the last term of Eq. 4.41, evaluated at the interface γ, to be dropped. Similarly, one can apply the above argument to the outside boundary Γ of the structural component and obtain the same form as Eq. 4.52, by dropping the last term evaluated at the outside boundary Γ.

Numerical calculations of design sensitivities are carried out to check the design sensitivity agreements between actual changes of constraint values (average stresses) and predictions.

The finite element model used is shown in Fig. 4.12. A total of 11 finite elements and 20 degrees of freedom are used to model the beam-truss built-up structure, including 10 beam elements and 1 truss element. The 11 finite elements are linked to two conventional design variables (heights and widths of the beam elements) and one shape design variable (supporting position of the truss).

The input data used in this calculation are as follows: elastic modulus $E = 3 \times 10^7$ psi, beam length $\ell = 100$ in., uniform height (width) of beam element $h = 1$ in. ($d = 0.4$ in.), cross-sectional area (length) of truss element $A = 5$ in. ($\bar{\ell} = 50$ in.), the original position of the supporting truss $\tilde{x} = 0.5\ell$, and uniformly distributed load $f = 0.1$ lb/in. on the beam.

Comparisons of design sensitivity calculations with the actual changes of constraint values after design modifications and the predictions for bending stress constraints of Eq. 4.34 are summarized in Table 4.4 for fixed domain and in Table 4.5 for variable domain, respectively. In Tables 4.4 and 4.5, Ψ_1 represents the constraint values at initial design, $\Delta\Psi$ represents the actual changes of constraint values after design modifications, and $\delta\Psi$ represent design sensitivity predictions. The last columns in Tables 4.4 and 4.5 denote the design sensitivity agreements in % between actual changes and predictions, defined as $\delta\Psi/\Delta\Psi \times 100$. In conventional design sensitivity comparison,

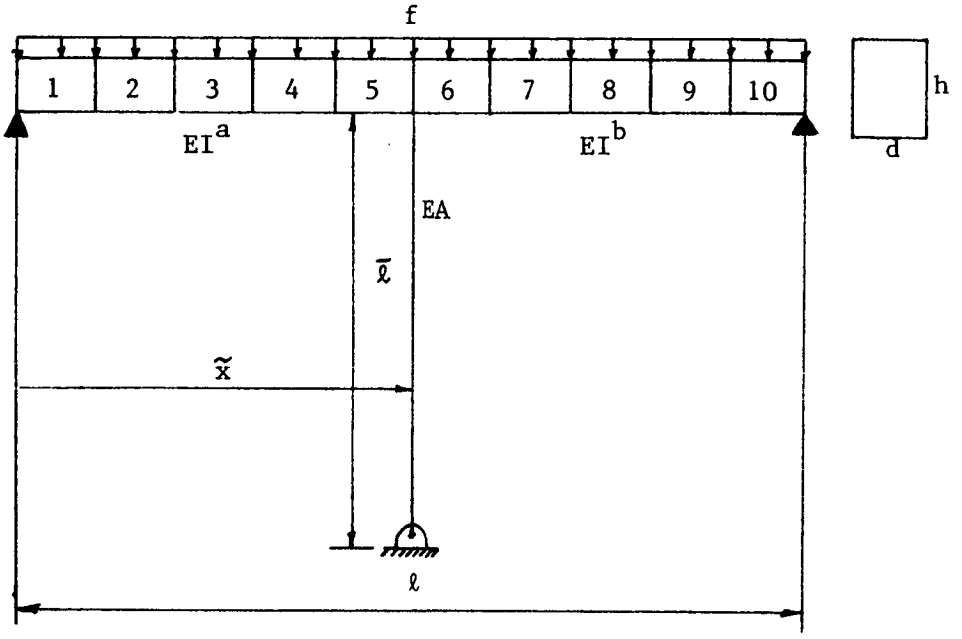

Figure 4.12 Finite Element Model for Beam-Truss Built-Up Structure

Table 4.4 Conventional Design Sensitivity Comparison for Truss-Beam Built-Up Structure

Element no.	Ψ_1	$\Delta\Psi$	$\delta\Psi$	$\delta\Psi/\Delta\Psi$ (%)
1	0.1156E 03	-0.1575E 02	-0.1734E 02	110.2
2	0.2469e 03	-0.3362E 02	-0.3703E 02	110.1
3	0.2281E 03	-0.3106E 02	-0.3422E 02	110.2
4	0.5940E 03	-0.8083E 01	-0.8905E 01	110.2
5	-0.2593E 03	0.3532E 02	0.3891E 02	110.2

Table 4.5 Shape Design Sensitivity Comparison for Truss-Beam Built-Up Structure

Element no.	Ψ_1	$\Delta\Psi$	$\delta\bar{\Psi}(\delta\bar{\Psi}/\Delta\Psi)$	$\delta\Psi(\delta\Psi/\Delta\Psi)$
1	0.1156E 03	0.1630E 02	0.1500E 02(92.0%)	0.1688E 02(103.5%)
2	0.2469E 03	0.3866E 02	0.3375E 02(87.3%)	0.3938E 02(101.8%)
3	0.2281E 03	0.4565E 02	0.3750E 02(82.1%)	0.4688E 02(102.7%)
4	0.5940E 03	0.3726E 02	0.2625E 02(70.5%)	0.3938E 02(105.7%)
5	-0.2593E 03	0.1349E 02	0.2347E-05(-----)	0.1688E 02(125.1%)
6	-0.2593E 03	-0.1901E 02	-0.2347E-05(-----)	-0.1688E 02(88.8%)
7	0.5940E 03	-0.4024E 02	-0.2625E 02(65.2%)	-0.3938E 02(97.8%)
8	0.2281E 03	-0.4685E 02	-0.3750E 02(80.0%)	-0.4688E 02(100.1%)
9	0.2469E 03	-0.3884E 02	-0.3375E 02(86.9%)	-0.3938E 02(101.4%)
10	0.1156E 03	-0.1620E 02	-0.1500E 02(92.6%)	-0.1688E 02(104.2%)

results for only half of the entire elements, due to symmetry of the structure, is tabulated in Table 4.4, with 5% uniform change of design variables. Table 4.4 shows good agreement of about 110% between actual changes and predictions for all elements. Table 4.5 shows the shape design sensitivity comparison with 5% change of shape design variable (position $\tilde{x}$). When the position $\tilde{x}$ moves with velocity V, it is assumed that each finite element domain also moves with a velocity V_i that is proportional to V, depending on the position, and the element boundary movement effect (Eq. 4.41) can apply. Particularly for calculating the design sensitivities for stress constraints defined on elements 5 and 6 of which boundaries coincide with the interface, Eq. 4.52 is used. In Table 4.5, the values in the column for $\delta\bar{\Psi}$ shows the design sensitivities by prediction without modification of third derivatives of the state variable.

Sensitivity predictions obtained for $\delta\bar{\Psi}$ in Table 4.5, using Eq. 4.52, show reasonably good agreement with actual changes, except in the 5th and 6th elements. However, using the extrapolation scheme for calculation of third derivatives of state variables (for uniformly distributed load) discussed in Section 4.2.1, one can obtain better sensitivity agreement of 88-125% as shown for $\delta\Psi$ in Table 4.5. These arguments and numerical tests provide the potential for design sensitivity calculations of a truss-beam-plate built-up structure, which is treated in Chapter 5.

CHAPTER 5

OPTIMAL DESIGN OF A TRUSS-BEAM-PLATE BUILT-UP STRUCTURE

5.1 Introduction

The design sensitivity analysis method developed in Chapters 2 and 3, with the aid of numerical methods discussed in Chapter 4, is used with a nonlinear programming method to iteratively optimize design of a truss-beam-plate built-up structure. Minimum weight will be sought, with constraints on compliance, displacement, stress, and natural frequency and bounds on design variables.

The variational formulation of system equations is presented in Section 5.2. The optimal design problem is formulated in Section 5.3 with the cost and constraint functionals defined. In Section 5.4, design sensitivity coefficients of the cost and constraint functionals for compliance, displacement, stress, and eigenvalue are obtained, using results from Chapters 2 and 3. The optimal design problem is solved using the linearization method of optimization [105]. Numerical results are presented and discussed in Section 5.5.

5.2 Description of System and Variational Formulation

A beam-plate built-up structure is supported by four 4-bar trusses, as shown in Fig. 5.1. A uniformly distributed load is applied to the plate components. The points supported by the trusses are at the intersections of two crossing beams nearest to the free edges of the structure. It is assumed that no external loads act on the beam and

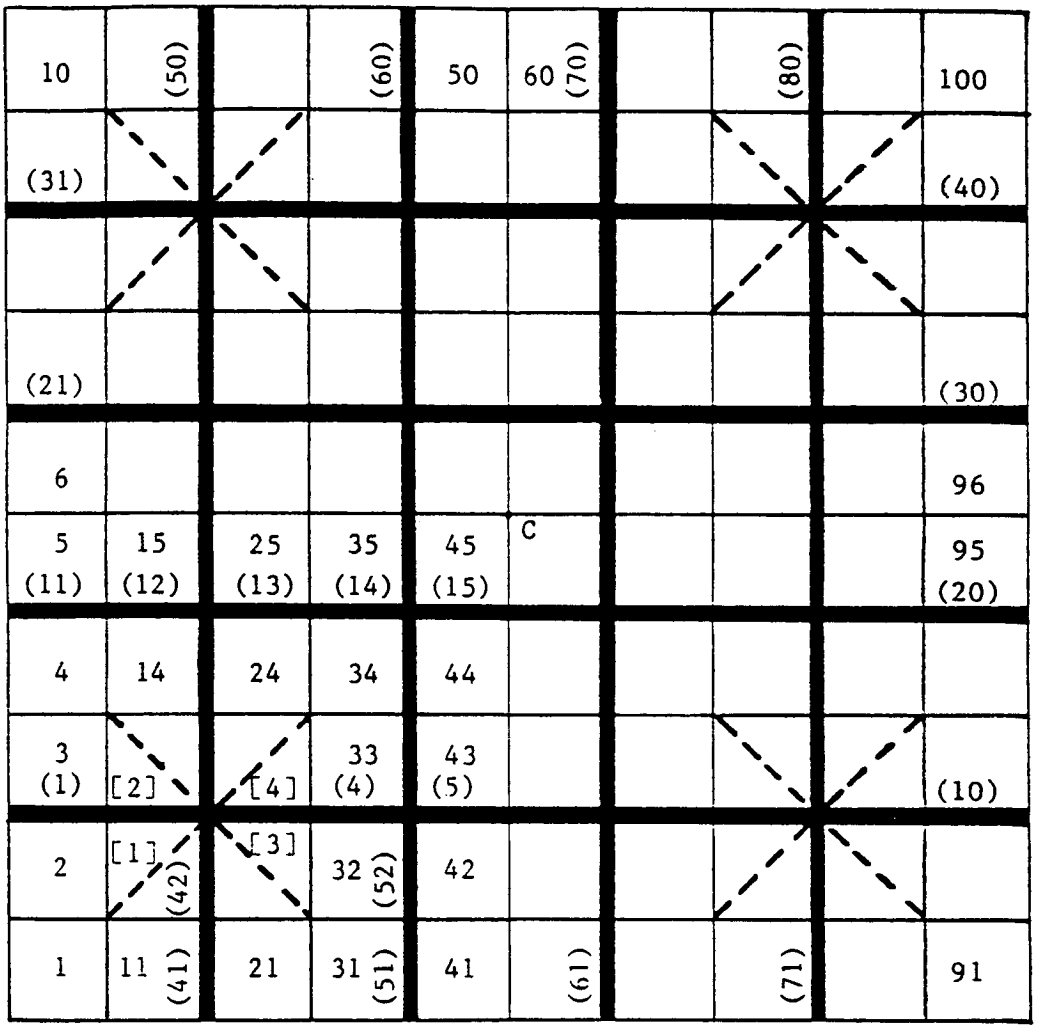

(a) Top View

(b) Side View

i : Plate Element No.
(i) : Beam Element No.
[i] : Truss Element No.

Figure 5.1 Truss-Beam-Plate Built-Up Structure

truss components and no external torques act on the beam. The plates and beams are assumed to be welded together. No dissipation of energy between plate and beam components is presumed to occur during bending and torsion. The derivation of state equations for the plate and beam is based on classical small-deflection theory [106].

Dimensions of the structure and the numbering and spacing of beams in both directions are shown in Fig. 5.1. Coordinates of intersection points of beams and plates are supposed to be in the mid-planes of the plates and neutral axes of the beams. The coordinates of intersection points are then

$$x_i = x_{i-1} + a_i , \qquad i = 1,\ldots,n \tag{5.1}$$

$$y_j = y_{j-1} + b_j , \qquad j = 1,\ldots,m \tag{5.2}$$

$$x_0 = y_0 = 0 \tag{5.3}$$

$$x_{n+1} = L_x , \; y_{m+1} = L_y \tag{5.4}$$

where n(m) is the number of transverse (longitudinal) beams, $a_i(b_j)$ is the distance from the (i-1)th to the ith transverse beam (from the (j-1)th to the jth longitudinal beam), and $L_x(L_y)$ is the dimension of the entire structure in the x(y)-direction.

Suppose applied loads are given as

$$f^{ij} \in L^2(\Omega^{ij}) \quad , \quad i = 1,\ldots,n+1, \quad j = 1,\ldots,m+1 \tag{5.5}$$

where f^{ij} is defined as a uniformly distributed load on the plate and

$$\Omega_1^{ij} = (x_{i-1},x_i) \times (y_{j-1},y_j),\ i = 1,\ldots,n+1,\ j = 1,\ldots,m+1 \qquad (5.6)$$

$$\Omega_2^{ij} = (x_{i-1},x_i),\ y_j \qquad ,\ i = 1,\ldots,n+1,\ j = 1,\ldots,m \qquad (5.7)$$

$$\Omega_3^{ij} = x_i,\ (y_{j-1},y_j) \qquad ,\ i = 1,\ldots,n,\ j = 1,\ldots,m+1 \qquad (5.8)$$

are domains of plates, longitudinal beams, and transverse beams, respectively. Define Γ_k^{ij} as the boundary of Ω_k^{ij}, k=1,2,3. Then, Ω_2^{ij} and Ω_3^{ij} are regarded as parts of Γ_1^{ij}. The superscripts i and j used in Eqs. 5.5 to 5.8 can be applied to the design variables and state variables to identify those values in each component.

The design variables for this built-up structure are the thickness $t^{ij}(x,y)$ of each plate component, the width $\tilde{d}^{ij}(x)$ and height $\tilde{h}^{ij}(x)$ of each longitudinal beam component, the width $\hat{d}^{ij}(y)$ and height $\hat{h}^{ij}(y)$ of each transverse beam component, the constant cross-sectional areas A_k^{ij}(i=1 and n, j=1 and m, k=1-4) of the 4-bar truss members, the positions $\tilde{x}^i$(i=1,...,n) of transverse beams, and the positions $\tilde{y}^j$(j=1,...,m) of longitudinal beams. In vector form, this is

$$u = (t^{ij},\ \tilde{d}^{ij},\ \tilde{h}^{ij},\ \hat{d}^{ij},\ \hat{h}^{ij},\ A_k^{ij},\ \tilde{x}^i,\ \tilde{y}^j) \quad L^\infty(\Omega_1^{ij}) \times L^\infty(\Omega_2^{ij})$$

$$\times L^\infty(\Omega_2^{ij}) \times L^\infty(\Omega_3^{ij}) \times L^\infty(\Omega_3^{ij}) \times (R^4)^4 \times R^n \times R^m \qquad (5.9)$$

It is presumed that the lengths of trusses are fixed, but that they may change their ground positions and that the outside boundary of the entire structure is fixed; i.e., only the locations of beams are variable.

The state variables for this built-up structure consist of the displacement function w^{ij} of each plate component, the displacement function $\tilde{v}^{ij}$ and the rotation $\tilde{\theta}^{ij}$ of each longitudinal beam component, the displacement function $\hat{v}^{ij}$ and the rotation $\tilde{\theta}^{ij}$ of each transverse beam component, and 12 nodal displacement coordinates q_k^{ij} (i=1 and n, j=1 and m, and k=1-3) of truss members.

In vector form, the state variables are thus

$$z \equiv (w^{ij}, \tilde{v}^{ij}, \tilde{\theta}^{ij}, \hat{v}^{ij}, \hat{\theta}^{ij}, q_k^{ij}) \tag{5.10}$$

Kinematic boundary and interface conditions are prerequisite for use of the principle of minimum total potential energy or the principle of virtual work and for design sensitivity calculations, since the displacement fields must satisfy kinematic boundary and interface conditions.

Consider first the kinematic boundary conditions at the interfaces, since there are no kinematic boundary conditions at the free edges. At the interfaces between plate components, the lateral deflections of the plate and beam components are the same. For longitudinal beams,

$$\tilde{v}^{ij} = w^{ij} = w^{i,j+1} \quad , \; i = 1,\ldots,n+1, \; j = 1,\ldots,m \tag{5.11}$$

and for transverse beams,

$$\hat{v}^{ij} = w^{ij} = w^{i+1,j} \quad , \; i = 1,\ldots,n \; , \; j = 1,\ldots,m+1 \tag{5.12}$$

The normal slopes of plate components are the same as the torsion angles of beam components that are attached at the interfaces of open

intervals. For plates and longitudinal beams,

$$\tilde{\theta}^{ij} = w_y^{ij} = w_y^{i,j+1} \quad , \quad i = 1,\ldots,n+1,\ j = 1,\ldots,m \tag{5.13}$$

and for plates and transverse beams,

$$\hat{\theta}^{ij} = w_x^{ij} = w_x^{i+1,j} \quad , \quad i = 1,\ldots,n,\ j = 1,\ldots,m+1 \tag{5.14}$$

The torsion angles of transverse beams and axial slopes of longitudinal beams must be the same at intersection of two beams; i.e.,

$$\hat{\theta}^{ij} = \tilde{\theta}^{ij} = \tilde{\theta}^{i+1,j} \quad , \quad i = 1,\ldots,n,\ j = 1,\ldots,m \tag{5.15}$$

Similarly, the torsion angles of longitudinal beams and axial slopes of transverse beams must be the same at intersection of two beams; i.e.,

$$\tilde{\theta}^{ij} = \hat{\theta}^{ij} = \hat{\theta}^{i,j+1} \quad , \quad i = 1,\ldots,n,\ j = 1,\ldots,m \tag{5.16}$$

It is assumed that each lateral displacement is evaluated at the middle plane of each plate and the neutral axis of each beam. Then, the lateral deflections of two crossing beams and trusses must be the same at the intersection points; i.e.,

$$\left.\begin{aligned} \tilde{v}^{ij} &= \tilde{v}^{i+1,j} \\ \hat{v}^{ij} &= \hat{v}^{i,j+1} \\ \tilde{v}^{ij} &= \hat{v}^{ij} \end{aligned}\right\} \quad i = 1,\ldots n,\ j = 1,\ldots,m \tag{5.17}$$

$$\tilde{v}^{ij} = \hat{v}^{ij} = q_3^{ij} \quad , \ i = 1 \text{ and } n,\ j = 1 \text{ and } m \tag{5.18}$$

With the assumption that there are no in-plane (axial) deformations in the plates (beams), the plates and beams resting on the four 4-bar trusses are presumed to move as a rigid body in the plane of the plates. Referring to Fig. 5.2, one can obtain relationships between horizontal displacements. Defining the position of point 1 in Fig. 5.2, after deformation, as $[(x_1+q_1^{11}), (y_1+q_2^{11})]$ and the rotation angle as ω, the coordinates of positions of points 2, 3, and 4 in Fig. 5.2 can be identified as follows:

For point 2,

$$\left.\begin{aligned} x_1 + q_1^{11} + (x_n - x_1)\cos\omega &= x_n + q_1^{n1} \\ y_1 + q_2^{11} + (x_n - x_1)\sin\omega &= y_1 + q_2^{n1} \end{aligned}\right\} \qquad (5.19)$$

For point 3,

$$\left.\begin{aligned} x_1 + q_1^{11} - (y_m - y_1)\sin\omega &= x_1 + q_1^{1m} \\ y_1 + q_2^{11} + (y_m - y_1)\cos\omega &= y_m + q_2^{1m} \end{aligned}\right\} \qquad (5.20)$$

For point 4,

$$\left.\begin{aligned} x_1 + q_1^{11} + (x_n - x_1)\cos\omega - (y_m - y_1)\sin\omega &= x_n + q_1^{nm} \\ y_1 + q_2^{11} + (x_n - x_1)\sin\omega + (y_m - y_1)\cos\omega &= y_m + q_2^{nm} \end{aligned}\right\} \qquad (5.21)$$

Assuming that the rotation angle ω is small, $\sin\omega \approx \omega$ and $\cos\omega \approx 1$. With this approximation, the system of equations of Eqs. 5.19 to 5.21 yields the following relationships among the unknown parameters q_1^{11}, q_2^{11}, and q_1^{nm}:

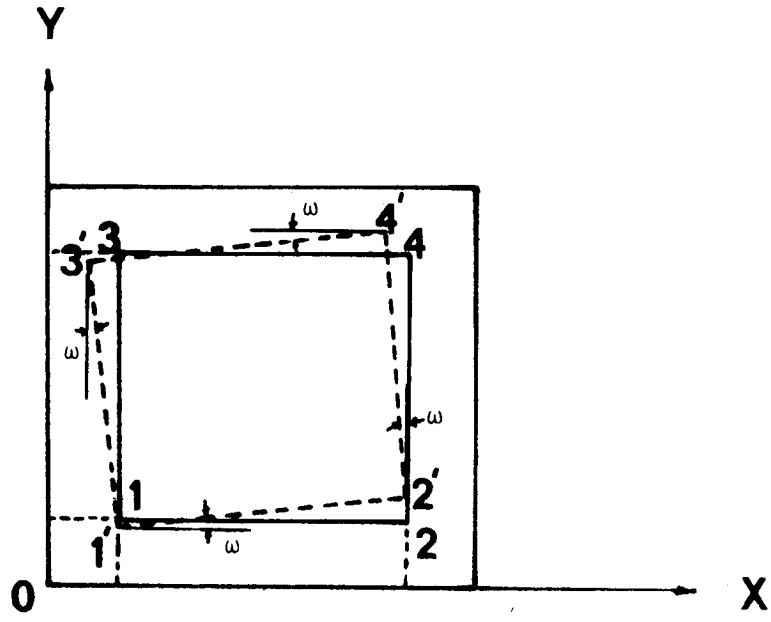

Figure 5.2 Horizontal Displacement of a Truss-Beam-Plate Built-Up Structure

$$q_1^{n1} = q_1^{11} \tag{5.22}$$

$$q_2^{n1} = q_2^{11} + (x_n - x_1)(q_1^{1m} - q_1^{11})/(y_m - y_1) \tag{5.23}$$

$$q_2^{1m} = q_2^{11} \tag{5.24}$$

$$q_1^{nm} = 2q_1^{11} - q_1^{1m} \tag{5.25}$$

$$q_2^{nm} = q_2^{11} + (x_n - x_1)(q_1^{nm} - q_1^{11})/(y_m - y_1) \tag{5.26}$$

One may now define the set Z of kinematically admissible displacement fields as follows:

$$Z = \{z = (w^{ij}, \tilde{v}^{ij}, \tilde{\theta}^{ij}, \hat{v}^{ij}, \hat{\theta}^{ij}, q_k^{11}, q_k^{n1}, q_k^{1m}, q_k^{nm}) \in H_0^2(\Omega_1^{ij}) \times H_0^2(\Omega_2^{ij}) \times H_0^1(\Omega_2^{ij}) \times H_0^2(\Omega_3^{ij}) \times H_0^1(\Omega_3^{ij}) \times R^3 \times R^3 \times R^3 \times R^3 ,$$

such that all the boundary conditions of Eqs. 5.11 to 5.26 are satisfied$\}$ (5.27)

Now consider the natural boundary conditions at the free edges and interfaces of plate components. At the four free edges, the bending moments and vertical edge forces are zero. For the plate components, at the free edges,

$$\left.\begin{aligned} M_x^{ij} &= 0 \\ V_x^{ij} &= 0 \end{aligned}\right\} \qquad i = 0 \text{ and } n+1,\ j = 1,\ldots,m+1 \tag{5.28}$$

$$\left.\begin{aligned} M_y^{ij} &= 0 \\ V_y^{ij} &= 0 \end{aligned}\right\} \qquad i = 1,\ldots,n+1,\ j = 0 \text{ and } m+1 \qquad (5.29)$$

where M_x, V_x, M_y, and V_y are defined in Table 3.2.

For the beam components at the free edges,

$$\left.\begin{aligned} \tilde{M}_x^{ij} &= 0 \\ \tilde{V}_x^{ij} &= 0 \end{aligned}\right\} \qquad i = 0 \text{ and } n+1,\ j = 1,\ldots,m \qquad (5.30)$$

$$\left.\begin{aligned} \tilde{M}_y^{ij} &= 0 \\ \tilde{V}_y^{ij} &= 0 \end{aligned}\right\} \qquad i = 1,\ldots,n,\ j = 0 \text{ and } m+1 \qquad (5.31)$$

where $\tilde{M}_x$, $\tilde{V}_x$, $\tilde{M}_y$, and $\tilde{V}_y$ are defined in Table 3.2.

At the interface of open intervals between plate components, the difference of effective shear forces [106,107] between adjacent plate components acts as the load on the beam component attached, while the difference of bending moments between adjacent plate components acts as the twisting moment on the beam component attached. For transverse beams,

$$\left.\begin{aligned} M_x^{ij} - M_x^{i+1,j} &= -G\hat{\hat{J}}v_{xyy}^{ij} \\ V_x^{ij} - V_x^{i+1,j} &= -(E\hat{\hat{I}}v_{yy}^{ij})_{yy} \end{aligned}\right\} \qquad i = 1,\ldots,n,\ j = 1,\ldots,m+1 \qquad (5.32)$$

Similarly, for longitudinal beams,

$$\left.\begin{aligned} M_y^{ij} - M_y^{i,j+1} &= -G\tilde{\tilde{J}}v_{xxy}^{ij} \\ V_y^{ij} - V_y^{i,j+1} &= -(E\tilde{\tilde{I}}v_{xx}^{ij})_{xx} \end{aligned}\right\} \qquad i = 1,\ldots,n+1,\ j = 1,\ldots,m \qquad (5.33)$$

where G is shear modulus and $\tilde{J}(\hat{J})$ is the torsion constant of longitudinal (transverse) beam component.

At intersection points of crossing beams, relationships between corner forces of plate components and shear forces of beam components are

$$2M_{xy}^{ij}-2M_{xy}^{i+1,j}-2M_{xy}^{i,j+1}+2M_{xy}^{i+1,j+1}+\tilde{V}_x^{i,j}-\tilde{V}_x^{i+1,j}+\tilde{V}_y^{i,j}-\tilde{V}_y^{i,j+1}=0 \qquad (5.34)$$

where M_{xy} is defined in Table 3.2.

The variational equation of Eq. 2.39, for static response, becomes

$$\begin{aligned}
a_{u,\Omega}(z,\bar{z}) = &\sum_{i=1}^{n+1}\sum_{j=1}^{m+1}\iint_{\Omega_1^{ij}} D^{ij}[(w_{xx}^{ij}+w_{yy}^{ij})(\bar{w}_{xx}^{ij}+\bar{w}_{yy}^{ij}) \\
&+(1-\nu)(2w_{xy}^{ij}\bar{w}_{xy}^{ij}-w_{xx}^{ij}\bar{w}_{yy}^{ij}-w_{yy}^{ij}\bar{w}_{xx}^{ij})]d\Omega_1 \\
&+\sum_{i=1}^{n+1}\sum_{j=1}^{m}\int_{\Omega_2^{ij}}(E\tilde{I}\tilde{v}_{xx}^{ij}\bar{\tilde{v}}_{xx}^{ij}+G\tilde{J}\tilde{v}_{xy}^{ij}\bar{\tilde{v}}_{xy}^{ij})d\Omega_2 \\
&+\sum_{i=1}^{n}\sum_{j=1}^{m+1}\int_{\Omega_3^{ij}}(E\hat{I}\hat{v}_{yy}^{ij}\bar{\hat{v}}_{yy}^{ij}+G\hat{J}\hat{v}_{xy}^{ij}\bar{\hat{v}}_{xy}^{ij})d\Omega_3 \\
&+q_k^{11T}K(A_\ell^{11})\bar{q}_k^{11}+q_k^{1mT}K(A_\ell^{1m})\bar{q}_k^{1m}+q_k^{n1T}K(A_\ell^{n1})\bar{q}_k^{n1} \\
&+q_k^{nmT}K(A_\ell^{nm})\bar{q}_k^{nm} \\
=&\sum_{i=1}^{n+1}\sum_{j=1}^{m+1}\iint_{\Omega_1^{ij}} f^{ij}\bar{w}^{ij}d\Omega_1=\ell_{u,\Omega}(\bar{z}) \qquad (5.35)
\end{aligned}$$

Similarly, the variational eigenvalue equation of Eq. 2.45 becomes [108]

$$a_{u,\Omega}(y,\bar{y}) = \varsigma[\sum_{i=1}^{n+1}\sum_{j=1}^{m+1}\iint_{\Omega_1^{ij}}\rho t^{ij}y^{ij}\bar{y}^{ij}d\Omega_1$$

$$+\sum_{i=1}^{n+1}\sum_{j=1}^{m}\int_{\Omega_2^{ij}}(\rho\tilde{d}^{ij}\tilde{h}^{ij}\tilde{y}^{ij}\bar{\tilde{y}}^{ij}+\tilde{I}^{ij}\tilde{y}_y^{ij}\bar{\tilde{y}}_y^{ij})d\Omega_2$$

$$+\sum_{i=1}^{n}\sum_{j=1}^{m+1}\int_{\Omega_3^{ij}}(\rho\hat{d}^{ij}\hat{h}^{ij}\hat{y}^{ij}\bar{\hat{y}}^{ij}+\hat{I}^{ij}\hat{y}_x^{ij}\bar{\hat{y}}_x^{ij})d\Omega_3$$

$$+\rho(A_\ell^{11}\ell_\ell^{11}y_k^{11}\bar{y}_k^{11}+A_\ell^{n1}\ell_\ell^{n1}y_k^{n1}\bar{y}_k^{n1}$$

$$+A_\ell^{1m}\ell_\ell^{1m}y_k^{1m}\bar{y}_k^{1m}+A_\ell^{nm}\ell_\ell^{nm}y_k^{nm}\bar{y}_k^{nm})] = \varsigma d_{u,\Omega}(y,\bar{y}) \qquad (5.36)$$

5.3 Formulation of the Optimal Design Problem

Minimum weight design of this truss-beam-plate built-up structure, subject to constraints that arise in most structures, is considered. Volume of the built-up structure is the cost functional to be minimized,

$$\Psi_0 = \sum_{i=1}^{n+1}\sum_{j=1}^{m+1}\iint_{\Omega_1^{ij}}t^{ij}d\Omega_1+\sum_{i=1}^{n+1}\sum_{j=1}^{m}\int_{\Omega_2^{ij}}\tilde{d}^{ij}\tilde{h}^{ij}d\Omega_2$$

$$+\sum_{i=1}^{n}\sum_{j=1}^{m+1}\int_{\Omega_3^{ij}}\hat{d}^{ij}\hat{h}^{ij}d\Omega_3+\sum_{i=1}^{16}A_i\ell_i \qquad (5.37)$$

where $A_i(\ell_i)$ is the cross-sectional area (length) of the ith truss member.

The design problem is to find the optimum distribution of design variables to minimize Ψ_0, subject to the following constraints:

Compliance Constraint;

$$\Psi_1 = \sum_{i=1}^{n+1}\sum_{j=1}^{m+1}\iint_{\Omega_1^{ij}}f^{ij}w^{ij}d\Omega - FW^a \leq 0 \qquad (5.38)$$

where FW^a is the maximum allowable value.

Displacement Constraint;

$$\psi_2 = \left| \iint_{\Omega_1^{ij}} \hat{\delta}(x-\hat{x}) w^{i_0 j_0} d\Omega \right| - z^a \leq 0 \tag{5.39}$$

where $\hat{x} \in \Omega_1^{i_0 j_0}$ is a fixed point, $\hat{\delta}(x)$ is the dirac measure in the plane acting at the origin, and z^a is the maximum allowable value.

Stress Constraint on Plate Elements;

The maximum stress for a thin plate occurs on the surface of the plate and is given in the form [107]

$$\left.\begin{aligned} \sigma_{xx} &= -\frac{Et}{2(1-\nu^2)} (w_{xx} + \nu w_{yy}) \\ \sigma_{yy} &= -\frac{Et}{2(1-\nu^2)} (w_{yy} + \nu w_{xx}) \\ \tau_{xy} &= -\frac{Et}{1+\nu} w_{xy} \end{aligned}\right\} \tag{5.40}$$

The Von-Mises failure criterion is [107]

$$\phi(\sigma) = (\sigma_{xx}^2 + \sigma_{yy}^2 + 3\tau_{xy}^2 - \sigma_{xx}\sigma_{yy})^{1/2} \tag{5.41}$$

One may transform the above pointwise constraint to integral form over plate finite elements, by weighting the stress field with a characteristic function. The averaged constraint on $\phi(\sigma)$ in this small region is

$$\psi_3 = \iint_{\Omega_1^{i_0 j_0}} \phi(\sigma) M_p d\Omega - \sigma_p^a \leq 0 \tag{5.42}$$

where M_p is a characteristic function that is defined on each plate element of $\Omega_1^{i_0 j_0}$ and is zero outside that plate element and σ_p^a is a given allowable yield stress.

Stress Constraint on Beam Elements;

The bending stress functional over beam finite elements is obtained by weighting the stress field with a characteristic function defined in that region as

$$\Psi_4 = \int_{\Omega_2^{i_0 j_0}} \sigma_b M_b d\Omega - \sigma_b^a \leq 0 \tag{5.43}$$

where M_b is a characteristic function that is defined on each beam element of $\Omega_2^{i_0 j_0}$ and is zero outside that beam element, σ_b^a is the given allowable stress on the beam element, and σ_b is the bending stress, defined as

$$\sigma_b = -\frac{E\tilde{h}}{2}\tilde{v}_{xx} \tag{5.44}$$

Similarly, stress constraints on transverse beam elements can be defined as in Eq. 5.43.

Eigenvalue Constraint;

The natural frequency bound must be met by the structure,

$$\Psi_5 = \zeta_0 - \zeta \leq 0 \tag{5.45}$$

where $\zeta = \omega^2$ is the computed smallest eigenvalue and ζ_0 is the lower bound.

Design Variable Bounds;

$$t_i^\ell < t_i < t_i^u \quad , i = 1,\ldots,NE \tag{5.46}$$

$$d_j^\ell < d_j < d_j^u \quad , j = 1,\ldots,NB \tag{5.47}$$

$$h_k^\ell < h_k < h_k^u \quad , k = 1,\ldots,NB \tag{5.48}$$

$$A_n^{\ell} < A_n < A_n^{u} \quad , n = 1,\ldots,NT \tag{5.49}$$

$$x_i^{\ell} < x_i < x_i^{u} \quad , i = 1,\ldots,n \tag{5.50}$$

$$y_j^{\ell} < y_j < y_j^{u} \quad , j = 1,\ldots,m \tag{5.51}$$

where NE is the number of plate elements, NB is the number of beam elements, NT is the number of trusses, n(m) is the number of transverse (longitudinal) beams, the superscript ℓ denotes lower bound, and the superscript u denotes upper bound.

5.4 Design Sensitivity Analysis

Design sensitivity analysis results of Chapter 2 and the shape design sensitivity technique of Chapter 3 are employed directly to obtain design sensitivity forms, with both design and shape variations, for the present model. Design derivatives of cost and constraint functionals considered in Section 5.3 are obtained. As discussed in the preceding chapters, the procedure for obtaining static design sensitivity, using the adjoint variable method, is identical with only a different adjoint load functional that depends on constraints. For the compliance and eigenvalue constraints, it is not required to introduce an adjoint variable.

The design derivative of the cost functional of Eq. 5.37 is calculated directly as

$$\Psi_0' = \sum_{i=1}^{n+1}\sum_{j=1}^{m+1} \iint_{\Omega_1^{ij}} \delta t^{ij} d\Omega_1 + \sum_{i=1}^{n+1}\sum_{j=1}^{m} \int_{\Omega_2^{ij}} (\tilde{d}^{ij}\delta\tilde{h}^{ij} + \tilde{h}^{ij}\delta\tilde{d}^{ij}) d\Omega_2$$

$$+ \sum_{i=1}^{n}\sum_{j=1}^{m+1} \int_{\Omega_3^{ij}} (\hat{d}^{ij}\delta\hat{h}^{ij} + \hat{h}^{ij}\delta\hat{d}^{ij}) d\Omega_3 + \sum_{i=1}^{16} \ell_i \delta A_i$$

$$+ \sum_{i=1}^{n}\sum_{j=1}^{m+1} \int_{\Gamma_1^{ij}} t^{ij}(v^{ij^T} n^{ij}) d\Gamma_1 + \sum_{i=1}^{n+1}\sum_{j=1}^{m} \int_{\Gamma_2^{ij}} \tilde{d}^{ij}\tilde{h}^{ij}(v^{ij^T} n^{ij}) d\Gamma_2$$

$$+ \sum_{i=1}^{n}\sum_{j=1}^{m+1} \int_{\Gamma_3^{ij}} \hat{d}^{ij}\hat{h}^{ij}(v^{ij^T} n^{ij}) d\Gamma_3 \qquad (5.52)$$

Consider first the design derivatives of the displacement constraint of Eq. 5.39. Since $\hat{\delta}(x-\hat{x})$ in Eq. 5.39 is defined on a neighborhood of $\bar{\Omega}_1^{i_0 j_0}$ by zero extension and $\hat{x}$ is fixed, $\hat{\delta}'(x-\hat{x}) = 0$. Thus, one can treat Eq. 5.39 as the functional form of Eq. 2.63 and the adjoint equation is, from Eq. 2.70,

$$a(\lambda,\bar{\lambda}) = \iint_{\Omega_1^{i_0 j_0}} \hat{\delta}(x-\hat{x})\bar{\bar{w}} d\Omega \qquad (5.53)$$

for all $\bar{\lambda} \in Z$. Equation 5.53 has a unique solution λ, which is the displacement due to a unit load at $\hat{x}$. That is, with smoothness assumptions, the variational equation of Eq. 5.53 is equivalent to the formal operator equation

$$\left.\begin{aligned} D^{i_0 j_0}\nabla^4 \bar{w}^{i_0 j_0} &= \hat{\delta}(x-\hat{x}) \quad , \quad x \in \Omega_1^{i_0 j_0} \\ D^{ij}\nabla^4 \bar{w}^{ij} &= 0 \quad , \quad x \in \Omega_1^{ij} \setminus \Omega_1^{i_0 j_0}, \quad i=1,\ldots,n+1, \quad j=1,\ldots,m+1 \end{aligned}\right\} \qquad (5.54)$$

where λ satisfies the boundary and interface conditions of Eqs. 5.11 to 5.34.

Once the adjoint variable is obtained by solving Eq. 5.54, one is in a position to evaluate the final design sensitivity forms of Eq. 2.72 for this displacement constraint as a combination of conventional and shape design sensitivities. The conventional design sensitivity, the first bracket of Eq. 2.72, is simply the explicit design derivatives of the constraint functional, load functional, and the variational equation of Eq. 5.35. For the shape design sensitivity, the second bracket of Eq. 2.72, a unified method for shape design sensitivity analysis can be employed as in Chapter 3 to obtain the final shape design sensitivity forms. Since the constraint and load functionals are independent of design variables, the final design sensitivities can be written as

$$
\begin{aligned}
\psi_2' = & - a'_{\delta u,\Omega}(z,\lambda) \\
& + \sum_{i=1}^{n+1} \sum_{j=1}^{m+1} \int_{\Gamma_1^{ij}} \Lambda_1^{ij}(z,\lambda) V^{ij^T} n^{ij} d\Gamma \\
& + \sum_{i=1}^{n+1} \sum_{j=1}^{m} \int_{\Gamma_2^{ij}} \Lambda_2^{ij}(z,\lambda) V^{ij^T} n^{ij} d\Gamma \\
& + \sum_{i=1}^{n} \sum_{j=1}^{m+1} \int_{\Gamma_3^{ij}} \Lambda_3^{ij}(z,\lambda) V^{ij^T} n^{ij} d\Gamma
\end{aligned}
\tag{5.55}
$$

where

$$
\begin{aligned}
a'_{\delta u,\Omega}(z,\lambda) = & \sum_{i=1}^{n+1} \sum_{j=1}^{m+1} \iint_{\Omega_1^{ij}} D_t^{ij} [(w_{xx}^{ij} + w_{yy}^{ij})(\bar{w}_{xx}^{ij} + \bar{w}_{yy}^{ij}) \\
& + (1-\nu)(2w_{xy}^{ij}\bar{w}_{xy}^{ij} - w_{xx}^{ij}\bar{w}_{yy}^{ij} - w_{yy}^{ij}\bar{w}_{xx}^{ij})] d\Omega_1
\end{aligned}
$$

$$+ \sum_{i=1}^{n+1} \sum_{j=1}^{m} \int_{\Omega_2^{ij}} (EI^{\tilde{b}^{ij}} v^{\tilde{ij}}_{xx} \bar{v}^{\tilde{ij}}_{xx} + GJ^{\tilde{b}^{ij}} v^{\tilde{ij}}_{xy} \bar{v}^{\tilde{ij}}_{xy}) d\Omega_2$$

$$+ \sum_{i=1}^{n} \sum_{j=1}^{m+1} \int_{\Omega_3^{ij}} (EI^{\hat{b}^{ij}} v^{\hat{ij}}_{yy} \bar{v}^{\hat{ij}}_{yy} + GJ^{\hat{b}^{ij}} v^{\hat{ij}}_{xy} \bar{v}^{\hat{ij}}_{xy}) d\Omega_3 \qquad (5.56)$$

$\tilde{b} = [\tilde{d},\tilde{h}]$, $\hat{b} = [\hat{d},\hat{h}]$, and

$$\Lambda_1(z,\lambda) = D\{w_{xx}\bar{w}_{xx} - w_{yy}\bar{w}_{yy} - (w_{xxx} + \nu w_{xyy})\bar{w}_x - (\bar{w}_{xxx} + \nu\bar{w}_{xyy})w_x\}$$

$$\text{at } x = x_i, \quad i = 1 - n \qquad (5.57)$$

$$\Lambda_1(z,\lambda) = D\{w_{yy}\bar{w}_{yy} - w_{xx}\bar{w}_{xx} - (w_{yyy} + \nu w_{xxy})\bar{w}_y - (\bar{w}_{yyy} + \nu\bar{w}_{xxy})w_y\}$$

$$\text{at } y = y_j, \quad j = 1 - m \qquad (5.58)$$

$$\Lambda_2(z,\lambda) = E\tilde{\tilde{I}}\tilde{v}_x\bar{\tilde{v}}_{xx} - (E\tilde{\tilde{I}}\tilde{v}_{xx})_x\bar{\tilde{v}}_x - (E\tilde{\tilde{I}}\bar{\tilde{v}}_{xx})_x\tilde{v}_x + G\tilde{\tilde{J}}\tilde{v}_{xy}\bar{\tilde{v}}_{xy}$$

$$\text{at } x = x_i, \quad i = 1 - n \qquad (5.59)$$

$$\Lambda_3(z,\lambda) = E\hat{\hat{I}}\hat{v}_{yy}\bar{\hat{v}}_{yy} - (E\hat{\hat{I}}\hat{v}_{yy})_y\bar{\hat{v}}_y - (E\hat{\hat{I}}\bar{\hat{v}}_{yy})_y\hat{v}_y + G\hat{\hat{J}}\hat{v}_{xy}\bar{\hat{v}}_{xy}$$

$$\text{at } y = y_j, \quad j = 1 - m \qquad (5.60)$$

For the design derivatives of the compliance constraint of Eq. 5.38, one notes that the integral of Eq. 5.38 depends on the load f^{ij}. However, since $f^{ij'} = 0$, one can treat Eq. 5.38 as the functional form of Eq. 2.63. Therefore, the adjoint equation is, from Eq. 2.70,

$$a(\lambda,\bar{\lambda}) = \sum_{i=1}^{n+1} \sum_{j=1}^{m+1} \iint_{\Omega_1^{ij}} f^{ij=}_{w} \, d\Omega \qquad (5.61)$$

for all $\bar{\lambda} \in Z$. The load functional on the right of Eq. 5.61 is precisely the same as the load functional for the original problem of Eq. 5.35. In this special case $\lambda = z$, so from Eq. 2.72 one obtains the same design sensitivity form of Eq. 5.55, with the adjoint variable λ replaced by state variable z; i.e.,

$$\psi_1' = - a'_{\delta u,\Omega}(z,z) + \sum_{i=1}^{n+1} \sum_{j=1}^{m+1} \int_{\Gamma_1^{ij}} \Lambda_1^{ij}(z,z) v^{ij^T} n^{ij} d\Gamma$$

$$+ \sum_{i=1}^{n+1} \sum_{j=1}^{m} \int_{\Gamma_2^{ij}} \Lambda_2^{ij}(z,z) v^{ij^T} n^{ij} d\Gamma + \sum_{i=1}^{n} \sum_{j=1}^{m+1} \int_{\Gamma_3^{ij}} \Lambda_3^{ij}(z,z) v^{ij^T} n^{ij} d\Gamma \tag{5.62}$$

where the terms in Eq. 5.62 are defined in Eqs. 5.56 to 5.60.

Consider next the stress constraint on a plate element of Eq. 5.42, treated as the functional form of Eq. 2.63 that depends on the second derivatives of the displacement functions. The adjoint equation is, from Eq. 2.70,

$$a(\lambda,\bar{\lambda}) = \iint_{\Omega_1^{i_0 j_0}} \frac{1}{2} (\sigma_{xx}^2 + \sigma_{yy}^2 + 3\tau_{xy}^2 - \sigma_{xx}\sigma_{yy})^{-\frac{1}{2}}$$

$$\left\{ - \frac{Et\sigma_{xx}}{(1-\nu)^2} (\bar{w}_{xx} + \nu \bar{w}_{yy}) - \frac{Et\sigma_{yy}}{(1-\nu^2)} (\bar{w}_{yy} + \nu \bar{w}_{xx}) \right.$$

$$- \frac{6Et\tau_{xy}}{(1+\nu)} \bar{w}_{xy} + \frac{Et\sigma_{xx}}{2(1-\nu^2)} (\bar{w}_{yy} + \nu \bar{w}_{xx})$$

$$\left. + \frac{Et\sigma_{yy}}{2(1-\nu^2)} (\bar{w}_{xx} + \nu \bar{w}_{yy}) \right\} M_p \, d\Omega \tag{5.63}$$

for all $\bar{\lambda} \in Z$. With smoothness assumptions, the variational equation of Eq. 5.63 is equivalent to the formal operator equation

$$D^{i_0j_0}\nabla^4 w - {}^{i_0j_0} = \frac{1}{2}\left(\sigma_{xx}^2 + \sigma_{yy}^2 + 3\tau_{xy}^2 - \sigma_{xx}\sigma_{yy}\right)^{-\frac{1}{2}}$$

$$\Big\{ -\frac{Et\sigma_{xx}}{(1-\nu^2)}\left(M_{p_{xx}} + \nu M_{p_{yy}}\right) - \frac{Et\sigma_{yy}}{(1-\nu^2)}\left(M_{p_{yy}} + \nu M_{p_{xx}}\right)$$

$$-\frac{6Et\tau_{xy}}{(1+\nu)} M_{p_{xy}} + \frac{Et\sigma_{xx}}{2(1-\nu^2)}\left(M_{p_{yy}} + \nu M_{p_{xx}}\right) + \frac{Et\sigma_{yy}}{2(1-\nu^2)}\left(M_{p_{xx}} + \nu M_{p_{yy}}\right)\Big\}$$

$$x \in \Omega_1^{i_0j_0},$$

$$D^{ij}\nabla^4 w^{ij} = 0 \quad , \qquad x \in \Omega_1^{ij} \setminus \Omega_1^{i_0j_0}, \quad i = 1,\ldots,n+1, \quad j = 1,\ldots,m+1 \tag{5.64}$$

where λ satisfies the boundary and interface conditions of Eqs. 5.11 to 5.34. By solving Eq. 5.64, one evaluates the final design sensitivity forms of Eq. 2.72 as in the displacement constraint with the same arguments discussed there. However, since the constraint functional in this case depends on the design variable explicitly, its design derivative is added to the conventional design sensitivity form of Eq. 5.55. Then, the final design sensitivity form is written, including the element boundary movement effect of Eq. 4.31, as

$$\psi_3' = \iint_{\Omega_1^{i_0j_0}} \frac{1}{2}\left(\sigma_{xx}^2 + \sigma_{yy}^2 + 3\tau_{xy}^2 - \sigma_{xx}\sigma_{yy}\right)^{-\frac{1}{2}} \Big[-\frac{E\sigma_{xx}}{(1-\nu^2)}\left(w_{xx} + \nu w_{yy}\right)$$

$$-\frac{E\sigma_{yy}}{(1-\nu^2)}\left(w_{yy} + \nu w_{xx}\right) - \frac{6E\tau_{xy}}{(1+\nu)} w_{xy} + \frac{E\sigma_{xx}}{2(1-\nu^2)}\left(w_{yy} + \nu w_{xx}\right)$$

$$+\frac{E\sigma_{yy}}{2(1-\nu^2)}\left(w_{xx} + \nu w_{yy}\right)\Big] M_p \, d\Omega - a'_{\delta u,\Omega}(z,\lambda)$$

$$+\sum_{i=1}^{n+1}\sum_{j=1}^{m+1}\int_{\Gamma_1^{ij}}\Lambda_1^{ij}(z,\lambda)V^{ij^T}n^{ij}d\Gamma+\sum_{i=1}^{n+1}\sum_{j=1}^{m}\int_{\Gamma_2^{ij}}\Lambda_2^{ij}(z,\lambda)V^{ij^T}n^{ij}d\Gamma$$

$$+\sum_{i=1}^{n}\sum_{j=1}^{m+1}\int_{\Gamma_3^{ij}}\Lambda_3^{ij}(z,\lambda)V^{ij^T}n^{ij}d\Gamma$$

$$-M_p^2\int_{\Gamma_M^{i_0j_0}}V^{M^T}nd\Gamma\int_{\Omega_1^{i_0j_0}}(\sigma_{xx}^2+\sigma_{yy}^2+3\tau_{xy}^2-\sigma_{xx}\sigma_{yy})^{\frac{1}{2}}d\Omega$$

$$+\int_{\Gamma_M^{i_0j_0}}(\sigma_{xx}^2+\sigma_{yy}^2+3\tau_{xy}^2-\sigma_{xx}\sigma_{yy})^{\frac{1}{2}}M_pV^{M^T}nd\Gamma \qquad (5.65)$$

where the terms in Eq. 5.65 are defined in Eqs. 5.56 to 5.60, $\Gamma_M^{i_0j_0}$ and V^M denote the element boundary and its velocity, respectively.

Similarly, for stress constraints on longitudinal beam elements of Eq. 5.43, the adjoint equation is, from Eq. 2.70,

$$a(\lambda,\bar{\lambda}) = -\int_{\Omega_2^{i_0j_0}}\frac{E\tilde{h}}{2}\tilde{\tilde{v}}_{xx}M_b d\Omega \qquad (5.66)$$

for all $\bar{\lambda}\in Z$. This is equivalent to the formal operator equation, with smoothness assumptions,

$$D^{ij}\nabla^4\bar{w}^{ij}=0,\quad x\in\Omega_1^{ij},\ i=1,\ldots,n+1,\ j=1,\ldots,m+1 \qquad (5.67)$$

where λ satisfies the boundary and interface conditions of Eqs. 5.11 to 5.34 except at the interface $\Gamma_1^{i_0j_0}$ (precisely $\Omega_2^{i_0j_0}$). At the interface $\Omega_2^{i_0j_0}$, different jump condition caused by the line load of Eq. 5.66 is made as

$$V_y^{i_0j_0}-V_y^{i_0j_0+1}=-(E\tilde{\tilde{I}}\tilde{\tilde{v}}_{xx})_{xx}-(\frac{E\tilde{h}}{2}M_b)_{xx},\quad x\in\Omega_2^{i_0j_0} \qquad (5.68)$$

With the adjoint variable obtained by solving Eq. 5.67, one can write the final design sensitivity form of Eq. 2.72, with design derivatives of the constraint functional for conventional design sensitivity as in the case of stress constraint on a plate element, as

$$\psi_4' = -\int_{\Omega_2} {}_{i_0}{}_{j_0} \frac{E}{2} \tilde{v}_{xx} M_b d\Omega - a'_{\delta u,\Omega}(z,\lambda) + \sum_{i=1}^{n+1}\sum_{j=1}^{m+1} \int_{\Gamma_1^{ij}} \Lambda_1^{ij}(z,\lambda) v^{ij^T} n^{ij} d\Gamma$$
$$+ \sum_{i=1}^{n+1}\sum_{j=1}^{m} \int_{\Gamma_2^{ij}} \Lambda_2^{ij}(z,\lambda) v^{ij^T} n^{ij} d\Gamma + \sum_{i=1}^{n}\sum_{j=1}^{m+1} \int_{\Gamma_3^{ij}} \Lambda_3^{ij}(z,\lambda) v^{ij^T} n^{ij} d\Gamma \tag{5.69}$$

where the terms in Eq. 5.69 are defined in Eqs. 5.56 to 5.60.

Finally, for the eigenvalue constraint of Eq. 5.45, the design derivatives of a simple eigenvalue, given by Eq. 2.78 are obtained. The conventional design sensitivity, the first bracket of Eq. 2.78, is the explicit design derivative of the variational eigenvalue equation of Eq. 5.36 and the shape design sensitivity, the second bracket of Eq. 2.78, can be obtained by using the unified method for shape design sensitivity analysis as in static response case and by imposing the boundary/interface conditions defined in Eqs. 5.11 through 5.34. Then, the final eigenvalue design sensitivities can be written, using the notion s instead of y for the eigenfunction in this section to avoid the confusion, as

$$\zeta' = a'_{\delta u,\Omega}(s,s) - \zeta d'_{\delta u,\Omega}(s,s) + \sum_{i=1}^{n+1}\sum_{j=1}^{m+1} \int_{\Gamma_1^{ij}} \bar{\Lambda}_1(s,s) v^{ij^T} n^{ij} d\Gamma$$
$$+ \sum_{i=1}^{n+1}\sum_{j=1}^{m} \int_{\Gamma_2^{ij}} \bar{\Lambda}_2^{ij}(s,s) v^{ij^T} n^{ij} d\Gamma + \sum_{i=1}^{n}\sum_{j=1}^{m+1} \int_{\Gamma_3^{ij}} \bar{\Lambda}_3^{ij}(s,s) v^{ij^T} n^{ij} d\Gamma \tag{5.70}$$

where $a'_{\delta u,\Omega}(s,s)$ is defined in Eq. 5.56 and

$$d'_{\delta u,\Omega}(s,s) = \sum_{i=1}^{n+1}\sum_{j=1}^{m+1} \iint_{\Omega_1^{ij}} \rho s^{ij\,2}\, d\Omega_1$$

$$+ \sum_{i=1}^{n+1}\sum_{j=1}^{m} \int_{\Omega_2^{ij}} [\rho(\tilde{d}^{ij}\tilde{h}^{ij})_{\tilde{b}^{ij}} \tilde{s}^{ij\,2} + \tilde{I}^{ij}_{\tilde{b}^{ij}} \tilde{s}_y^{ij\,2}]\, d\Omega_2$$

$$+ \sum_{i=1}^{n}\sum_{j=1}^{m+1} \int_{\Omega_3^{ij}} [\rho(\hat{d}^{ij}\hat{h}^{ij})_{\hat{b}^{ij}} \hat{s}^{ij\,2} + \hat{I}^{ij}_{\hat{b}^{ij}} \hat{s}_x^{ij\,2}]\, d\Omega_3 \qquad (5.71)$$

$$\bar{\Lambda}_1(s,s) = D\{-s_{xx}^2 + s_{yy}^2 + 2(s_{xxx} + \nu s_{xyy})s_x\} - \zeta\rho t s^2$$

$$\text{at } x = \tilde{x}_i\,, \quad i = 1\text{-}n \qquad (5.72)$$

$$\bar{\Lambda}_1(s,s) = D\{-s_{yy}^2 + s_{xx}^2 + 2(s_{yyy} + \nu s_{xxy})s_y\} - \zeta\rho t s^2$$

$$\text{at } y = \tilde{y}_j\,, \quad j = 1\text{-}m \qquad (5.73)$$

$$\bar{\Lambda}_2(s,s) = 2(E\tilde{\tilde{I}}\tilde{s}_{xx})_x \tilde{s}_x - E\tilde{\tilde{I}}\tilde{s}_{xx}^2 - G\tilde{\tilde{J}}\tilde{s}_{xy}^2 - \zeta(\rho\tilde{\tilde{d}}\tilde{\tilde{h}}\tilde{s}^2 + \tilde{\tilde{I}}\tilde{s}_y^2)$$

$$\text{at } x = \tilde{x}_i\,, \quad i = 1\text{-}n \qquad (5.74)$$

$$\bar{\Lambda}_3(s,s) = 2(E\hat{\hat{I}}\hat{s}_{yy})_y \hat{s}_y - E\hat{\hat{I}}\hat{s}_{yy}^2 - G\hat{\hat{J}}\hat{s}_{xy}^2 - \zeta(\rho\hat{\hat{d}}\hat{\hat{h}}\hat{s}^2 + \hat{\hat{I}}\hat{s}_x^2)$$

$$\text{at } y = \tilde{y}_j\,, \quad j = 1\text{-}m \qquad (5.75)$$

The calculation of derivatives of design variable bounds of Eqs. 5.46 to 5.51 is trivial.

5.5 Numerical Results and Discussion

Numerical calculation of design sensitivities for the constraints presented in Sections 5.3 and 5.4 for the present model is carried out using the finite element method. A finite dimensional optimization method [101] is employed for the present problem, to match the accuracy of the finite element analysis. Numerical considerations discussed in Chapter 4 are applied to solve this problem.

For structural analysis of this built-up structure, in the first stage, the stiffness and mass matrices of the plate are constructed by the non-conforming method discussed in Section 4.2.2. The explicit forms of stiffness and mass matrices have been published in many papers such as Refs. 62 and 73. In the present problem, isotropic plates with Hook's law in the standard form [73] are considered. In the second stage, the stiffness and mass matrices of longitudinal and transverse beams with respect to torsion and flexure rigidity are obtained [62] by transformation from local to global coordinate systems. In the final stage, the stiffness and mass matrices of truss members are obtained [62]. The three stages are then assembled to form the global stiffness and mass matrices for this problem, imposing interface conditions. Similarly, global load vectors are assembled from element load vectors of each structural component [73].

To solve the static and eigenvalue equations, the symbolic factorization technique presented in Section 4.5 is used to take advantage of sparsity of the global stiffness and mass matrices of the built-up structure. The subspace iteration method [102] is employed for solving the eigenvalue problem.

Structural analysis results are checked by using the finite element program SPAR and show good agreements up to 3 significant digits.

Conventional design sensitivity and shape design sensitivity calculations are carried out separately, with different finite element models. The finite element model used for conventional design sensitivity calculation is shown in Fig. 5.3. A total of 196 finite elements and 363 degrees of freedom are used to model the truss-beam-plate built-up structure, including 100 rectangular plate elements, 80 beam elements, and 16 truss elements. The 196 finite elements are linked to 6 kinds of independent design variables (thickness of plate elements, height and width of longitudinal beam elements, height and width of transverse beam elements, and cross-sectional area of truss members).

The input data used are as follows: elastic modulus $E = 3 \times 10^7$ psi, Poisson's ratio $\nu = 0.3$, the overall dimension $L_x \times L_y = 15$ in. $\times$ 15 in., uniform thickness of plate element $t = 0.1$ in., uniform height (width) of beam element $h = 0.5$ in. ($d = 0.15$ in.), cross-sectional area (length) of truss element $A = 0.1$ in. ($L = 5.364$ in.), equal spacing of beams $L_b = 3$ in., and uniformly distributed load $f = 0.1$ lb/in.^{2} on the plate. Mass density for the entire structure is taken as $\rho = 0.1$ lb/in.^{3} for the eigenvalue problem.

Comparison of conventional design sensitivities with actual changes after design modifications and predictions for constraints considered in Section 5.3 are summarized in Table 5.1. A 5% uniform change of all design variables with fixed cross-sectional areas and lengths of truss

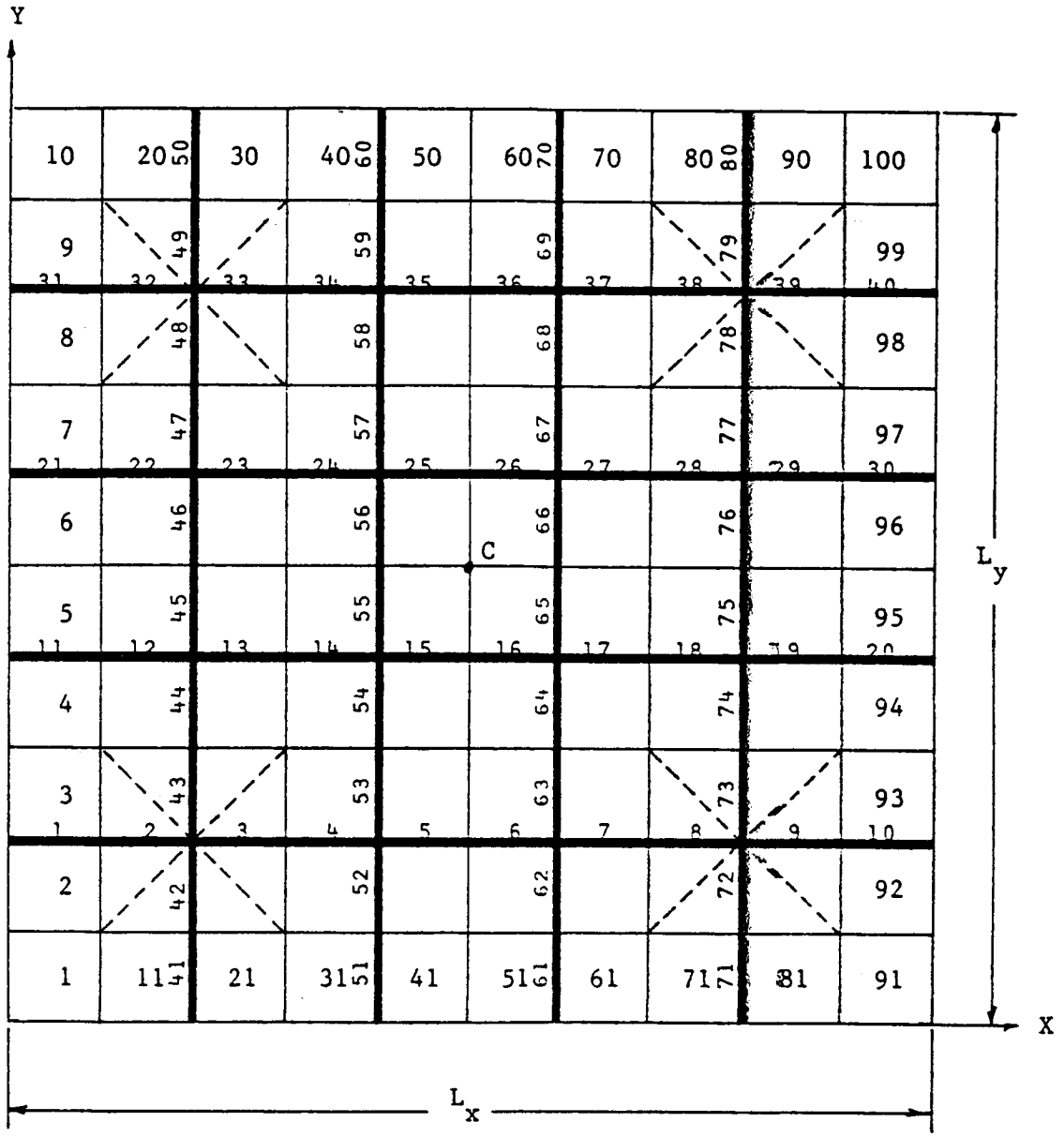

Figure 5.3 Finite Element Model of a Truss-Beam-Plate Built-Up Structure for Fixed Domain

Table 5.1 Conventional Design Sensitivity Comparison for Truss-Beam-Plate Built-Up Structure

Constraint		Ψ_1	$\Delta\Psi$	$\delta\Psi$	$\delta\Psi/\Delta\Psi$ (%)
Displace-ment	C	0.4775E-03	-0.8052E-04	-0.9071E-04	112.7
Stress on plate element	1	0.1484E 02	-0.7100E 00	-0.6750E 00	95.1
	2	0.5829E 02	-0.5980E 01	-0.6780E 01	113.4
	3	0.5263E 02	-0.5220E 01	-0.5810E 01	111.3
	4	0.5256E 02	-0.5760E 01	-0.6320E 01	109.7
	5	0.8497E 02	-0.1028E 02	-0.1126E 02	109.5
	11	0.5829E 02	-0.5980E 01	-0.6780E 01	113.4
	12	0.6780E 02	-0.7870E 01	-0.8630E 01	109.7
	13	0.5827E 02	-0.6720E 01	-0.7580E 01	112.8
	14	0.5269E 02	-0.6240E 01	-0.6830E 01	109.5
	15	0.7658E 02	-0.9360E 01	-0.1034E 02	110.5
	21	0.5263E 02	-0.5220E 01	-0.5810E 01	111.3
	22	0.5827E 02	-0.6720E 01	-0.7580E 01	112.8
	23	0.5450E 02	-0.6690E 01	-0.7300E 01	109.1
	24	0.5850E 02	-0.6990E 01	-0.8060E 01	115.3
	25	0.6155E 02	-0.7740E 01	-0.8500E 01	109.8
	31	0.5256E 02	-0.5760E 01	-0.6320E 01	109.7
	32	0.5269E 02	-0.6240E 01	-0.6830E 01	109.5
	33	0.5850E 02	-0.6990E 01	-0.8060E 01	115.3
	34	0.4697E 02	-0.6030E 01	-0.6340E 01	105.1
	35	0.4621E 02	-0.5880E 01	-0.6770E 01	115.1
	41	0.8497E 02	-0.1028E 02	-0.1126E 02	109.5
	42	0.7658E 02	-0.9360E 01	-0.1034E 02	110.5
	43	0.6155E 02	-0.7740E 01	-0.8500E 01	109.8
	44	0.4621E 02	-0.5880E 01	-0.6770E 01	115.1
	45	0.3975E 02	-0.5250E 01	-0.5980E 01	113.9
Stress on beam element	1	0.2956E 02	-0.3640E 01	-0.3960E 01	108.8
	2	0.1850E 03	-0.2428E 02	-0.2672E 02	110.0
	3	0.1200E 03	-0.1608E 02	-0.1764E 02	109.7
	4	0.2041E 03	-0.2552E 02	-0.2792E 02	109.4
	5	0.3549E 03	-0.4444E 02	-0.4872E 02	109.6
	11	0.1656E 02	-0.2360E 01	-0.2520E 01	106.8
	12	0.6312E 02	-0.7920E 01	-0.8680E 01	109.6
	13	0.2192E 02	-0.2400E 01	-0.2640E 01	110.0
	14	0.7964E 02	-0.1088E 02	-0.1192E 02	109.6
	15	0.1454E 03	-0.1960E 02	-0.2140E 02	109.2
Eigen-value		0.1242E 04	0.2408E 03	0.2199E 03	91.3

members is used. In Table 5.1, Ψ_1 represents the constraint value at initial design, $\Delta\Psi$ represents the actual change of constraint value after design modification, and $\delta\Psi$ represents the sensitivity prediction. The last column in Table 5.1 denotes the sensitivity agreement in % between actual change and prediction, defined as $\delta\Psi/\Delta\Psi \times 100$. This definition is also used to Table 5.2. Results in Table 5.1 show the conventional design sensitivity comparison for one quarter of the structure, due to symmetry (Fig. 5.3), and show good agreements of 91-115% for all constraints considered between sensitivity predictions and constraint reevaluations after design modifications. The accuracy is is more than adequate for iterative design.

During numerical calculation, it has been shown that the finite element model of Fig. 5.3, which was used for conventional design sensitivity calculation is not suitable for shape design sensitivity calculation because of the coarse grid. The reason the finer grid for shape design sensitivity calculations is required is that the shape design sensitivity forms are defined as an integration over component boundaries, while conventional design sensitivity forms are defined as an integration over their domains. Sensitivity evaluation at the component boundary is a major source of numerical inaccuracy, stemming from finite element analysis in shape optimization of built-up structures.

A finer grid finite element model for shape design sensitivity calculation is shown in Fig. 5.4. Only one quarter of the entire structure is shown in Fig. 5.4, due to symmetry. A total of 484 finite

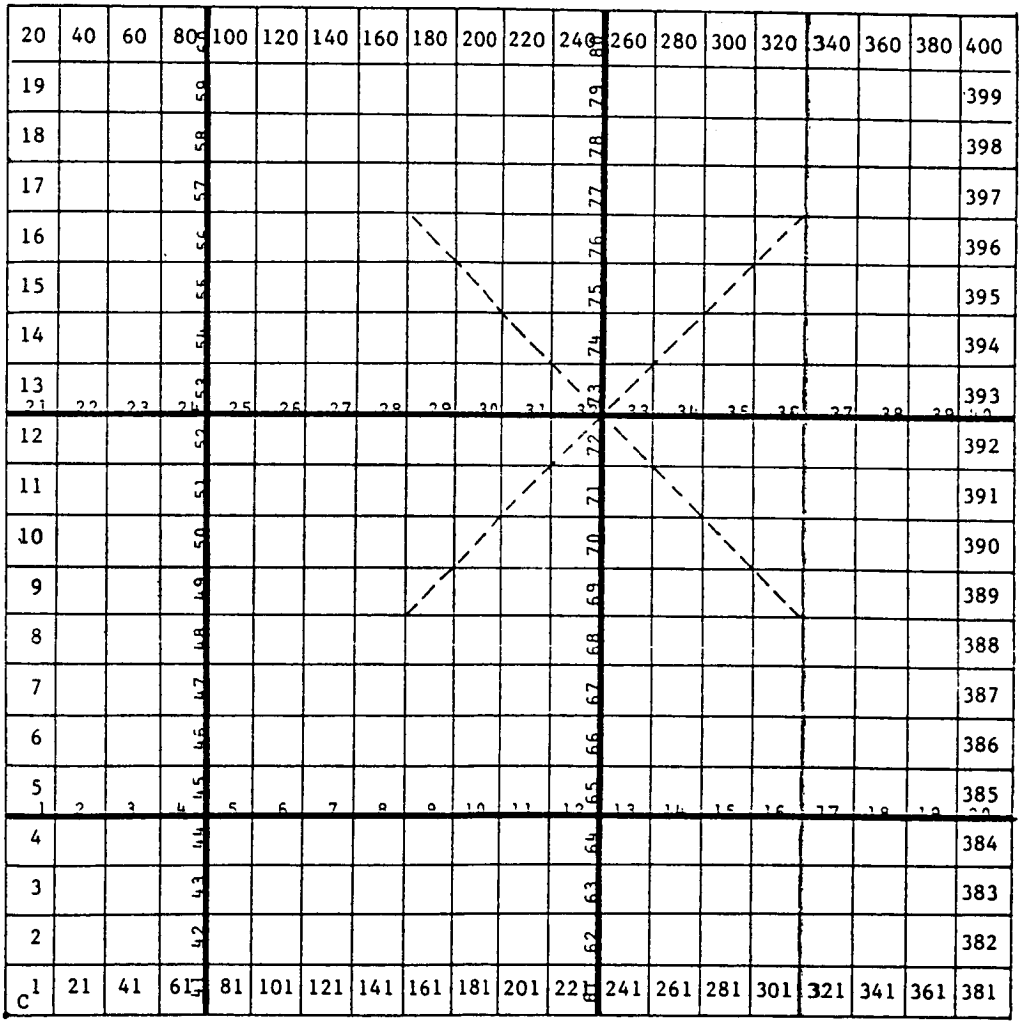

Figure 5.4 Finite Element Model of a Truss-Beam-Plate Built-Up Structure for Shape Variation

elements and 1281 degrees of freedom are used to model the structure, including 400 rectangular plate elements, 80 beam elements and 4 truss elements. Since conventional design variables are suppressed, the design variables for shape variation are the positions $\tilde{x}^i$, i=1,2, of transverse beams and the positions $\tilde{y}^j$, j=1,2, of longitudinal beams. During shape variations, it is presumed that the outside boundary is fixed and the lengths of truss members are constant, that is, the ground support of the truss moves according to the change of the beam position. The same input data that are used in conventional design sensitivity calculation are employed.

Comparison of shape design sensitivities with actual changes after design modification and predictions by formulas for constraints considered in Section 5.3 are summarized in Table 5.2, with 5 % change in position of each side of the plate components. Due to symmetry of the finite element model (Fig. 5.4), design sensitivity comparison for stress constraints of all beam elements and every other plate element in the upper triangular part, in addition to other constraints considered in Section 5.3, is listed in Table 5.2. As in the truss-beam built-up structure of Section 4.6, it is considered that the component boundary movement affects the element boundary movement with a distributed velocity, depending on the position, which is proportional to the velocity of the component boundary, to treat the stress constraint that is defined on the plate or beam element. Element boundary movement effect in Section 4.4 for sensitivity calculation is applied, in which the effect is shown to be critical in the present problem. As discussed

Table 5.2 Shape Design Sensitivity Comparison for Truss-Beam-Plate Built-Up Structure

Constraint		Ψ_1	$\Delta\Psi$	$\delta\Psi$	$\delta\Psi/\Delta\Psi$ (%)
Displace-ment		0.477630E-03	0.639000E-04	0.623050E-04	97.5
Stress on plate element	1	0.491283E 02	0.578430E 01	0.582313E 01	100.7
	3	0.404290E 02	0.507150E 01	0.503782E 01	99.3
	5	0.342734E 02	0.372610E 01	0.177060E 02	475.2*
	7	0.503317E 02	0.447630E 01	0.458831E 01	102.5
	9	0.621425E 02	0.461810E 01	0.471064E 01	102.0
	11	0.678413E 02	0.443210E 01	0.432144E 01	97.5
	13	0.770758E 02	0.449140E 01	0.199737E 02	444.7*
	15	0.836097E 02	0.495960E 01	0.497955E 01	100.4
	17	0.927545E 02	0.584630E 01	0.588408E 01	100.6
	19	0.102907E 03	0.711600E 01	0.737359E 01	103.6
	22	0.442618E 02	0.537550E 01	0.548079E 01	102.0
	24	0.330396E 02	0.431410E 01	0.637451E 01	147.8*
	26	0.426660E 02	0.419350E 01	0.430971E 01	102.8
	28	0.559439E 02	0.465430E 01	0.478683E 01	102.8
	30	0.635225E 02	0.455650E 01	0.462942E 01	101.6
	32	0.696483E 02	0.433590E 01	-0.271092E 01	- *
	34	0.779308E 02	0.472420E 01	0.474039E 01	100.3
	36	0.855177E 02	0.538780E 01	0.544000E 01	101.0
	38	0.918679E 02	0.632470E 01	0.636981E 01	100.7
	40	0.104643E 03	0.754400E 01	0.740095E 01	98.1
	44	0.333483E 02	0.433940E 01	0.476834E 01	109.9*
	46	0.442882E 02	0.420580E 01	0.457845E 01	108.9
	48	0.524977E 02	0.465790E 01	0.472717E 01	101.5
	50	0.585271E 02	0.449740E 01	0.471797E 01	104.9
	52	0.675386E 02	0.425440E 01	-0.417631E 01	- *
	54	0.754992E 02	0.478350E 01	0.486093E 01	101.6
	56	0.790451E 02	0.548130E 01	0.561322E 01	102.4
	58	0.812659E 02	0.589370E 01	0.581995E 01	98.7
	60	0.898351E 02	0.702590E 01	0.873431E 01	124.3
	65	0.384293E 02	0.410100E 01	0.885964E 01	216.0*
	67	0.448857E 02	0.440390E 01	0.716955E 01	162.8*
	69	0.460618E 02	0.419510E 01	0.103754E 01	24.7*
	71	0.560286E 02	0.402320E 01	0.854381E 01	212.4*
	73	0.707552E 02	0.433660E 01	0.161278E 02	371.9*
	75	0.683784E 02	0.534000E 01	0.606585E 01	113.6*
	77	0.671276E 02	0.552770E 01	0.663759E 01	120.1*
	79	0.650156E 02	0.500740E 01	0.508216E 01	101.5*
	85	0.383067E 02	0.418290E 01	0.787511E 01	188.3*
	87	0.405797E 02	0.386490E 01	0.742288E 01	192.1*
	89	0.478572E 02	0.365830E 01	0.292377E 01	79.9*
	91	0.601870E 02	0.366820E 01	-0.216160E 01	- *
	93	0.678691E 02	0.406780E 01	0.122838E 02	302.0*
	95	0.641141E 02	0.489870E 01	0.520101E 01	106.2*
	97	0.627188E 02	0.567790E 01	0.602441E 01	106.1*
	99	0.644332E 02	0.646100E 01	0.648722E 01	100.4*
	106	0.430485E 02	0.400810E 01	0.368377E 01	91.9
	108	0.515961E 02	0.377600E 01	0.362389E 01	96.0
	110	0.591465E 02	0.367630E 01	0.350028E 01	95.2

Table 5.2 Continued

112	0.622421E 02	0.352580E 01	0.475202E 01	134.8*
114	0.560415E 02	0.412800E 01	0.387695E 01	93.9
116	0.572092E 02	0.481830E 01	0.468990E 01	97.3
118	0.592701E 02	0.544530E 01	0.499216E 01	91.7
120	0.653244E 02	0.629920E 01	0.866491E 01	137.6
128	0.551221E 02	0.377870E 01	0.369667E 01	97.8
130	0.582628E 02	0.362570E 01	0.358268E 01	98.8
132	0.591416E 02	0.278540E 01	0.112804E 02	405.2*
134	0.480085E 02	0.382730E 01	0.399422E 01	104.4
136	0.470503E 02	0.454920E 01	0.430866E 01	94.7
138	0.497518E 02	0.501480E 01	0.460304E 01	91.8
140	0.568233E 02	0.578470E 01	0.579408E 01	100.2
149	0.555054E 02	0.365210E 01	0.360337E 01	98.7
151	0.532211E 02	0.291820E 01	0.279312E 01	95.7
153	0.555484E 02	0.199770E 01	0.762408E 01	381.6*
155	0.369989E 02	0.406490E 01	0.399285E 01	98.2
157	0.351428E 02	0.469500E 01	0.441864E 01	94.1
159	0.379014E 02	0.517780E 01	0.509654E 01	98.4
169	0.520786E 02	0.347340E 01	0.339814E 01	97.8
171	0.488632E 02	0.212230E 01	0.190147E 01	89.6
173	0.563002E 02	0.986300E 00	0.507594E 01	515.5*
175	0.327010E 02	0.319860E 01	0.293605E 01	91.8
177	0.233698E 02	0.438970E 01	0.420271E 01	95.7
179	0.232539E 02	0.498540E 01	0.481146E 01	96.5
190	0.452829E 02	0.225560E 01	0.184213E 01	81.7
192	0.613298E 02	-0.287800E 00	0.887028E 01	- *
194	0.477629E 02	0.850300E 00	0.620269E 00	72.9
196	0.320130E 02	0.162980E 01	0.133533E 01	81.9
198	0.270660E 02	0.193730E 01	0.212358E 01	109.6
200	0.348251E 02	0.246970E 01	0.146149E 01	59.2
212	0.676872E 02	-0.108820E 01	0.435962E 01	- *
214	0.601710E 02	-0.525400E 00	-0.575288E 00	109.5
216	0.533533E 02	-0.389700E 00	-0.584231E 00	149.9
218	0.552964E 02	-0.327000E-01	0.301678E 00	-
220	0.657858E 02	0.754300E 00	-0.214753E 01	-
233	0.814806E 02	-0.165530E 01	0.137769E 02	- *
235	0.827060E 02	-0.150610E 01	0.119062E 01	- *
237	0.900454E 02	-0.102090E 01	-0.458401E 00	449.0*
239	0.100982E 03	0.318000E 00	0.948578E 00	298.3*
253	0.820499E 02	-0.201040E 01	0.205777E 02	- *
255	0.795086E 02	-0.190830E 01	0.230174E 01	- *
257	0.900398E 02	-0.173330E 01	-0.137223E 01	79.2*
259	0.101662E 03	-0.176000E 01	-0.244327E 01	138.8*
274	0.673588E 02	-0.176060E 01	-0.985639E 00	56.0
276	0.612991E 02	-0.143850E 01	-0.146266E 01	101.7
278	0.648550E 02	-0.119740E 01	-0.104803E 01	87.5
280	0.753538E 02	-0.118920E 01	-0.448313E 01	377.0
296	0.456086E 02	-0.122760E 01	-0.117749E 01	95.9
298	0.425431E 02	-0.898100E 00	-0.744751E 00	82.9
300	0.493462E 02	-0.807200E 00	-0.121862E 01	151.0
317	0.297704E 02	-0.103000E 01	-0.904167E 00	87.8
319	0.278978E 02	-0.811600E 00	-0.101897E 01	125.6

Table 5.2 Continued

	337	0.218492E 02	-0.115130E 01	-0.104685E 01	90.9
	339	0.181100E 02	-0.120480E 01	-0.139737E 01	116.0
	358	0.145541E 02	-0.155840E 01	-0.164168E 01	105.3
	360	0.149387E 02	-0.151100E 01	-0.174274E 01	115.3
	380	0.121912E 02	-0.132390E 01	-0.149064E 01	112.6
	400	0.846174E 01	-0.843500E 00	-0.938432E 00	111.3
Stress on beam element	1	0.160415E 03	0.195140E 02	0.194400E 02	99.6
	2	0.154422E 03	0.188550E 02	0.187802E 02	99.6
	3	0.143154E 03	0.176080E 02	0.174085E 02	98.9
	4	0.128072E 03	0.159270E 02	0.156410E 02	98.2
	21	0.365447E 03	0.237300E 02	0.236590E 02	99.7
	22	0.360604E 03	0.231890E 02	0.231229E 02	99.7
	23	0.351645E 03	0.221520E 02	0.219809E 02	99.2
	24	0.340254E 03	0.207440E 02	0.208615E 02	100.6
	25	0.305855E 03	0.191690E 02	0.193528E 02	101.0
	26	0.240941E 03	0.178240E 02	0.179433E 02	100.7
	27	0.172152E 03	0.164840E 02	0.164213E 02	99.6
	28	0.979993E 02	0.151517E 02	0.150810E 02	99.5
	29	0.175804E 02	0.138385E 02	0.137983E 02	99.7
	30	-0.693616E 02	0.125603E 02	0.125568E 02	100.0
	31	-0.162326E 03	0.113270E 02	0.112652E 02	99.5
	32	-0.259741E 03	0.101420E 02	0.104919E 02	103.5
	45	0.106547E 03	0.141790E 02	0.139345E 02	98.3
	46	0.901367E 02	0.130483E 02	0.131937E 02	101.1
	47	0.721165E 02	0.119729E 02	0.120849E 02	100.9
	48	0.504898E 02	0.109112E 02	0.110551E 02	101.3
	49	0.245700E 02	0.982590E 01	0.999583E 01	101.7
	50	-0.547858E 01	0.869336E 01	0.885654E 01	101.9
	51	-0.388750E 02	0.750090E 01	0.747266E 01	99.6
	52	-0.743968E 02	0.623580E 01	0.604437E 01	96.9
	53	-0.904410E 02	0.456870E 01	0.438521E 01	96.0
	54	-0.740261E 02	0.331260E 01	0.350239E 01	105.7
	55	-0.573423E 02	0.219220E 01	0.225943E 01	103.1
	56	-0.423233E 02	0.125110E 01	0.129765E 01	103.7
	57	-0.298151E 02	0.510400E 00	0.562454E 00	110.2
	58	-0.199104E 02	-0.710000E-02	0.118288E 00	-
	59	-0.119784E 02	-0.265500E 00	0.289746E 00	-
	60	-0.478911E 01	-0.214640E 00	0.235848E 01	-
	73	-0.270690E 03	0.842100E 01	0.885263E 01	105.1
	74	-0.207475E 03	0.614300E 01	0.642310E 01	104.6
	75	-0.150720E 03	0.416000E 01	0.422678E 01	101.6
	76	-0.101488E 03	0.253470E 01	0.256681E 01	101.3
	77	-0.606386E 02	0.129380E 01	0.134459E 01	103.9
	78	-0.288523E 02	0.439900E 00	0.602348E 00	136.9
	79	-0.713844E 01	-0.277000E-01	0.630721E 00	-
	80	0.214113E 01	-0.103470E 00	0.268880E 01	-
Compliance		0.977450E-03	0.110150E-03	0.101664E-03	92.3
Eigenvalue		0.121510E 04	-0.222000E 02	0.211944E 02	95.5

in Section 4.6, to treat a stress constraint that is defined on an element adjacent to the interface, the argument presented in Section 4.6 is applied to calculate the sensitivity coefficients.

As suggested in previous sections, the non-conforming method for plate analysis is used, which allows displacement continuity at the element boundary and nodal points, and slope continuity at the nodal points between elements. Since the normal slopes at the element boundaries must be continuous (interface condition), the average values of normal slopes at the component boundaries (interface) between components are taken to evaluate shape design sensitivity coefficients. A numerical test shows that this averaging scheme yields better sensitivity results. As discussed in Section 4.6, to evaluate the third derivatives of state variable, an extrapolation scheme is used.

Results in Table 5.2 show reasonably good agreement between sensitivity prediction and constraint reevaluation after design modification, for all constraints except a few stress constraints defined on plate and beam elements. Note that some of the sensitivities for the stress constraints on plate elements adjacent to the interface marked by * in Table 5.2 are poor (even opposite sign in some constraints). The reason for poor sensitivity results for these constraints is that the adjoint load is acting at the interface (element boundary) and hence the non-continuity of normal slopes (even taking average of these values) degrades sensitivity accuracy. However, for stress constraints defined on beam elements adjacent to the interface, since the slope is continuous at the nodal points between components,

good sensitivity agreement is obtained, as shown in Table 5.2. For a few stress constraints on plate and beam elements near free boundary, since the amount of change of constraint values are relatively small, the sensitivity agreement is poor, due to approximation error. Numerical tests show that these poor sensitivities can be improved by a larger perturbation of design, within the range of linear approxiition. To improve the poor shape design sensitivity agreement for the stress constraints defined on plate and beam elements adjacent to interfaces or free boundaries, which is one of the most numerically difficult tasks in built-up structure optimization, a conforming method for plate analysis, as discussed in Section 4.2.2, or the boundary element method for treating elements close to component boundaries is suggested.

Once acceptable design sensitivity coefficients are obtained, one can directly utilize a nonlinear programming method to obtain an optimum design, without any appreciable difficulty. With the design sensitivity coefficients obtained, the linearization method [105] is applied to obtain the optimum distribution of design variables for the present problem, with a fixed domain (Fig. 5.3). Minimum weight design of the entire structure subject to displacement, stress on plate and beam elements, and natural frequency constraints is considered. The initial design (b_0) is selected as $t_0 = 0.1$ in., $\tilde{d}_0 = \hat{d}_0 = 0.15$ in., $\tilde{h}_0 = \hat{h}_0 = 0.5$ in., and $A_0 = 0.1$ in., with the lower and upper bound $b_\ell = 0.8\ b_0$ and $b_u = 1.2 b_0$, respectively, with ratio $R = b_u/b_\ell = 1.5$. Allowable bounds for each constraint are given

as: $z^a = 0.0006$ in., $\sigma_\rho^a = 100$ psi, $\sigma_b^a = 400$ psi, and $\zeta^a = 800$ $(\text{rad/sec})^2$.

The solution in Table 5.3 shows the optimum design for the present problem, where one quarter of design variables appear, due to symmetry. The cost is reduced from 41.68 to 32.40, which is 22.3% reduction, while the L-2 norm of the direction vector as a convergence criteria, is reduced from 34.69 to 0.791×10^{-3} after 17 iterations.

Reviewing the history of iterative design, the cross-sectional area of truss member and the beam width tend to approach the lower bounds in the early iterations. When the beam height is significantly dominant to the plate thickness, the plate thickness tends to go to the lower bound in the early stage, in which the optimum solution is obtained by controlling the beam height. For this case, the outer beams that are close to the free edges have the characteristic of a build up in beam height, particularly conspicuous around the middle portion of the beam.

Also, one can notice that whenever the ratio of upper and lower bounds of design variables becomes smaller, the smoother distribution of design variables is expected. However, if the beam height is not significantly large compared to plate thickness, the optimum design may be obtained by controlling both plate thickness and beam height.

Table 5.3 Optimal Design Results for Truss-Beam-Plate Built-Up Structure

		Initial	Final			Initial	Final
Plate thickness (× 0.1)	(1)	1.0000	0.80008	Beam width	(1)	0.1500	0.12000
	(2)	-	0.80009		(2)	-	0.12000
	(3)	-	0.80010		(3)	-	0.12000
	(4)	-	0.80010		(4)		0.12001
	(5)	-	0.80010		(5)		0.12001
	(11)		0.80009		(11)		0.12000
	(12)		0.80009		(12)		0.12000
	(13)		0.80009		(13)	-	0.12000
	(14)		0.80009		(14)	-	0.12000
	(15)		0.80009		(15)	0.1500	0.12000
	(21)		0.80010	Beam height	(1)	0.5000	0.40005
	(22)		0.80009		(2)	-	0.43199
	(23)		0.80009		(3)	-	0.40005
	(24)		0.80009		(4)		0.50015
	(25)		0.80008		(5)		0.59996
	(31)		0.80010		(11)		0.40005
	(32)		0.80009		(12)		0.40004
	(33)		0.80009		(13)	-	0.40004
	(34)		0.80010		(14)	-	0.40008
	(35)		0.80005		(15)	0.5000	0.40986
	(41)	-	0.80010	Truss area (× 0.1)	(1)	1.0000	0.80009
	(42)	-	0.80009		(2)	-	0.80009
	(43)	-	0.80008		(3)	-	0.80009
	(44)	-	0.80005		(4)	1.0000	0.80009
	(45)	1.0000	0.80009				

CHAPTER 6

DISCUSSION AND CONCLUSIONS

Methods of design sensitivity analysis and optimization of built-up structures have been studied using distributed parameter structural theory. The studies clearly demonstrate the advantage of the variational formulation of boundary-value problems in design sensitivity analysis. The material derivative idea from continuum mechanics is employed for shape variation analysis. A unified method of shape design sensitivity analysis is developed, in which the shape design sensitivity coefficients are easily obtained by imposing boundary and interface conditions in built-up structure problems, without carrying out the complete procedure of shape design sensitivity analysis. An iterative optimization algorithm is then utilized to obtain an optimum solution. This procedure is applied for optimal design of a truss-beam-plate built-up structure, as a numerical feasibility study. In view of the theory and results presented, there should be no fundamental difficulties in applying the procedure to other classes of built-up structural optimization problems.

Numerical experimentation with the procedure developed shows that the inherent approximation error caused by using distributed parameter structural theory instead of matrix/finite element method for design sensitivity calculation is not significant, but that the choice of numerical methods for calculation, especially the finite element method,

plays a crucial role in the procedure's success. This is mainly due to the fact that one obtains relatively poor design sensitivity results for stress constraints near the component boundary (interface) where interface or boundary conditions are imposed.

Further development and application of the present design method for built-up structure optimization may be envisioned in several fields. The present study on optimization of relatively simple geometry under general constraints clearly indicates the feasibility of extending the present optimal design problem for more complex built-up structures, including curved beam and shell components, where the configurations of combined structures are more complex and constraints and loading conditions are more varied.

REFERENCES

1. Venkayya, V.B., "Structural Optimization: A Review and Some Recommendations," Int. J. Num. Meth. Eng., Vol. 13, No. 2, 1978, pp. 203-228.

2. Morris, A.J., "An Introduction to the Solution of Optimal Structural Design Problems Using the Finite Element Method," Optimization of Distributed Parameter Structures (Ed. E.J. Haug and J. Cea), Sijthoff & Noordhoff, Alphen ann den Rijn, Netherlands, 1981.

3. Haug, E.J. and Cea, J., Optimization of Distributed Parameter Structures, Sijthoff & Noordhoff, Alphen ann den Rijn, Netherlands, 1981.

4. Fichera, G., "Existence Theorem in Elasticity," Handbuch Der Physik, Vol. VI a/2, 1972, pp. 347-389.

5. Haug, E.J., Choi, K.K., and Komkov, V., Design Sensitivity Analysis of Structural Systems, Academic Press, New York, to appear 1984.

6. Ciarlet, P.G., The Finite Element Method for Elliptic Problems, North-Holland, New York, 1978.

7. Catchpole, E.J., "The Optimum Design of Compression Surfaces having Unflanged Integral Stiffeners," Journal of the Royal Aeronautical Society, Vol. 58, Nov. 1954, pp. 765-768.

8. Symonds, M.F., "Minimum Weight Design of a Simply Supported Transversely Stiffened Plate Loaded in Shear," Journal of the Aeronautical Societies, July 1956, pp. 685-693.

9. Nickel, E.H. and Crawford, R.F., "Optimum Ring Stiffened Cylinders Subjected to a Uniform Hydrostatic Pressure," Society of Automotive Engineers, Reprint 578F, 1962.

10. Crawford, R.F. and Burns, A.B., "Minimum Weight Potentials for Stiffened Plates and Shells," AIAA J. 1(4), 1963, pp. 879-886.

11. Cohen, G.A., "Optimum Design of Truss-Core Sandwich Cylinders under Axial Compression," AIAA J. 1(7), 1963, pp. 1626-1630.

12. Burns, A.B. and Almroth, B.O., "Structural Optimization of Axially Compressed, Ring-Stringer Stiffened Cylinders," J. Spacecraft Rockets 3(1), 1966, pp. 19-25.

13. Gerard, G. and Papirno, R., "Minimum Weight Design of Stiffened Cylinders for Launch Vehicle Applications," NASA CR-53315, 1964.

14. Burns. A.B. and Skogh J., "Combined Loads Minimum Weight Analysis of Stiffened Plates and Shells," J. Spacecraft Rockets 3(2), 1966, pp. 235-240.

15. Burns, A.B., "Structural Optimization of Axially Compressed Cylinders, Considering Ring-Stringer Eccentricity Effects," J. Spacecraft Rockets 3(8). 1966, pp. 1263-1268.

16. Burns, A.B., "Minimum Weight, Hydrostatically Compressed, Ring Stiffened Cones," J. Spacecraft Rockets, 3, 1966, pp. 387-392.

17. Burns, A.B., "Optimum Cylinders with Contrasting Materials and Various Ring-Stringer Configurations," J. Spacecraft Rockets, 4, 1967.

18. Burns, A.B., "Optimum Stiffened Cylinders for Combined Axial Compression and Internal or External Pressure," J. Spacecraft Rockets 5(6), 1968, pp.690-699.

19. Gerard, G., "Optimum Structural Design Concepts for Aerospace Vehicles," J. Spacecraft Rockets 3(1), 1966, pp. 5-18.

20. Lakshmikantham, C. and Becker, H., "Minimum Weight Design Aspects of Stiffened Cylinders under Compression," NASA CR-963, 1967.

21. Block, D.L., "Minimum Weight Design for Axially Compressed Ring and Stringer Stiffened Cylindrical Shells," NASA CR-1766, July 1971.

22. Shideler, J.L., Anderson, M.S., and Jackson, L.R., "Optimum Mass Strength Analysis for Orthotropic Ring Stiffened Cylinders under Axial Compression," NASA TN D-6772, 1972.

23. Shanley, F.D., Weight Strength Analysis of Aircraft Structures, Dover, New York, 1960.

24. Schmit, L.A., "Structural Design by Systematic Synthesis," Proceedings of the 2nd National Conference on Electronic Computation, American Society of Civil Engineers, Structural Division, New York, 1960, pp. 105-132.

25. Kicher, T.P., "Structural Synthesis of Integrally Stiffened Cylinders", J. Spacecraft Rockets, 5 (1), 1968, pp. 62-67.

26. Schmit, L.A., Morrow, W.M., and Kicher, T.P., "A Structural Synthesis Capability for Integrally Stiffened Cylindrical Shells," AIAA Paper 68-327, Palm Springs, Calif., 1968.

27. Morrow, W.M. and Schmit, L.A., Jr., "Structural Synthesis of a Stiffened Cylinder," NASA CR-1217, 1968.

28. Pappas M. and Amba-Rao, C.L., "A Direct Search Algorithm for Automated Optimum Structure Design," AIAA J. 9(3), 1971, pp. 387-393.

29. Thornton, W.A., "Synthesis of Stiffened Conical Shells," J. Spacecraft Rockets, Vol. 9, March 1972, pp. 189-195.

30. Jones, R.T. and Hague, D.S., "Application of Multi-Variable Search Technique to Structural Design Optimization," NASA CR-2038, Jan. 1972.

31. Pappas, M. and Allentuch, A., "Structural Synthesis of Frame Reinforced Submersible, Circular, Cylindrical Hulls," Computers & Structures, Vol. 4, 1974, pp. 253-280.

32. Pappas, M. and Allentuch, A., "Optimal Design Properties of Frame Reinforced, Submersible, Circular, Cylindrical Hulls," J. of Ship Research, 17(4), 1973, pp.208-216.

33. Pappas, M. and Allentuch, A., "Automated Optimal Design of Frame Reinforced, Submersible, Circular, Cylindrical Shells," J. of Ship Research, Vol. 17, No. 4, 1973, pp. 208-216.

34. Stroud, W.J. and Sykes, N.P., "Minimum Weight Stiffened Shells with Slight Meridional Curvature Designed to Support Axial Compressive Loads," AIAA J. 7(8), 1969, pp. 1599-1601.

35. Lakshmikantham, C. and Gerard, G., "Minimum Weight Design of Stiffened Cylinders," Aeronautical Quarterly, 21(2), 1970, pp. 49-68.

36. Kicher, T.P. and Chao, T.L., "Minimum Weight Design of Stiffend Fiber Composite Cylinders," J. Aircraft, 8(7), 1971, pp. 562-569.

37. Manevich, A.I. and Kaganov, M.Y., "Stability and Weight Optimization of Reinforced Spherical Shells under External Pressure," Prikladnaya Mekhanika, Vol. 9, Nr. 1, 1973, pp. 20-26.

38. Tvergaard, V., "Influence of Post-Buckling Behaviour on Optimum Design of Stiffened Panels," Int. J. of Solids Structures, Vol. 9, 1973, pp. 1519-1534.

39. Rehfield, L.W., "Design of Stiffened Cylinders to Resist Axial Compression," J. Spacecraft Rockets, 10(5), 1973, pp. 346-349.

40. Pappas, M. and Allentuch, A., "Extended Capability for Automated Design of Frame-Stiffened, Submersible, Cylindrical Shells," Computers & Structures, Vol. 4, 1974, pp. 1025-1059.

41. Simitses, G.T. and Aswani, M., "Minimum Weight Design of Stiffend Cylinder under Hydrostatic Pressure," J. of Ship Research, Vol. 21, No. 4, 1977, pp. 217-224.

42. Pappas, M. and Allentuch, A., "Pressure Hull Optimization Using General Instability Equation Admitting More Than One Longitudinal Buckling Half-Wave," J. of Ship Research, Vol. 19, No. 1, 1975, pp. 18-22.

43. Simitses, G.J. and Ungbhakorn, V., "Minimum Weight Design of Stiffened Cylinders under Axial Compression," AIAA J., 13(6), 1975, pp. 750-755.

44. Simitses, G.J. and Ungbhakorn, V., "Weight Optimization of Stiffened Cylinders under Axial Compression," Computers & Structures, Vol. 5, 1975, pp. 305-314.

45. Kunoo, K. and Yang, T.Y., "Minimum Weight Design of an Orthogonally Stiffened Waffle Cylindrical Shell with Buckling Constraint," J. Spacecraft Rockets, 13(3), 1976, pp. 137-143.

46. Kunoo, K. and Yang, T.Y., "Minimum Weight Design of Cylindrical Shell with Multiple Stiffener Sizes," AIAA J., Vol. 16, No. 1, 1978, pp. 35-40.

47. Pappas, M. and Moradi, J., "Optimal Design of Ring Stiffened Cylindrical Shells Using Multiple Stiffener Sizes," AIAA J., Vol. 18, No. 2, 1980, pp. 1020-1022.

48. Richards, D.M., "Optimum Design of Stiffened Shear Webs with Supplementary Skin Stabilization," Int. J. of Solids Structures, Vol. 12, 1976, pp. 791-802.

49. Sφreide, T.H., Moan, T., and Nordsve, N.T., "On the Behaviour and Design of Stiffened Plates in Ultimate Limit State," J. of Ship Research, Vol. 22, No. 4, Dec. 1978, pp. 238-244.

50. Libai, A., "Optimization of a Stiffened Square Panel Subjected to Compressive Edge Loads," AIAA J., Vol. 17, No. 12, Dec. 1979, pp. 1379-1380.

51. Majumder, D.K. and Thornton, W.A., "Design of Efficient Stiffened Shells of Revolution," Int. J. Num. Meth. Eng., Vol. 10, 1976, pp. 535-549.

52. Simitses, G.J. and Giri, J., "Minimum Weight Design of Stiffened Cylinders Subjected to Pure Torsion," Computers & Structures, Vol. 7, 1977, pp. 667-677.

53. Simitses, G.J. and Giri, J., "Optimum Weight Design of Stiffened Cylinders Subjected to Torsion Combined with Axial Compression With and Without Lateral Pressure," Computers & Structures, Vol. 8, 1978, pp. 19-30.

54. Toakley, A.R. and Williams, D.G., "The Optimum Design of Stiffened Panels Subject to Compression Loading," Engineering Optimization, Vol. 2, 1977, pp. 239-250.

55. Simitses, G.J. and Sheinman, I., "Minimum-Weight Design of Stiffened Cylindrical Panels under Combined Loads," J. Aircraft, Vol. 14, No. 5, May 1977, pp. 419-420.

56. Bronowicki, A.J., Nelson, R.B., Felton, L.P., and Schmit, L.A. Jr., "Optimization of Ring Stiffened Cylindrical Shells," AIAA J. 13(10), 1975, pp. 1319-1325.

57. Patnaik, S.N. and Sankaran, G.V., "Optimum Design of Stiffened Cylindrical Panels with Constraint on the Frequency in the Presence of Initial Stresses," Int. J. Num. Meth. Eng., Vol. 10, 1976, pp. 283-299.

58. Dobbs, M.W. and Nelson, R.B., "Minimum Weight Design of Stiffened Panels with Fracture Constraints," Computers & Structures, Vol. 8, 1978, pp. 753-759.

59. Rao, S.S. and Reddy, E.S., "Optimum Design of Stiffened Cylindrical Shells with Natural Frequency Constraints," Computers & Structures, Vol. 12, 1980, pp. 211-219.

60. Simitses, G.J. and Sheinman, I., "Optimization of Geometrically Imperfect Stiffened Cylindrical Shells under Axial Compression," Computers & Structures, Vol. 9, 1978, pp. 377-381.

61. Patel, J.M. and Patel, T.S., "Minimum Weight Design of the Stiffened Cylindrical Shell under Pure Bending," Computers & Structures, Vol. 11, 1980, pp. 559-563.

62. Przemieniecki, J.S., Theory of Matrix Structural Analysis, McGraw-Hill, 1968.

63. Roark, R.J. and Young, W.C., Formulas for Stress and Strain, McGraw-Hill, 5th Ed., 1975.

64. Gallagher, R.H., Finite Element Analysis, Fundamentals, Prentice-Hall, Englewood Cliffs, N.J., 1975.

65. Reed, M., and Simon, B., "Methods of Modern Mathematical Physics I: Functional Analysis, Academic Press, London, 1972.

66. Aubin, J-P., Applied Functional Analysis, Wiley-Interscience, New York, 1979.

67. Aubin, J-P., Approximation of Elliptic Boundary-Value Problems, Wiley-Interscience, New York, 1972.

68. Sokolnikoff, I.S., Mathematical Theory of Elasticity, McGraw-Hill, New York, 1956.

69. Fung, Y. C., Foundation of Solid Mechanics, Prentice-Hall, Englewood Cliffs, N.J., 1973.

70. Goldstein, H., Classical Mechanics, 2nd Ed., Addison-Wesley Publishing Co., 1980.

71. Rosenberg, R.M., Analytical Dynamics of Discrete Systems, Plenum Press, New York, 1977.

72. Yoo, Y.M., Shape Optimal Design of Elastic Structural Components, TR No. 82-8, Center for Computer Aided Design, The University of Iowa, Dec. 1982.

73. Zienkiewicz, O.C., The Finite Element Method, McGraw-Hill, 3rd Ed., 1977.

74. Zienkiewicz, O.C. and Cheung, Y.K., "The Finite Element Method for Analysis of Elastic Isotropic and Orthotropic Slabs," Proc. Inst. Civ. Eng., 28, 1964, pp. 471-488.

75. Adini, A. and Clough, R.W., Analysis of Plate Bending by the Finite Element Method and Report to Nat. Sci. Found/U.S.A., G.7337, 1961.

76. Bogner, F.K., Fox, R.L., and Schmit, L.A., "The Generation of Interelement-Compatible Stiffness and Mass Matrices by the Use of Interpolation Formulae," Proc. Conf. Matrix Methods in Struct. Mech., Air Force Inst. of Tech., Wright Patterson A.F. Base, Ohio, 1965.

77. Fraeijs de Veubeke, B., "A Conforming Finite Element for Plate Bending," Int. J. Solids Struct., 4, 1968, pp. 95-108.

78. Bron, J and Dhatt, G., "Mixed Quadrilateral Elements for Bending," AIAA J., 10, 1972, pp. 1359-1361.

79. Morley, L.S.D., "The Triangular Equilibrium Element in the Solution of Plate Bending Problems," Aero Quart., 19, 1968, pp. 149-169.

80. Bazeley, G.P., Cheung, Y.K., Irons, B.M., and Zienkiewicz, O.C., "Triangular Elements in Bending-Conforming and Non-Conforming Solutions," Proc. Conf. Matrix Methods in Struct. Mech., Air Force Inst. of Tech., Wright Patterson A.F. Base, Ohio, 1965.

81. Razzaque, A., "Program for Triangular Bending Element with Derivative Smoothing," Int. J. Num. Meth. Eng., 5, 1973, pp. 588-589.

82. Fellipa, C.A., Refined Finite Element Analysis of Linear and Non-linear Two-Dimensional Structures, Ph.D., Struct. Eng. Univ. of Calif., Berkeley, 1966.

83. Irons, B.M. and Razzaque, A., "Experience with the Patch Test," in Mathematical Foundations of the Finite Element Method, pp. 557-587 (Ed. Aziz, A.R.), Academic Press, 1972.

84. Strang, G. and Fix, G.J., An Analysis of the Finite Element Method, Prentice-Hall, Englewood Cliffs, N.J., 1973.

85. Argyris, J.H., Fried, I., and Scharpf, D.W., "The TUBA Family of Plate Elements for the Matrix Displacement Method," The Aeronautical J. R. Ae. S., 72, 701-709, 1968.

86. Bell, K., "A Refined Triangular Plate Bending Element," Int. J. Num. Meth. Eng., 1, 1969, pp. 101-122.

87. Bosshard, W., "Ein neues vollvertragliches endliches Element für Plattenbiegung," Mt. Assoc. Bridge Struc. Eng. Bulletin, 28, 1968, pp. 27-40.

88. Irons, B.M., "A Conforming Quartic Triangular Element for Plate Bending," Int. J. Num. Meth. Eng., 1, 1969, pp. 29-46.

89. Visser, W., The Finite Element Method in Deformation and Heat Conduction Problems, Dr. W. Dissertation, T.H., Delft, 1968.

90. Cowper, G.R., Kosko, E., Lindberg, G.M., and Olson, M.D., "Formulation of a New Triangular Plate Bending Element," Trans. Canad. Aero-Space Inst., 1, 1968, pp. 86-90.

91. Butlin, G.A. and Ford, R., "A Compatible Plate Bending Element," Univ. of Leicester Eng. Dept. Report, 68-15, 1968.

92. Withum, D., Berechnung von Platten nach dem Ritzsehen verfahren mit Wilfe dreieckförmiger Meshnetze, Mittl. Inst. Statik Tech. Hochschule, Hanover, 1966.

93. Zenisek, A., "Interpolation Polynomials on the Triangle," Int. J. Num. Meth. Eng., 10, 1976, pp. 283-296.

94. Kopal, Z., Numerical Analysis, John Wiley & Sons, New York, 1955.

95. Stroud, A.H. and Secrest, D., Gaussian Quadrature Formulas, Prentice-Hall, Englewood Cliffs, N.J., 1966.

96. Hinton, H. and Campbell, J.S., "Local and Global Smoothing of Discontinuous Finite Element Functions Using a Least Squares Method," Int. J. Num. Meth. Eng., Vol. 8, No.3, 1974, pp. 461-480.

97. Argyris, J.H. and William, K.J., "Some Considerations for the Evaluation of Finite Element Models," NucEDe, Vol. 28, No.1. 1974, pp. 76-96.

98. Hinton, E., Scott, F.C., and Ricketts, R.E., "Local Least Squares Smoothing for Parabolic Isoparametric Elements," Int. J. Num. Meth. Eng., Vol. 9, No. 1, 1975, pp. 235-238.

99. Barlow, J., "Optimal Stress Locations in Finite Element Models," Int. J. Num. Meth. Eng., Vol.10, No.2, 1976, pp. 243-251 (Discussion: Vol. 11, No. 3, p. 604).

100. Cook, R.D., Concepts and Applications of Finite Element Analysis, John Wiley & Sons, 2nd Ed., 1981.

101. Haug, E.J. and Arora, J.S., Applied Optimal Design, Wiley-Interscience, New York, 1979.

102. Bathe, K-J. and Wilson, E.L., Numerical Methods in Finite Element Analysis, Prentice-Hall, Englewood Cliffs, N.J., 1976.

103. Lam, H.L., Choi, K.K., and Haug, E.J., "A Sparse Matrix Finite Element Technique for Iterative Structural Optimization," Computers & Structures, Vol. 16, No. 1-4, 1983, pp. 289-295.

104. Harwell Subroutine Library, A Catalogue of Subroutine, Computer Science and Systems Division, AERE-R 9185, Harwell, Oxfordshire, 1980.

105. Choi, K.K., Haug, E.J., Hou, J.W., and Sohoni, V.N., "Pshenichny's Linearization Method for Mechanical System Optimization", ASME Journal of Mechanisms, Transmissions, and Automation in Design, Vol. 105, March 1983, pp. 97-103.

106. Dym, C.L. and Shames, J.H., Solid Mechanics, A Variational Approach, McGraw-Hill, 1973.

107. Ugral, A.C. and Fenster, S.K., Advanced Strength and Applied Elasticity, Elsevier, New York, 1975.

108. Meirovitch, L., Analytical Methods in Vibrations, New York, Macmillan, 1967.